# An electrophysiological investigation of normal and scrapie-infected dorsal lateral geniculate neurones *in vitro*

by

**Catherine J. Black**

**Submitted for the degree of**

**Doctor of Philosophy**

**in the Faculty of Medicine, The University of Edinburgh**

**September 1995**

*for my parents and Tim*

## Declaration

I declare that this thesis was composed by myself. The contributions of others to this work are clearly indicated.

Catherine J. Black

**Acknowledgments**

I would like to thank the BBSRC, Dr. J.R. Fraser and Dr N.K. MacLeod for the opportunity to work on this project, and for the provision of laboratory and computing facilities.

My time in the Physiology Department certainly has been memorable. My sincerest thanks go to Mayank Dutia, Gareth Leng and John Russell for their generous support and advice during my period of study, and with whom I have been privileged to discuss my work.

I am very grateful for the technical and administrative help I have received from Elizabeth Tweedale, Brendan McGrory, Tom MacKenzie and Pete Frew.

Also thanks go to the staff at the Neuropathogenesis Unit for making me welcome during my many visits, particularly to Debbie Brown for the considerable amount of time spent transferring various materials for this project to and from the Physiology Department. Thanks also to Martin Jeffrey for helpful discussions during this project.

There are several people whose tolerance and patience have known no bounds. Alex Johnston has been both an invaluable friend and mentor to me during the last three years. I have benefited considerably from the time we have spent in discussions of matters electrophysiological and otherwise. Colin Brown has been a good friend to me and unfailing in his advice and support. I would like to thank him for the many helpful discussions during the writing of this thesis, especially with regards to the statistics. I cannot thank Jan Fraser enough for her guidance during this project, having an essential sense of humour and showing unstinting enthusiasm during the writing up of this project.

"No one is an island entire of itself;
every one is a piece of the continent,
a part of the main."

John Donne (1573 - 1631)

Therefore there are those without whom my completion of this project just would not have been possible, namely Jill, Justin, mum, dad and Tim.

Finally I would like to say it has been a pleasure making Simone Meddle's acquaintance these last months and discussing with herself and Niall Murphy the challenging experience of "writing up".

**Contents**

**Abstract**

This thesis reports the results of an intracellular investigation of the electrophysiological properties of dorsal lateral geniculate nucleus (dLGN) relay neurones in normal and scrapie-infected mice. Scrapie is an infectious, fatal neurodegenerative disease naturally occurring in sheep; it is categorised with similar diseases in humans and animals as a transmissible spongiform encephalopathy. These diseases are characterised by a prolonged incubation period from the time of infection, with the late appearance of clinical symptoms. Typical pathological features are vacuolation of the neuropil, gliosis, deposition of an abnormal protein (PrP) and neuronal loss; an acute immune response is absent. The causal agent has unconventional properties but its precise nature is unknown and the mechanisms preceding neuronal loss that accompany such infections are not well understood. Scrapie has been successfully transmitted to rodents. By the intraocular route, infectivity and pathology of the ME7 strain of scrapie targets the central visual pathways including the dLGN in the thalamus. In this scrapie model there is a profound loss of neurones in the dLGN.

In this study the functional integrity of relay neurones and their afferent input from optic tract fibres was monitored in the scrapie-infected dLGN throughout the incubation period. The aim of this study was to elucidate the mechanisms of scrapie-associated dysfunction at the level of the neuronal membrane. The properties of murine relay cells have not been well characterised; a study of the membrane properties of these cells was carried out in order to ascertain if they were similar to rat and guinea-pig relay cells, and thus if the results of the scrapie investigation could be interpreted in terms of the extensive literature on relay cell physiology in these species.

The technique of intracellular recording from brain slices was used to evaluate the properties of dLGN relay cells in untreated (normal), normal brain inoculated (control) and scrapie-inoculated mice. The inoculated mice received an intraocular injection of either ME7 scrapie-infected or normal brain homogenate and recordings were made from coronal brain slice preparations of the dLGN at approximately 28 day intervals from 60 days post-inoculation. The incubation period in this model was approximately 270 days; two experimental series of inoculated mice were studied. Basic membrane properties (resting membrane potential, action potential threshold, input resistance and time constant), properties of averaged action potential shapes, the integrity of the synaptic response evoked

by afferent optic tract stimulation and the membrane responses to current injection were studied in normal, control and scrapie-inoculated mice. In addition the morphology of cells in the control and scrapie-inoculated mice was monitored by iontophoresis of dye via the recording electrode.

The study of normal mice demonstrated that relay neurones in the dLGN exhibited membrane response properties and responses to optic tract stimulation typical of those in the rat and guinea-pig. The basic membrane and action potential properties quantified were also similar to published studies. In terms of both their basic membrane and action potential properties murine dLGN relay cells constituted a homogeneous population. Both a fast and slow after-hyperpolarisation (AHP) followed the action potentials in murine dLGN relay cells; the slow AHP was apamin-sensitive indicating that it was mediated by the calcium-activated potassium current, $I_{AHP}$. This current appeared to have a role in regulating the rate of action potential discharge. This study demonstrated that murine dLGN relay cells function as a homogenous population and possess similar properties to rat and guinea-pig dLGN relay cells. This is the first report of the current $I_{AHP}$ in dLGN relay cells.

In the investigation of scrapie-inoculated mice intracellular recordings in the dLGN were obtained until day 230 in the first, and day 200 in the second series of animals studied. This study demonstrated that relay cells with normal membrane, action potential and optic tract evoked synaptic properties were recorded in the scrapie-infected dLGN throughout, and even at advanced stages of the incubation period; neurones with dysfunctional properties were not recorded in the dLGN. A similar range of membrane responses to current injection and optic tract stimulation were evident in cells in both control and scrapie-inoculated mice which were indistinguishable from the recordings in normal mice. Plots of the relationships between the basic membrane and the action potential properties in normal, control and scrapie-inoculated mice indicated that the experimental groups collectively behaved as a single population. Thus in contrast to the expectation of a progressive degeneration in the function of cells in the scrapie-infected dLGN, relay neurones with normal intrinsic and optic tract evoked synaptic properties were evident even in the presence of marked pathological changes and a profound neuronal loss. The possibility that the cells recorded in this study were pre-infected or infected without compromised function, is discussed.

# Chapter 1

# Introduction to scrapie

## 1.1 Scrapie: A historical perspective

The spongiform encephalopathies are neurodegenerative diseases in which clinical signs are not apparent until just prior to death. The encephalopathies include Creutzfeld-Jacob disease, Gerstmann-Straussler-Scheinker disease and Kuru in humans; scrapie in sheep, mink encephalopathy, bovine spongiform encephalopathy and chronic wasting disease in deer and elks. Experimentally, these diseases can be transmitted to a variety of species; whilst the infectious agent appears to be unconventional its exact nature is unknown. The histological features of this group of diseases have often been referred to as a triad of vacuolation of the neuropil, gliosis and neuronal loss in the brain although few studies have actually quantified the extent of neuronal degeneration. The term "status spongiosis" was introduced by Spielmeyer in 1922 to describe the gross vacuolation seen histologically in the brains of patients with Creutzfeldt-Jacob disease.

In 1957, following their expeditions to the Highlands of Papua New Guinea, Gajdusek and Zigas described a new neurodegenerative disease illness known to the natives as "Kuru"; it was Carleton Gajdusek's investigation of Kuru which led to him being awarded the Nobel Prize for Medicine. Kuru (which means to shake or shiver) is a fatal disease unique to the Fore tribe and their ancestry and during the 1950's the incidence of this disease reached endemic proportions. Kuru predominantly affected the women and children, but oddly not those marrying into the tribe or coming into close contact with the disease. In fact, natural transmission was found to be related to the mourning ritual of the Fore people which, in a (slightly unusual) quest for their knowledge, consisted of the cannibalistic consumption of the tissues and brains of their deceased relatives. The woman and children were engaged in the food preparation and, more so than the men, consumed the less well-cooked offal including the brain, thus accounting for their apparent increased susceptibility to the disease.

The similarities between Kuru and scrapie, particularly on histopathological grounds, were first noted by Hadlow in 1959 and soon Kuru was linked to Creutzfeldt-Jacob disease, the infectious nature of which was confirmed by transmission to chimpanzees in the late 1960's (e.g. Gajdusek et al., 1966). Scrapie itself has been recognized in Europe since 1732 (see M'Gowan, 1914), and its significance in Britain can be gauged from the fact that it was included together with tuberculosis and Zinc poisoning in the first Government grant for research at the London Royal Veterinary college in 1910.

Interest in scrapie somewhat intensified in 1986 following the outbreak of bovine spongiform encephalopathy (BSE). Epidemiological studies linked the source of BSE to the meat-and-bone meal incorporated into cattle feed supplements (Wilesmith et al., 1991). Sheep offal has, for many years, been a major source of protein-supplements in animal foodstuffs. During the late 1970's offal rendering plants altered their processes of tallow extraction, restricting their use of both heat treatment and solvent extraction to purify the material. This altered processing is though to have permitted the invasion of high scrapie infectivity levels into cattle through their ingestion of contaminated feed; it is thought that is the major factor responsible for the clinical presentation of BSE.

Since the first documented case of scrapie, in 1732, there is in fact no evidence that the consumption of scrapie offal by man has been perceived as a health threat. This is exemplified by the recipes for both haggis and sheep brain broth in both the 1962 and 1978 editions of *The Glasgow Cookbook* (see Appendix). Whilst, for traditional reasons, it is difficult to envisage a dent in the enthusiasm for haggis, in the light of the BSE epidemic, it remains to be seen if sheep brain broth is included in the 1996 edition of this cookbook.

Despite the wayward suggestion by Roche-Lubin, (1848) that scrapie was caused by "sexual excess and lightning", to date the exact nature of the agent causing scrapie, or indeed that of any of the spongiform encephalopathies, is unknown. This has been a subject of heated debate for many years. The agent was at first thought to be a virus and Sigurdsson, (1954) termed these diseases "slow viruses" of the central nervous system. However this idea was challenged by the failure to isolate a virus (or any immunological response to it) and the large body of evidence suggesting that the properties of the agent were both highly unconventional, and inconsistent with those of any known viral agent. On the basis of the association of a protein with infectivity the term "prion" was introduced by Prusiner, (1982) to distinguish the pathogen from viruses or viroids. In the absence of a characterised agent, there is not a generic term for scrapie which, over the years, has been termed "the goggles" in England, "la tremblante" (the tremble) in France and in Germany "gnubberkrankheit" (the itching disease). However a Scottish term has been universally adopted, "scrapie" aptly describing the tendency of infected sheep to rub their flanks bare against objects such as fencing, walls and barbed wire.

In France in 1936, Cuillé and Chelle laid claim to the first experimental transmission of scrapie, by the intraocular inoculation of healthy goats with spinal cord material from an infected sheep. However the early investigations of scrapie were hindered

by the length of the incubation period with workers having to wait, in some cases, as long as 4 years for the appearance of clinical signs and therefore the necessary evidence of successful transmission. It was therefore a significant step forward when, in 1961, Chandler successfully transmitted scrapie to the laboratory mouse; the uniform susceptibility and incubation period displayed in this species made it possible for the first time to perform accurate quantitative experiments on the disease process.

Approximately 18 different strain of scrapie have been transmitted to mice, each characterised by the severity and distribution of pathological lesions in the brain, and the length of the incubation period. Scrapie infection can be initiated by a number of routes e.g. intraperitoneal, intracerebral or intraocular. Following intraocular infection, scrapie pathology is targeted to the central visual pathways including the dorsal lateral geniculate nucleus (dLGN) in the thalamus (Fraser, 1982; Scott et al., 1992; Jeffrey et al., 1995) (see fig. 1). The ME7 strain was originally derived from natural scrapie in Suffolk sheep; in recent years a considerable amount of information has been collated concerning the pathology and infectivity targeted to the murine dLGN following intraocular injection of this strain. The pattern of pathological lesions in the dLGN are highly repeatable and the incubation period length, whilst strictly repeatable for a given mouse genotype, ranges from 240 and 300 days depending on the genotype of mouse used.

The physiology of the thalamic nuclei, including the dLGN, have been extensively investigated in coronal brain slice preparations in the rat and guinea-pig. The specific targeting of scrapie pathology and neuronal loss to the dLGN, makes this a model of choice for the study of the pathophysiological effects of scrapie. In reviewing scrapie pathology, this introduction will focus largely on what has been learned of the pathological effects of scrapie in the ME7-infected dLGN.

### 1.2 PrP and the nature of the scrapie agent

There are presently two major theories as to the nature of scrapie agent; that it is (i) a "virino", a viral nucleic acid enveloped by an unusually robust protein coat (Kimberlin, 1982) or (ii) a "prion", a novel infectious protein (Griffith, 1967; Prusiner, 1982). Progenitors of the virino hypothesis hold that in order to explain the diverse pathology of the different scrapie strains, an independent information molecule such as a nucleic acid must be associated with the infectious agent; according to this theory each strain would

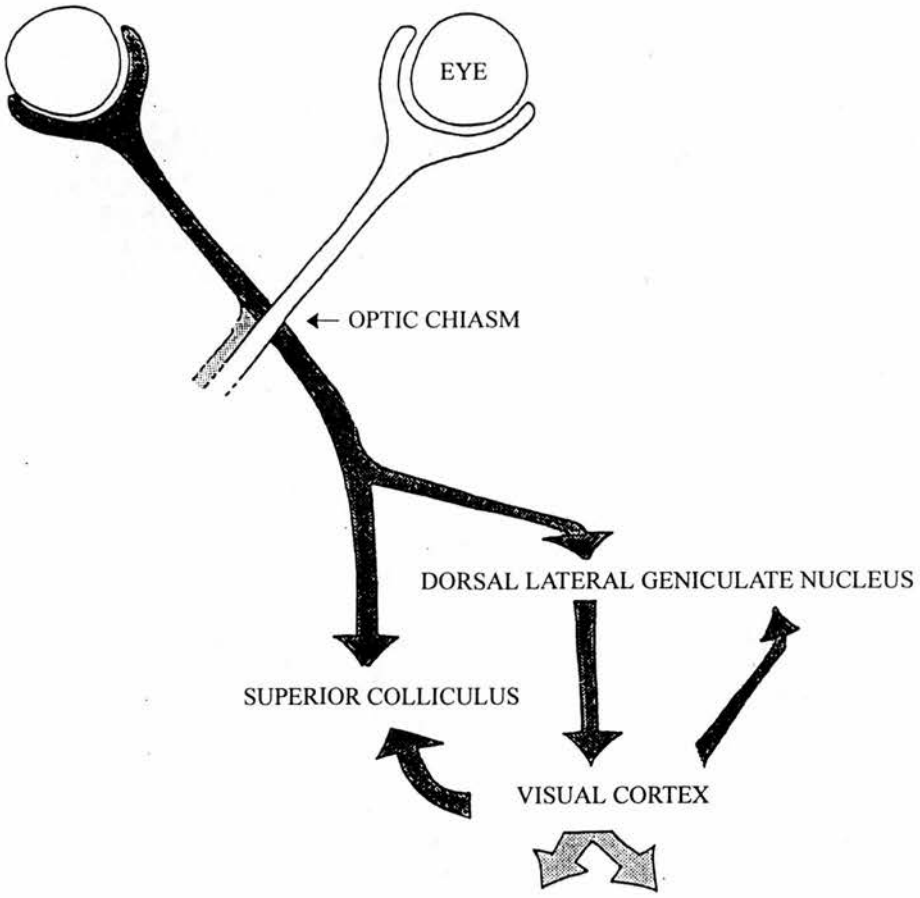


**Fig. 1.** Schematic diagram of the main pathways in the rodent visual system (adapted from Sefton and Dreher, 1985). In rodents there is almost complete decussation at the optic chiasm.

genetically encode the synthesis of a different form of the agent, presumably conferring upon the agent its ability to selectively target neuronal populations (see Bruce et al., 1994). Scrapie infectivity is resistant to treatments that degrade and denature nucleic acids (e.g. ionising radiation: Alper et al., 1967; DNases and RNases: Prusiner, 1982; Bellinger-Kawahar et al., 1987) and whilst a population of short and variable length nucleic acids have been isolated from infectious brain fractions, a class of scrapie-specific nucleic acids has not yet been detected (Meyer et al., 1991).

Prion protein, $PrP^{C}$ is a normal cell surface glycoprotein of molecular mass 33-35 kD which is attached to the cell membranes by a glycoinositol-phospholipid (GPI) anchor (Caughey et al., 1990). $PrP^{C}$ is found in the cells of a number of tissues in the body, but is present in its highest concentrations in the brain (Kretzchmar et al., 1986). In scrapie infected brains an additional, conformationally altered form of $PrP^{C}$ ($PrP^{SC}$) is found (Pan et al., 1993). $PrP^{SC}$ can be separated from $PrP^{C}$ on the basis of its resistance to proteolysis, yielding a protease-resistant core of 27 - 30 Kd; to date this protein is the only characterised molecule found in purified fractions of scrapie-infected brain (McKinley et al., 1983). Denaturation or other modifications such as proteolysis reduce scrapie infectivity titres detected by bioassay (Prusiner et al., 1980; Prusiner, 1982), therefore collectively this evidence indicates that a protein is essential for disease propagation.. These findings forms the basis of the protein-only or "prion" hypothesis (Prusiner, 1982).

Despite differing in their physical properties, $PrP^{SC}$ and $PrP^{C}$ possess an identical amino-acid sequence (Basler et al., 1986). $PrP^{SC}$ can be isolated biochemically, on the basis of its protease resistance, and employing this method cell culture studies have shown that $PrP^{SC}$ is formed at a slower rate than $PrP^{C}$ (Borschelt et al., 1990; Caughey et al., 1992). PrP mRNA is not upregulated in scrapie infected brains (Oesch et al., 1985) and $PrP^{C}$ levels remain constant throughout the incubation period despite the presence of $PrP^{SC}$ in amounts twenty times that of $PrP^{C}$ (Meyer et al., 1986). Collectively these findings suggests a post-translational modification is responsible for the production of $PrP^{SC}$ and that, given the excess $PrP^{SC}$ quantities, there may be a breakdown in the endocytic processes normally responsible for the degradation of $PrP^{C}$ (Caughey et al., 1992).

The "prion" hypothesis proposes that a given molecule of $PrP^{SC}$ invades the host, and interacts with and converts $PrP^{C}$ to another $PrP^{SC}$ molecule; this then becomes a self-propagating and multiplicative process. The PrP gene has two N-terminal glycosylation sites and it has been calculated that potentially 401 different PrP isoforms may exist when both

asparginine residues are glycosylated (Endo et al., 1989). It is therefore possible to speculate that PrP glycoform diversity may account for the variance of scrapie strains i.e. an infectious $PrP^{SC}$ glycoform will target and convert a $PrP^{C}$ of similar glycosylation, with potentially each neuronal population housing different (population of) $PrP^{C}$ glycoform(s).

$PrP^{C}$ is highly conserved amongst species, however the functional role of this protein is unknown. Transgenic 'PrP-null' mice have been developed in which the PrP gene is ablated (Bueler et al., 1992). These animals develop normally, do not show impaired learning ability, live for a normal lifespan and are not susceptible to scrapie (Bueler, et al., 1992; Prusiner et al., 1993). These findings demonstrate that $PrP^{C}$ is essentially involved in the pathogenesis of scrapie infection. However in the light of the apparent phenotypic normality of the PrP-null mice, these observations questioned the existence of a physiological role for the normal cell surface protein.

Hippocampal CA1 pyramidal cell function has been monitored in PrP-null mice in which impaired $GABA_A$-mediated synaptic inhibition and a loss of the a slow calcium-activated potassium conductance (mediating the slow phase of spike after-hyperpolarisation) has been reported in these cells (Collinge et al., 1994; Colling et al., 1995). The results of these studies suggest that a loss of function of the normal cellular protein, $PrP^{C}$, may contribute to scrapie-associated neurological dysfunction, as opposed to this being purely due to the accumulation of $PrP^{SC}$. However investigations of the PrP content of scrapie infected and control hamster brains indicate that there is no difference in the quantity of $PrP^{C}$ extracted from the two groups (Meyer et al., 1991). $PrP^{C}$ is present in cells in other non-neural tissues where its functional role is not known (Bendheim et al., 1992). This introduces the possibility that the physiological consequences of $PrP^{C}$ removal (or possibly conversion during infection) may differ between cell types.

One criticism of the "protein only" model is that the necessary variety of isoforms of $PrP^{C}$ required to explain strain diversity of neuronal targeting (Bruce et al., 1994), have not yet been proven to exist. Amphoteracin-B prolongs the scrapie incubation period without altering the dynamics of $PrP^{SC}$ accumulation suggesting that scrapie infectivity and the production of $PrP^{SC}$ are not inextricably linked (Xi et al., 1992). The existence of an "infectious protein" lacking a nuclear information molecule is clearly a new concept in biological terms. However Kocisko et al, (1994) recently demonstrated the cell-free conversion of $PrP^{C}$ by, and into $PrP^{SC}$. Therefore, on balance, the experimental evidence reported to date suggests that $PrP^{SC}$ is a likely candidate for the infectious scrapie agent.

## 1.3 Neuropathology in rodent scrapie

### *1.3.1 Infectivity*

The precise nature of the scrapie agent is unknown therefore infectivity is detected by bioassay. This involves the inoculation of dilutions of homogenized infected brain into a group of animals and comparing the length of the incubation period with a dose response curve for that strain.

Following the intraocular inoculation of mice with ME7 scrapie infectivity is first detected by bioassay in the dLGN after 77 days in the 240 day incubation period model; thereafter, infectivity titres rise rapidly between 100 and 140 days after which time the accumulation slows towards the end of the incubation period (Scott et al., 1992). In the same model, infectivity in retinal ganglion cell axons is detected at the later stage of 100 days and although these levels increase during the incubation period, the maximum titres attained are approximately 10 % of those in the dLGN; that detectable infectivity is not found until after high levels are found in the dLGN introduced the possibility that there is retrograde transfer from the relay to retinal ganglion cells (Scott et al., 1992). Infectivity levels in the visual cortex are first detected at 100 days, and by 160 and 180 day reach, and thereafter maintain, a level similar to in the dLGN.

Enucleation experiments, commencing at day one post-inoculation, have demonstrated that a minimum of 14 days is required for vacuolar lesions to become established in the central visual pathways; in fact in animals enucleated after 28 days, similar numbers as in the unenucleated group developed signs of infective pathology in central visual areas (Scott, J. et al., 1989). This progression of infectivity, at a rate of 1 - 2 mm a day, is consistent with an anterograde spread of the agent through the visual pathways by slow axonal transport (see Grafstein and Forman, 1980). This is slower than the rate of spread of conventional viruses by the intraocular route e.g. herpes simplex virus II which accesses the dLGN 3 days following inoculation (Kristensson et al., 1974). Although the enucleation experiment clearly demonstrates that infectivity has accessed central visual areas by approximately a month after injection, as mentioned above, sufficient levels to be detected by bioassay are not found until 77 days post-inoculation (Scott et al., 1992).

It is therefore most probably that infectivity accesses the dLGN by crossing the synapses between the retinal ganglion and relay and/ or interneuronal cells. The cellular and molecular mechanisms involved in the uptake and transport of infectivity are unknown.

*1.3.2 Incubation period*

The scrapie incubation period is the length of time from inoculation to the time point at which mice are sacrificed at a standard clinical endpoint (Dickinson et al., 1968). The length of the incubation period varies between strains, but for a given host phenotype and scrapie strain this time interval is highly repeatable. Generally speaking the infection of a group of mice with scrapie results in a standard error of less than 3 % of the mean incubation period. In mice, the *Sinc* gene influences the length of the incubation period by controlling the initiation of replication (Scott et al., 1991); the *s* allele corresponds to the *short* incubation in mice homozygous for this genotype and the *p* allele represents the observed incubation period *prolongation* in mice of this genotype. Each strain of scrapie has a reproducible length of incubation period in mice of the same *Sinc* genotype (Bruce et al., 1991). To date, in all mice strains studied, the two *Sinc* alleles are consistently associated with PrP molecules that differ by two amino acids indicating the close linkage and perhaps also the homology of the *Sinc* and PrP encoding (*Prn-p*) genes (Hunter et al., 1992).

*1.3.3 Vacuolation*

In murine scrapie a system of scoring specific areas in the brain for vacuolation is used to construct a "lesion profile" that is unique for a given scrapie strain and mouse genotype (Fraser and Dickinson, 1968). Fraser, (1982) first described the presence of vacuolation in the dLGN following intraocular infection. In the dLGN contralateral to the infected eye vacuolation is first seen by light microscopy at 150 days post-inoculation and increases in intensity throughout the 240 day incubation period (Jeffrey et al., 1995). The severity of vacuolation bilaterally in the dLGN throughout the incubation period is shown in fig 2.

The sub-cellular location of vacuoles in the superior colliculus, of the intraocularly ME7 infected brain, has been examined by electron microscopy (Jeffrey et al., 1991); the superior colliculus is the main afferent target of the retinal ganglion cell axons, collaterals of which innervate the dLGN (see 2.4 and fig.1). Vacuoles are commonly found within dendrites, and are more sparsely located in axons, axon terminals and neuronal somata. The

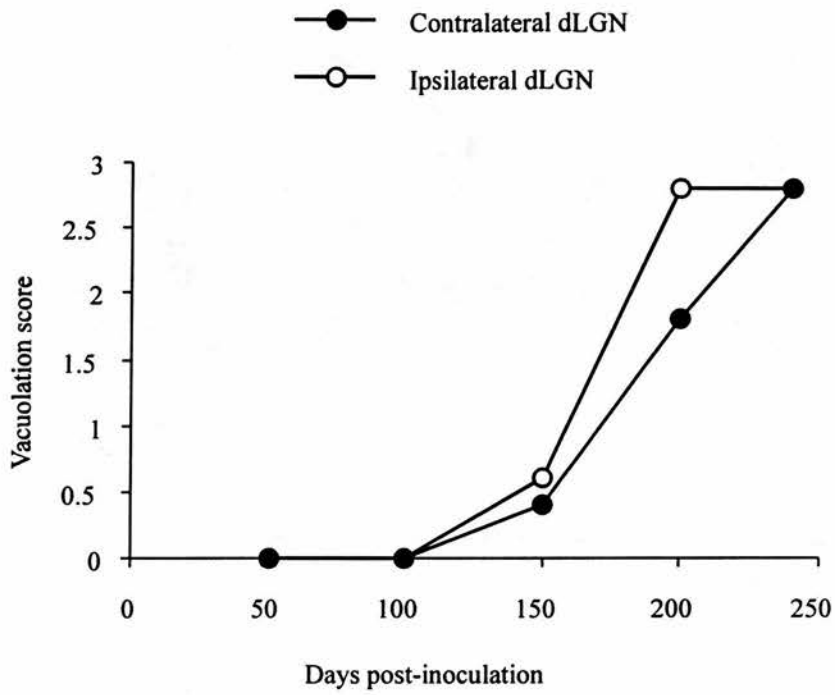


**Fig. 2.** Vacuolation scores in the murine dLGN contralateral (closed circles) and ipsilateral (open circles) to the eye inoculated with ME7 scrapie (adapted from Jeffrey et al., 1995). The incubation period in this model was 240 days.

cellular location of these vacuoles is therefore consistent with the neuronal distribution pattern in natural sheep scrapie (Bignami and Parry, 1972), other murine scrapie models (Lampert et al., 1971), Creutzfeldt-Jacob disease (Chou et al., 1980) and rodents experimentally infected with Creutzfeldt-Jacob disease (Sato et al., 1980). In these studies, single membrane or unbounded disease-specific vacuoles are discernible from non-specific vacuoles in uninfected tissues, by the presence of membrane and granular debris. To summarise the results of these studies, vacuoles may arise from a variety of sub-cellular organelles e.g. smooth endoplasmic reticulum and mitochondria, or may emanate from dendritic processes due to dissolution of the cytoskeleton.

Following intraocular ME7 infection the onset of vacuolation in the dLGN, at 150 days post-inoculation, is coincident with the first signs of neuronal loss. In mice at 150 days post-inoculation, there is a significant negative correlation between the vacuolation scores and surviving cell numbers in the dLGN; vacuolation scores in the dLGN increase with progression of the incubation period (Jeffrey et al., 1995).

*1.3.4. PrP deposition*

To date, antibodies are not available that can distinguish between cellular ($PrP^{C}$) and scrapie-associated ($PrP^{SC}$) prion protein. In published studies, immunolabelled deposits of "$PrP^{SC}$" refer to disease-specific PrP accumulations i.e. those deposits observed in infected tissue that are visibly distinct from the background levels in untreated, normal brain-inoculated or sham-inoculated mice. A similar terminology that will be adopted in this thesis.

In the uninfected brain, $PrP^{C}$ staining is observed predominantly within neuronal perikarya and only occasionally surrounding the dendritic processes of neurones (DeArmond et al., 1987; Bruce et al., 1994). The relative density of $PrP^{SC}$ deposition in brain areas at the terminal (clinical) stage of differs between scrapie strains; however within targeted areas, characteristic profiles of staining are seen (Bruce et al., 1989): Under light microscopy, scrapie-specific accumulations are seen as diffuse or punctate deposits in the neuropil; these often concentrate in areas of severe vacuolation and gliosis (DeArmond et al., 1987); in some scrapie strains especially dense and focal areas of $PrP^{SC}$ accumulation, termed "plaques", intermingle with the diffuse staining. These plaques are groups of radiating "amyloid fibrils" (aggregated chains $PrP^{SC}$ molecules: Merz et al., 1981). Dense

staining is often seen surrounding the cell bodies and dendritic process of neurones (perineuronal staining) and this is a common feature of ME7 scrapie (Bruce et al., 1994).

$PrP^{SC}$ is first detected as diffuse deposits in the contralateral dLGN 150 days after inoculation with ME7 scrapie; modest staining at this stage is also evident in the ipsilateral nucleus (Jeffrey et al., 1995). At the terminal stage of disease diffuse $PrP^{SC}$ labeling is apparent throughout the brain but this is especially dense in the dLGN where focal plaques are evident.

Early subcellular fractionation studies performed on cultured cells derived from mouse brain tissue (Clarke and Millson, 1976) demonstrated that scrapie infectivity, detected by bioassay, was associated with the plasma membrane. In context of the proposed link between PrP and infectivity, there have not been any ultrastructural studies of neurones in ME7 scrapie-infected mice that have addressed the subcellular location, or production site of scrapie associated PrP in this strain. However in 87V scrapie ultrastructural findings suggest that $PrP^{SC}$ is released from the plasma membrane into the extracellular space before diffusing around different processes in the neuropil; the majority of scrapie-specific PrP labeling was found in the vicinity of the plasma membrane of dendrites, with only occasional labeling of the lysosomes and perikarya (Jeffrey et al., 1994). The sites associated with the initial release and accumulation of $PrP^{SC}$ appear morphologically normal; at diffusion sites where $PrP^{SC}$ appeared to have accumulated over a period of time, single amyloid fibrils are apparently coincident with the first signs of invasion by microglial processes.

*1.3.5 Neuronal loss*

Neuronal loss has often been quoted as a prominent pathological feature of spongiform encephalopathies but few studies have actually quantified the extent of neuronal degeneration. The surviving neuronal numbers in the dLGN following intraocular infection with ME7 scrapie have been quantified throughout the 240 day incubation period in this model (Jeffrey et al., 1995). The neuronal loss in the contralateral and ipsilateral dLGN at 150 days is not significant however in mice at this stage there is a negative correlation between the surviving neuronal number and vacuolation score (also 1.3.3). By 200 days a significant neuronal loss is evident bilaterally in comparison to normal brain-inoculated mice, and there is a significant difference in neuronal numbers between the ipsilateral and contralateral dLGN. At the terminal stage of disease there was a reduction from

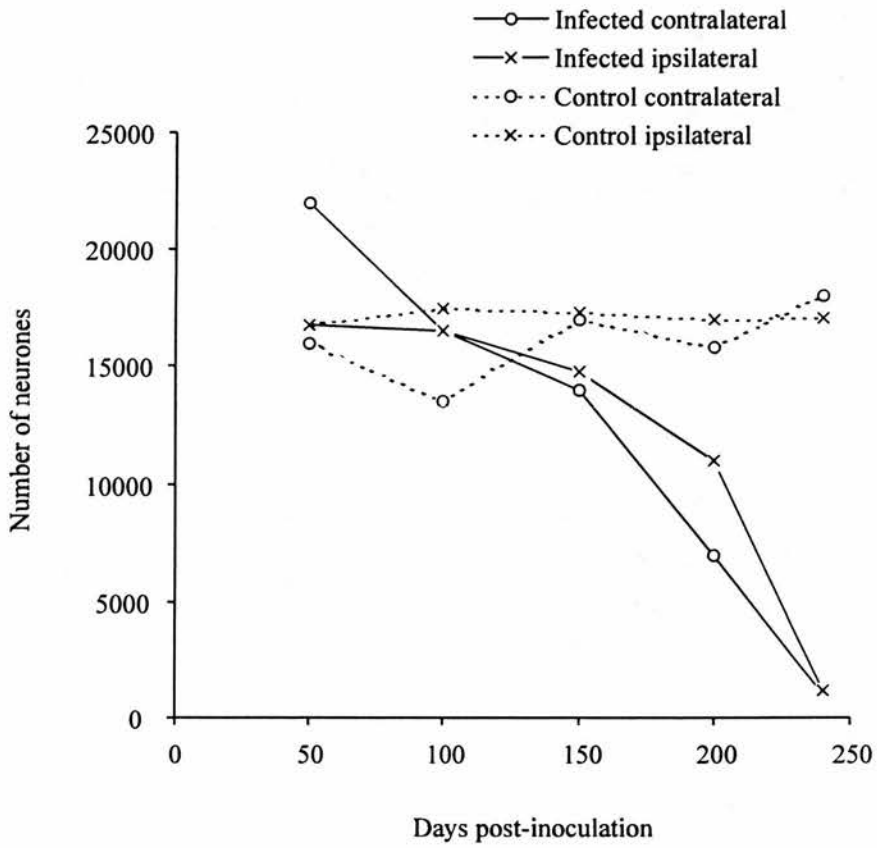


**Fig. 3.** The mean surviving neuronal number counted in the dLGN both ipsilateral and contralateral to the inoculated eye in normal brain-inoculated (control) and scrapie-infected mice (adapted from Jeffrey et al., 1995). The incubation period in the scrapie-infected mice was 240 days.

approximately 22,000 to 1000 cells in the contralateral dLGN. The temporal profile of neuronal loss in the dLGN of this model, throughout the 240 day incubation period is illustrated in fig. 3.

Quantitative analysis of the GABAergic nuclei in the rat dLGN has shown that approximately one quarter of dLGN cells are interneurones (Gabbott et al., 1986). Fig. 3 demonstrates that by the experimental end stage of disease there is almost entire cell loss in the murine dLGN; assuming a similar ratio of interneurones to relay cells in the dLGN, both populations of cells must degenerate. The order (if any) in which interneurones and relay cells are lost is not known. Neuronal loss appears to be selective in different strains of scrapie: photoreceptor cells are lost following intraocular inoculation of 139A but this population is not diminished following inoculation of ME7. In addition, although dLGN cells degenerate with intraocular ME7 scrapie, the retinal ganglion cell population, that mediate the transfer of infectivity to the dLGN, do not appear to decline in number (Scott et al., 1992).

*1.3.6 Synaptic vesicle loss in the scrapie-infected dLGN*

Synaptophysin is a glycoprotein which is common to most if not all synaptic vesicle membranes (Sudhof and Jahn, 1991). The intensity of synaptophysin immmunostaining has become an established method of indirectly assessing synaptic density in the post-mortem brain. This approach is considered an effective alternative to the (time consuming) method of counting individual synapses at the ultrastructural level (Masliah and Terry, 1993).

Clinton et al., (1993) studied the synaptophysin content of cortical, midbrain and cerebellar regions in cases of the human spongiform encephalopathies: Creutzfeld Jacob Disease (CJD) and Gerstmann Straussler Scheinker Syndrome (GSS); some of these patients had presented with atypical neurological symptoms. There was no obvious correlation between symptom prevalence and the extent of vacuolar and PrP pathology however, in each of the brains examined, a similar significant loss of synaptophysin labeling was evident. The authors hypothesised that a loss of synaptic connections may underlie the development of functional deficits and dementia in the human encephalopathies.

In the dLGN of mice intraocularly infected with ME7 scrapie there was a marked and uniform reduction in synaptophysin throughout the ipsilateral and contralateral dLGN in terminally ill scrapie-infected mice (Jeffrey et al., 1995). At approximately 200 days post infection, in the 240 day incubation period, there is a less obvious reduction in staining in

the contralateral dLGN. A this stage, the deficit in staining was more pronounced in the contralalateral and ipsilateral dLGN; a reduction in synaptophysin staining was not obvious prior to 200 days. The extent of labeling in the visual cortex did not appear altered at any stage in the incubation period. The results of this study in the dLGN clearly demonstrate that neuronal loss is well established before there is a detectable loss of synaptic vesicles; this may suggest that axonal terminal degeneration is secondary to neuronal loss and argue against dLGN cell degeneration due to de-afferentation (Jeffrey et al., 1995).

*1.3.7 Gliosis*

Although there is an absence of a classical, acute inflammatory response in scrapie there is both astrocytic hypertrophy and proliferation (astrocytosis). In both mouse and hamster scrapie models astrocytosis, whilst widespread, is particularly marked in areas exhibiting vacuolation and $PrP^{SC}$ accumulation (DeArmond et al., 1987; Williams et al., 1994). In a study of the scrapie-infected hippocampus the glial reaction appeared to increase in parallel with progressive neuronal loss (Scott and Fraser, 1984).

Wegiel and Wisniewski, (1990) reported a structural relationship between amyloid fibrils and microglia in Alzheimer's Disease, prompting the suggestion that the microglia may be responsible for the production of $PrP^{SC}$. Correlated light and ultrastructural studies have demonstrated that $PrP^{SC}$ labeled in the lysosomes of microglial cells is associated with the punctate distributions of $PrP^{SC}$, as opposed to the diffuse labeling seen in the neuropil (Bruce et al., 1989; Jeffrey et al., 1992). In murine 87V scrapie, $PrP^{SC}$ accumulation has been demonstrated in areas lacking morphologically identified microglial processes; the subsequent invasion of microglia in this model, suggests these cells are fulfilling their phagocytic role in an attempt to degrade the excess amount of abnormal PrP (Jeffrey et al., 1994).

In intraocular ME7 scrapie, immunolabelling for glial fibrillary acid protein (GFAP) identified a mild gliosis seen bilaterally in the dLGN at 150 days post-infection; at this stage gliosis was found only in those mice with the highest vacuolation scores, and the most severe neuronal loss (Jeffrey et al., 1995). In the same study a marked gliosis, evident as increased numbers of astrocytic and microglial nuclei in the dLGN, is apparent in mice at 200 days post-infection and in those culled at the clinical end point of disease.

This synchronous detection of glial proliferation in association with the onset of vacuolation, PrP deposition and neuronal loss, and after the invasion of infectivity suggests these pathological effects may be secondary to the accumulation of infectivity.

### 1.4 Neuronal morphology

Subjectively, dendritic spine loss of biocytin-labelled CA1 neurones is observed from approximately 180 days into the incubation period of mice intracerebrally infected with ME7 scrapie (Johnston et al., 1995 and A.R. Johnston, personal communication); large translucent swellings, thought to be vacuoles, are also present on the neuronal dendrites.

Disease-specific axonal and dendritic "varicosities" and dendritic spine loss are observed in Golgi-impregnated cortical cells of hamsters infected with Creutzfeldt-Jacob disease (Kim and Manueldis, 1987). In infected animals, irregularly shaped cortical cell perikaya were seen which possessed hole-like empty spaces; the apical dendrites of these cells were also unusually thinned. Spine loss on the dendritic processes of both motor and visual layer 3 Golgi-impregnated cortical neurones has been quantified in hamsters infected with the 263K scrapie strain (Hogan et al., 1987); a significant spine loss was evident on the apical shaft of these neurones and an average of 18 spherical bodies, measuring 7 to 25 μm in diameter, were found on 80 % of cells in scrapie infected animals. Less than 2 % of control cells exhibited these varicosities, which when present, numbered less than 3 per cell. Landis et al., (1981) observed morphological abnormalities in cortical neurones of post mortem brains of Creutzfeldt-Jacob disease patients. Abnormal features included a reduced diameter, a decrease in the number of spines per unit length and focal, spherical or ovoid swellings in the dendrites. Dendritic changes arose in distal before proximal portions of the dendritic arbor and alterations of primary dendritic segments and pyramidal apical shafts were apparent only when there were pathological changes on the more distal dendritic tree. Swellings in the neuronal processes were seen which dilated the dendrites by four to ten times their normal diameter. The ultrastructural examination of tissue from these patients showed that there were vacuolated axon terminals opposed to dendritic spines with normal morphology. The changes in dendritic profile that accompanied spine loss were more severe than observed following experimental denervation, suggesting that the dendrites were a primary pathological target of the disease (Landis et al., 1981).

The morphological studies of scrapie and Creutzfeld-Jacob Disease to date, suggest that morphological abnormalities are common to neurones during the terminal stages of encephalopathic disease.

### 1.5 Pathophysiological consequences of scrapie infection

The association of scrapie infectivity with membrane fractions prompted investigations into the integrity of membrane-localised neurotransmitter receptors in rodent scrapie models. These biochemical investigations do not include any studies of ME7 scrapie, however a brief description of findings in murine and the 263K hamster scrapie models are included in this section,. Altered 5HT receptor affinities have been detected in hamsters infected with 263K scrapie (Pocchiari et al., 1985a) and in the same model a reduction in the functional pool of the inhibitory neurotransmitter, gamma-aminobutyric acid (GABA) was detected in the brain (Pocchiari et al., 1985b). 22L murine scrapie targets vacuolar lesions to the granule cell layer in the cerebellum; in this region modest but specific reductions in adenosine receptor affinity and glutamic decarboxylase (GAD) activity are detected (Quinn et al., 1988). In 139A scrapie, choline acetyl transferase (ChAT) and GAD levels remain unaltered however the enzyme responsible for degrading acetylcholine, acetylcholine-esterase (AChE), is reduced by 20 % in the infected mice (Iqbal et al., 1985).

It appears that scrapie can specifically target enzymes and transmitters involved in synaptic transmission. However in the absence of correlated electrophysiological and biochemical studies on these animals it is not possible to assess functional impact of these changes, and if they are primary of secondary to the disease process.

Electroencephalography (EEG) studies in scrapie-infected rats have detected network dysfunction prior to the onset of clinical illness (Bassant, et al., 1984; Bassant et al., 1987). In terms of the lengthy history of research into scrapie it is, however, only recently that intracellular and extracellular recording techniques have been employed to monitor the response properties of neurones in the rodent scrapie models. When this study began, in 1992, there had been no published reports of the electrophysiological properties of single neurones recorded in scrapie-infected rodents or any other models of the spongiform encephalopathies.

Jefferys et al., (1994) reported details of the membrane, action potential and synaptic properties of hippocampal CA1 and cortical neurones in brain slice preparations from transgenic, scrapie-infected mice. These mice express (multiple copies of) the hamster PrP gene and are susceptible to intracerebral inoculation of the 263K strain of hamster scrapie; the pathological lesions in the brains of these mice are characteristic of hamster scrapie and this includes intense grey matter vacuolation and plaque deposition in the hippocampal and cortical areas (Scott, M et al., 1989; Prusiner et al., 1990). The incubation period in this model is approximately 60 days. In this study the electrical stimulation of the afferent pathways was employed to monitor the synaptic input to cortical and CA1 neurones, respectively. In both brain areas, abnormal extracellular field potentials were onset between 30 and 40 days in the incubation period. Epileptiform activity in both these areas was evident as "all or none" large depolarisations in the cortical cells and multiple population spikes in the hippocampal CA1 neurones. Intracellularly recorded synaptic responses, recorded in both hippocampal and cortical cells, displayed prolonged excitatory post-synaptic potentials (EPSP's) supporting an increased number of action potentials; these observations were attendant with a subjective loss of inhibitory post-synaptic potentials (IPSP's) in the CA1 and layer 4/ 5 cortical cells tested, and a possible loss of these potentials in the layer 2 cortical cells. The resting membrane potentials and input resistances of these cells appeared normal throughout the approximately 60 day incubation period in this model. Abnormal, calcium-mediated shoulders were observed on the action potential repolarisation phase in 30 % of hippocampal and cortical cells during the last few days (the clinical stage) of the disease incubation period. In this study it was suggested there may be a link between this observation and the abnormalities in calcium observed in scrapie-infected cultured cell lines (Kristensson et al., 1993).

The functional integrity of hippocampal CA1 neurones has also been monitored in brain slice preparations in mice intracerebrally inoculated with the ME7 scrapie, in which the incubation period is approximately 220 days (Johnston et al., 1994). By this route ME7 targets scrapie pathology to the hippocampus (J.Fraser, personal communication). The membrane response properties of the CA1 cells were unaltered even at terminal stages of the incubation period however increasing numbers of cells exhibited spontaneous activity; 70% of cells were spontaneously active by the terminal stage of disease. From 180 days there was up to a five-fold increase in the threshold stimulus required to evoke the maximum field potential in scrapie-infected mice, the maximum amplitude of which

progressively diminished such that it was abolished by the terminal stage of disease. Intracellularly, the EPSP and both fast and slow IPSP's recorded in CA1 neurones gradually declined in amplitude from approximately 180 days in the incubation period. The onset of electrophysiological abnormalities in this model was coincident with a subjective loss of spines and the occurrence of translucent swellings in the dendrites in hippocampal cells.

Clearly there is evidence for both intrinsic and network dysfunction in the cortex and hippocampus of mice infected with scrapie. Although $PrP^{SC}$ accumulation is a feature in these brain areas investigated in the above studies, there are no published reports of the temporal pattern of neuronal or synaptic vesicle loss, parameters which have been investigated in the intraocular ME7 model (see 1.3.5 and 1.3.6).

# Chapter 2

## Introduction to relay cells in the rodent dorsal lateral geniculate nucleus

## 2.1 The visual system

The dorsal lateral geniculate nucleus (dLGN) is involved in the central processing of visual information where it functions as both a gateway and an integration site regulating the flow of visual signals to the cortex (see Martin, 1988; Sherman and Koch, 1990; Steriade et al., 1990b). Light entering the eye is transduced to neural activity by the photoreceptor cells of the retina and this activity is relayed by axons of the retinal ganglion cells to the dLGN in the thalamus. The dLGN contains both intrinsic interneurones and relay cells; the relay cells transfer, via their axonal projections, the neural activity coding for vision to a specific area of the cortex, the visual or "striate" cortex (see Sherman and Koch, 1990). In addition to receiving a retinal input, the projection cells in the dLGN are reciprocally innervated by neurones in the thalamic reticular nucleus and the visual cortex; relay cells also receive innervation from brainstem, hypothalamic and forebrain nuclei (see Steriade and McCarley, 1990). In terms of the relative size of the inputs, the retinal ganglion cells account for approximately 15 %, the interneurones 20 %, reticular nucleus 20 %, the cortex 40 % and the remaining inputs 5 % of the synapses converging on dLGN relay cells (see Sherman and Koch, 1986). Fig. 4 is a simplified representation of the major connections of dorsal lateral geniculate nucleus in the visual pathway of rat (adapted from Ohara et al., 1983).

Whilst the mammalian visual system has been extensively investigated in the cat, the pathways in the rat are also well documented. Fewer studies have concentrated on the murine visual system, but there is no evidence to suggest that the connectivity markedly differs between the mouse and rat. A considerable amount of information concerning the functional properties of relay neurones has been gained from recordings in single cells in guinea-pig and rat brain slices; published reports of murine relay cells are limited to a description of whole cell recordings in Warren et al., (1994). Relay cells in both guinea-pig and rat possess similar intrinsic properties, and collectively function as a homogeneous population.

During this project the functional properties of dLGN relay cells in normal and scrapie-infected mice were monitored. In view of the apparent similarity between these species, the visual anatomy presented in this introduction will concentrate on the rat, and details of the murine visual system will be included where possible; the morphology of the dLGN cell types, the regional organisation of the nucleus and the topographic localisation of

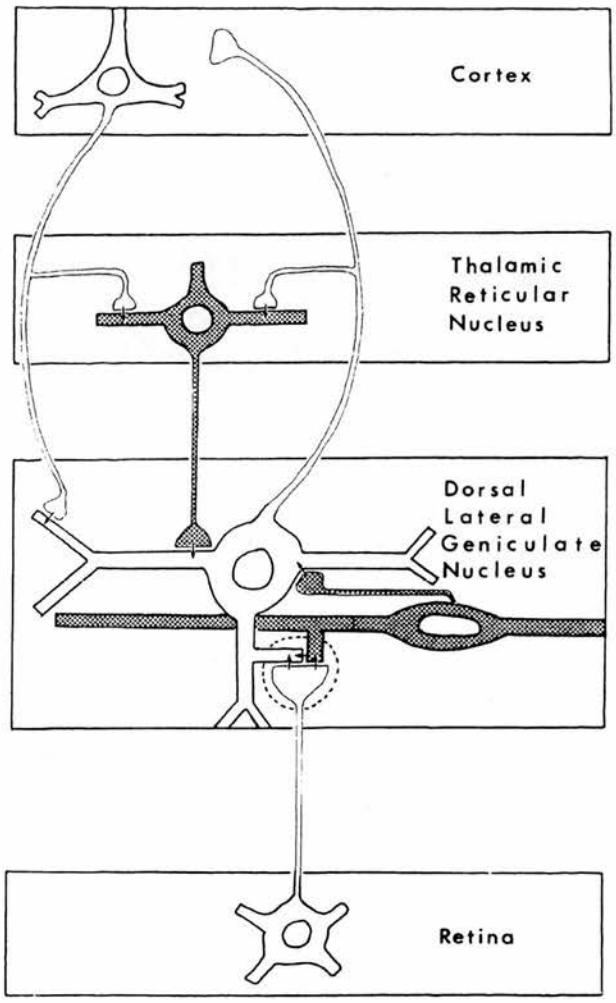


**Fig. 4.** Schematic diagram of the intrinsic and extrinsic connectivity of the dLGN in the rat visual system (adapted from Ohara et al., 1983). The source of the inputs from the brainstem, hypothalamic and forebrain nuclei, which account for 5 % of synaptic contacts on relay cells, are not shown. The inhibitory neurones of the thalamic reticular nucleus and the interneurones in the dLGN are shaded in grey.

the synaptic contacts on relay cells will be described. Due to the functional homology between rat and guinea-pig relay cells, and the lack of information on the electrophysiological properties in the mouse, the description of the membrane properties of relay cells *in vitro*, will concentrate on these species; the functional organisation of the convergent neurotransmitter systems, and the ionic currents underlying the membrane response properties of relay cells, will be reviewed.

## 2.2 Morphology of cells in the dLGN

In sections of Golgi-impregnated mouse and rat brain, two morphological dLGN cell types have been identified. The cells with axons that project to the cortex are defined as relay neurones and the cells with processes that generally do not project beyond the confines of the nucleus are termed intrinsic interneurones [rat: Grossman et al., (1973); Parnavelas et al., (1977); mouse: Rafols and Valverde, (1973); Iwahori and Mizuno, (1984)]. The typical morphology of a relay cell and interneurone in the murine dLGN are shown in fig. 5. This figure is adapted from Iwahori and Mizuno, (1984).

Similar to the rat, relay cells in the mouse possess a "brush-like" dendritic arbor and a thick unbranched axon (Rafols and Valverde, 1973); the oval somata are 15 - 25 μm at their longest diameter and between 5 and 10 primary dendrites (1.5 - 2 μm in diameter) radiate from the cell body. Three to five secondary branches radiate in all planes from each primary dendrite, conferring on these cells a "tufted" appearance. Protrusions or swellings, varying in size, are seen on the largest diameter dendrites and often at the points of primary dendritic branching. Ultrastructural examination of Golgi preparations is necessary to reveal the irregularly spaced, short and blunt spines on the dendrites. Spines are also observed protruding from the dendritic swellings. Relay cells axons originate from the cell body or a major dendrite. The axon follows a "twisting and meandering course" within the dendritic arbor before projecting medially to join the optic (superior thalamic) radiation. In a separate Golgi study in the mouse, Iwahori and Mazuno, (1984) reported similar morphological findings for dLGN relay cells.

Crunelli et al., (1987a) intracellularly labeled presumed relay cells with horseradish peroxidase (HRP) in brain slice preparations from the rat but the iontophoretic labeling of murine relay cells has not been reported. The morphology of the cells labeled by HRP was consistent with the published reports of Golgi-impregnated relay cells in this species

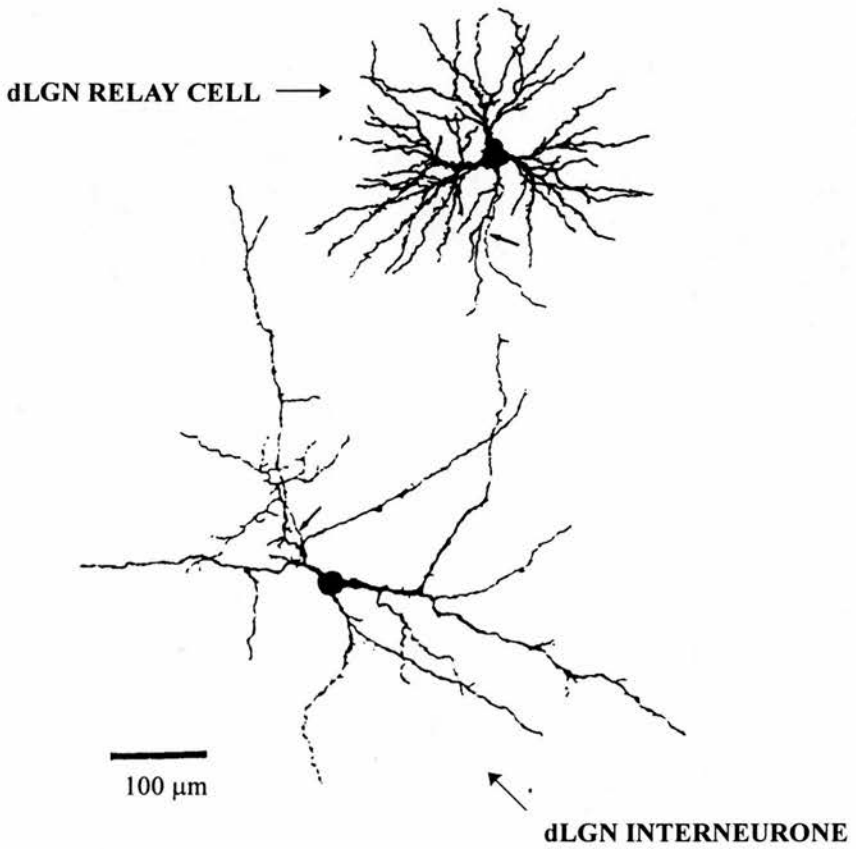


**Fig. 5.** Typical relay cell and intrinsic interneurone morphology in the murine dLGN (adapted from Iwahori and Mazuno, 1984). From these examples of Golgi-impregnated cells, it is clear that interneurones and relay cells possess a distinct morphology.

suggesting that the somatic and dendritic profile of relay cells can be accurately monitored by dye injection through the recording electrode.

The Golgi studies are also consistent in their findings of a distinct interneurone morphology. The cell bodies of interneurones are spindle-like, and generally smaller (10 - 20 μm) than those of relay cells (Rafols and Valverde, 1973). The 2 - 3 major dendrites emanating from the soma are restricted to secondary branch points, and the bipolar spread of the dendrites lends the interneurones an elongated appearance. A prominent feature of interneurones are the single, clustered or strings of spheroid bodies attached by fine processes to the dendritic surface. Iwahori and Mazuno, (1984) also reported few dendritic branch points and smaller elongated somas in dLGN interneurones.

In summary, the relay cells and interneurones in the murine dLGN possess a distinct morphology and are homologous in profile with the cells in rat Golgi studies (see Grossman et al., 1973; Parnavelas et al., 1977). The cell bodies of relay cells are larger and the extensive branching of the radiating dendrites confers on these cells a bushy appearance. Interneurones possess fewer dendrites and their restricted branch pattern results in a more elongated profile of these cells. There is no agreement as to a morphological sub-classification of relay cells in the rat or mouse in the dLGN therefore no detectable laminar distribution of these cells in the rodent nucleus.

### 2.3 Synaptic organisation in the dLGN

E.G. Gray in 1963 described two common types of central synaptic profile in central nervous tissue prepared using electron microscope (EM) fixatives:- Gray type 1 synapses are normally excitatory with spherical synaptic vesicles, a wide synaptic cleft and an obvious dendritic post-synaptic density; Gray type 2 are normally inhibitory with eliptical synaptic vesicles, a narrower synaptic cleft and no obvious post-synaptic density.

In a combined Golgi and electron microscope study, three types of axon terminal profiles have been identified making either Gray type 1 or 2 synaptic contacts with murine dLGN cells (Rafols and Valverde, 1973). The synaptic connectivity between retinal ganglion cells, interneurones and relay cells dendrites in the dLGN is summarised in fig. 6. The axon terminals of retinal ganglion cells make Gray type 1 synaptic contacts with dendrites of dLGN relay cells. Retinal terminals are interspersed between, or are directly opposed to individual spines. More commonly the retinal terminals make contact with the

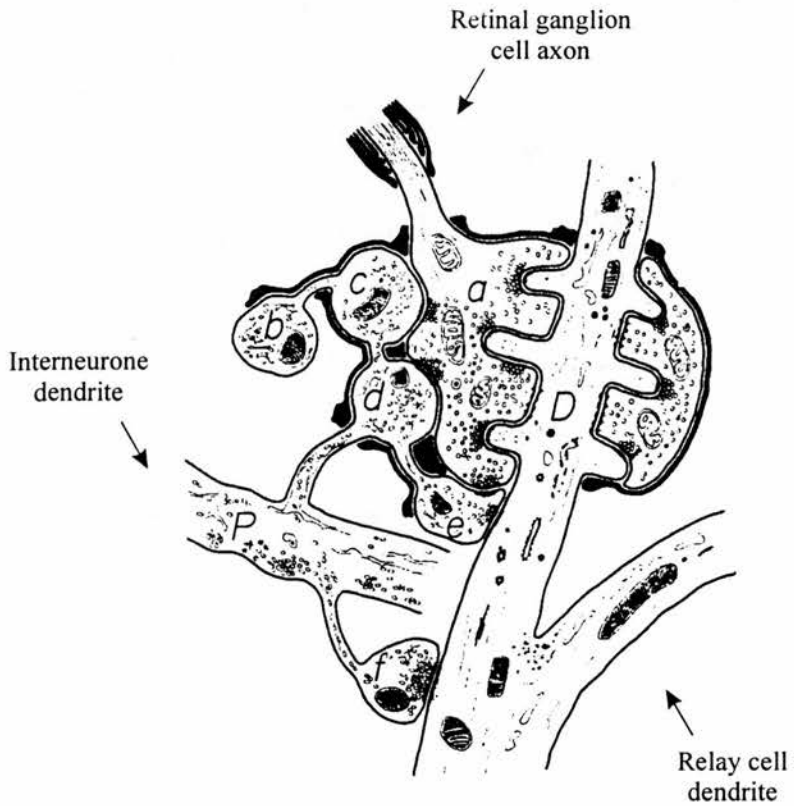


**Fig. 6.** Typical synaptic connectivity between a retinal ganglion cell (a), interneurone (P) and relay cell dendrite (D) in the Golgi-impregnated murine dLGN (adapted from Rafols and Valverde, 1973). See 2.3 for details.

spiny swellings or enlargements in the dendrites and the spines are seen to invaginate into the mass of the axon terminal. Synaptic contacts are found at the tip, base or stem of the spine as well as on the smooth dendritic surface (see *a* in fig. 6). Retinal contacts were also found at distal dendritic sites where spines and dendritic enlargements are lacking.

The spheroid bodies attached to the dendrites of interneurones (see 2.2) make Gray type 2 synaptic contacts with the dendrites of relay cells (see *f* in fig. 6). Interneurone terminals are also found in a complex arrangement with the synaptic boutons of retinal ganglion cells: Often an interneurone axon terminal receives a pre-synaptic input from a single retinal terminal that is also pre-synaptic to a relay cell (see *c* and *d* in fig. 6). A variant of the latter complex is found when an interneurone shares a retinal input with a relay cell, but at the same time is pre-synaptic to the same relay cell (see *e* in fig. 6). This tri-synaptic arrangement is known as a "glomerulus" (Famiglietti and Peters, 1972). Similar arrangements of synaptic contact between retinal ganglion cell and interneurone terminals and the dendrites of dLGN cells have been identified ultrastructurally in the rat (Lieberman and Webster, 1972 and 1974).

In this study a third type of synaptic contact (Gray type 1) of undetermined origin is found at indiscriminate locations on murine relay cell dendrites; these terminals are not associated with the glomerulus and are similar to the Gray type 1 extraglomerlular synaptic contacts in the rat dLGN that originate in the cortex (Lund and Cunningham, 1972). In the rat, axon terminals originating in the reticular nucleus form Gray type 2 synapses on the dendrites of relay cells (Ohara et al., 1983).

The synaptic connectivity between the retinal ganglion cells, interneurones, dLGN relay cells in the mouse and rat is clearly similar. The extraglomerular Gray type 1 synapses on murine relay cells, that have not been characterised, may be cortical in origin as in the rat although the possibility that these excitatory inputs arise from other brain areas cannot be ruled out. Given the absence of a basis to discriminate between the synaptic organisation in the rat and mouse, it is reasonable to assume that murine relay cells also receive inputs from the reticular nucleus.

### 2.4 Regional organisation of the retinal inputs to the dLGN

In the rodent there is almost complete decussation at the optic chiasm (see fig.1); radiolabelling and enucleation experiments in mice have demonstrated that that 90-95 % of

retinal axons from each eye project to the contralateral dLGN (Valverde, 1968; Drager, 1974). In albino strains the contribution of ganglion cells axons to the ipsilateral pathway somewhat reduced, with approximately 99 % of the axons projecting to the contralateral dLGN (Drager, 1974). A similar decussation is reported in albino and pigmented rats (Dreher et al., 1985; Lund, 1965) and similar numbers of retinal ganglion cells are found in pigmented and albino strains (Fukuda et al., 1982). Unlike in the cat, there is no evidence of a laminar arrangement of the retinal inputs from the contralateral and ipsilateral eyes in the dLGN of the rat and mouse. Montero et al., (1968) found that relay cells receiving ipsilateral input were intermingled with contralateral ones in the medial half of the nucleus. In the mouse, relay cells receiving ipsilateral input are clustered adjacent to medial border of the nucleus surrounded by contralateral retinorecipient cells (Metin et al., 1983).

In the rat, most retinal ganglion cells are labeled following HRP injection of the superior colliculus, suggesting that the dLGN is innervated by axon collaterals of ganglion cells (Linden and Perry, 1983). For each relay cell there is thought to be one ganglion cell innervating the dLGN although there is axonal branching near the target nuclei (Sefton and Dreher, 1985). Golgi-impregnation of the murine dLGN has found that individual relay cells are contacted by more than one ganglion cell (Iwahori and Mazuno, 1984).

On the basis of axonal diameter, three classes of retinal ganglion cell have been identified in Golgi-impregnation (Perry, 1979) and HRP retrograde labeling studies in the rat (Ni and Dreher, 1981). In the Golgi-impregnated murine dLGN large, medium and small diameter retinal fibres have been identified (Iwahori and Mazuno, 1984). In a combined electrophysiological and histological study Fukuda, (1977) identified fibres of fast, medium and slow conduction velocities innervated the dLGN which corresponded to large, medium and small diameter ganglion cell axons. Enucleation experiments in the rat have demonstrated that degeneration in this nucleus occurs in three stages, each stage possessing both a unique latency to onset and spatial location in the nucleus (Lund et al., 1976). The regional termination of the retinal axons appeared to relate to fibre diameter, with the largest diameter axons taking the greatest length of time to degenerate.

Retrograde degeneration studies first identified a topographic relationship in the projection pattern from the retina to the dLGN in the rat; ganglion cells located at different quadrants of the retina project to oblique columns of cells situated anteromedially in the nucleus (Lashley, 1934). Metin et al., (1983) recorded from mouse dLGN cells during

stimulation of areas of the retina, and found a similar topographic relationship between retinal areas and segregated columns of cells in the dLGN.

Whilst in terms of their morphology relay cells in the rat and mouse dLGN constitute a homogeneous population, there is a laminar arrangement of the retinal ganglion cell inputs to the dLGN such that large, medium and small diameter axons terminate in spatially distinct sectors of the nucleus. Anatomically, the major retinal input to the dLGN (approximately 95 % of axons) is from the contralateral as opposed to the ipsilateral eye. There is a reduced contribution in albino strains such that the ipsilateral eye only contributes approximately 1% of the retinal input to the ipsilateral dLGN.

## 2.5 Ionic conductances in dLGN relay cells

### *2.5.1 Voltage-activated currents*

The intrinsic properties of thalamic relay cells have been extensively investigated in rat and guinea-pig brain slices. Jahnsen and Llinas (1984a) first demonstrated that relay cells in different thalamic nuclei, including the dLGN, function as a homogeneous population. Crunelli et al., (1987a) established that the properties of relay cells in the rat are the same as those in the guinea-pig.

Both fast and slow sodium currents have been identified in relay cells by their sensitivity to the Japanese puffer fish poison, Tetrodoxin (TTX). The fast activating and rapidly inactivating sodium current, $I_{Na}$ is responsible for the upstroke of the action potential in thalamic relay cells (Jahnsen and Llinas, 1984b; Crunelli, 1987a; Leresche et al., 1991). The persistent and non-inactivating sodium conductance, $I_{NaP}$ is activate in a voltage range sub-threshold to that of $I_{Na}$; this current can generate a plateau depolarisation in relay cells, promoting the rhythmic firing of action potentials (Jahnsen and Llinas, 1984b).

Inward calcium currents with both a low and high threshold of activation have been identified in thalamic relay cells. In voltage clamp the low threshold calcium current, $I_T$ is largely inactivated at membrane potentials positive to -65 mV and this inactivation is gradually removed as the membrane approaches -100 mV. The inward movement of calcium ions depolarises the cell to a plateau of around -20 mV; this current is sensitive to extracellular nickel ions and a minimum of 500 ms is required for removal of inactivation (Crunelli et al., 1989; Hernandez-Cruz and Pape, 1989). In current clamp, the activation of $I_T$ is seen as a slowly rising and decaying triangular shaped potential, 30 -50 ms in duration

(Jahnsen and Llinas, 1984a; Crunelli et al., 1987a; McCormick and Pape, 1990a; Leresche et al., 1991). This is termed a low threshold spike after a similar calcium potential, first described in inferior olivary neurones (Llinas and Yarom, 1981). In depolarising the relay cell membrane potential into the activation range for $I_{Na}$, the low threshold spike triggers a high frequency burst of sodium-mediated action potentials (Jahnsen and Llinas, 1984a; Crunelli et al., 1987a; McCormick and Pape, 1990a; Leresche et al., 1991). In voltage clamp the high threshold calcium current $I_L$ is activated between approximately -30 mV and 5 mV and the peak amplitude of this current occurs between 6 and 30 ms after onset; the inactivation follows a very slow time course. The activation range of $I_L$ is therefore distinct from that of the low threshold current $I_T$, but it is also blocked by nickel ions (Hernandez-Cruz and Pape, 1989). In current clamp, high threshold calcium spikes are occluded by the powerful inward and outward currents shaping the action potential; in the presence of TTX, depolarisation of the membrane to approximately -20 mV evokes high threshold spikes which are abolished by low extracellular calcium (Jahnsen and Llinas, 1984b).

Under voltage clamp, hyperpolarisation of relay cells beyond -60 mV activates an inward mixed sodium and potassium current, $I_H$ which can be blocked by extracellular caesium; activation of this current depolarises the cell towards the equilibrium potential for $I_H$ which is approximately -40 mV (McCormick and Pape, 1990a). The time course of activation of this current ranges from a few seconds at -60 mV to several hundred milliseconds at -95 mV and maximal activation is achieved with hyperpolarisation of the membrane to approximately -100 mV. Activation of $I_H$ in current clamp is seen as a depolarising "sag" of the membrane potential towards rest. The activation ranges of $I_T$ and $I_H$ are similar and hence the depolarisation of the membrane caused by activation of $I_H$ can evoke a low threshold spike in relay cells. Consequently, the inactivation of $I_H$, due to the peak depolarisation of the low threshold spike, assists in the repolarisation of the calcium potential (Solstesz et al., 1991).

In relay neurones the rapidly activating and rapidly inactivating (transient) potassium current $I_A$ is activated by depolarisation from approximately -70 mV; this current is sensitive to millimolar concentrations of 4-aminopyridine (4-AP) (Huguenard et al., 1991; Budde et al., 1992). In current clamp, activation of $I_A$ delays the onset of the low threshold calcium spike (Jahnsen and Llinas, 1984b). In voltage clamp an outward potassium current $I_{AS}$ with a similar fast activation, but much slower inactivation rate has been identified in thalamic relay cells (McCormick, 1991). This current is activated by depolarisation above -

65 mV and is blocked by micromolar concentrations of 4-AP. In current clamp there is often a delay to the onset of the first spike of a train initiated by depolarising from -60 to -70 mV. In relay cells this delay is due to the activation of both $I_A$ and $I_{AS}$. The slow inactivation rate of $I_{AS}$ also confers on relay cells a marked outward rectification during depolarisations from -60 to -70 mV (McCormick, 1991). An outward potassium current, relatively linear in the voltage range 120 to -60 mV, and which contributes to the resting leak conductance of the cell, has been identified in voltage clamp studies of relay cells ($I_{KL}$: McCormick and Wang, 1991; McCormick and Williamson, 1991; McCormick, 1992).

*2.5.2 Calcium-activated currents*

Pennefather et al., (1985) identified two main types of calcium-activated potassium conductances in mammalian cells. $I_C$ is voltage dependent and blocked by both tetraethylammonium (TEA) and charybdotoxin, and is mediated by large conductance (BK) calcium-activated potassium channels (Marty, 1981). The current $I_C$ possesses fast activation kinetics and in current clamp contributes to the repolarisation of the action potential, generating the fast after-hyperpolarisation (AHP) in mammalian neurones (Lancaster and Nicoll, 1987; Storm, 1987; Johnston et al., 1994). The current $I_{AHP}$ possesses slower activation and inactivation kinetics and is abolished by apamin (Pennefather et al., 1985); apamin selectively blocks small conductance calcium-activated potassium channels (SK channels: Blatz and Magleby, 1986). Activation of $I_{AHP}$ generates a hyperpolarisation of up to 200 ms in duration in mammalian neurones (Pennefather et al., 1985; Avanzini et al., 1989; Osmanovic et al., 1990; Viana, et al., 1993; Johnston et al., 1994). In the study by Pennefather et al., (1985) $I_{AHP}$ was reduced by muscarinic receptor activation; the apamin sensitive-AHP in a number of mammalian cell types has not been tested for muscarinic sensitivity but Johnston et al., (1994) found that the slow AHP mediated by SK channels in MVN neurones, is carbachol-insensitive. A second type of calcium dependent slow AHP has been identified in hippocampal cells that is similar to the $I_{AHP}$ characterised by Pennefather et al., (1985); it is sensitive to muscarinic agonists, insensitive to TEA and charybdotoxin and possesses slow activation and inactivation kinetics (Lancaster and Adams, 1986; Lancaster and Nicoll, 1987). However the slow AHP in hippocampal cells is not sensitive to apamin and therefore is not mediated by SK channels (Lancaster and Nicoll, 1987).

In the first *in vitro* study of thalamic neurones Jahnsen and Llinas, (1984b) demonstrated that the biphasic AHP of the action potentials was calcium dependent. Voltage clamp studies of thalamic neurones have characterised a current with properties similar to $I_C$. However the conductance underlying the slow AHP in relay cells has not been identified. The muscarinic mediated slow depolarisation in guinea-pig relay cells persists after the blockade of membrane calcium channels; this observation prompted the suggestion that a slow calcium-activated calcium conductance is not present in these cells (McCormick, 1992). However in this context the effects of the SK channel blocker, apamin, on thalamic relay cells have not been reported.

## 2.6 Afferent projections to dLGN relay cells

The rat dLGN receives minor anatomical inputs from other retinorecipient nuclei: the superior colliculus and parabigeminal nucleus of the midbrain, and the pretectal nucleus of the optic tract (see Sefton and Dreher, 1985). The physiology and neurochemistry of these projections have not been characterised. More information is available concerning the afferent input to dLGN cells from the ascending neurotransmitter systems, the cortex, thalamic reticular nucleus, retinal ganglion cells and intrinsic interneurones. Estimates in the cat suggest that in proportion these inputs account for 5:40:20:15:20 of the synaptic contacts on relay cells (see Sherman and Koch, 1986).

### *2.6.1 Retinal ganglion cells*

The neurotransmitter released by the retinal ganglion cell terminals is the excitatory amino-acid (EAA) glutamate: At the ultrastructural level immunogold labeling demonstrates that synaptic terminals of retinal and cortical origin contain large concentrations of glutamate (Montero and Wenthold, 1989) and in the rat thalamus binding sites for both *N*-methyl-*D*-aspartate (NMDA) and non-NMDA glutamergic receptor subtypes are found (Monaghen and Cotman, 1982; Monaghen et al., 1984). Electrical stimulation of the optic tract axons in a coronal brain slice preparation in the rat results in a fast excitatory post-synaptic potential (EPSP) in dLGN relay cells that is specifically blocked by the EAA antagonist γ-D-glutamylglycine (DGG) (Crunelli et al., 1987b). Contributions of the *N*-methyl-*D*-Aspartate (NMDA) and non-NMDA glutamergic receptor subtypes to the fast EPSP have been investigated using the NMDA antagonist D-2-

[3H]amino-5-phosphopentanoate (APV), and the non-NMDA antagonist 6-cyano-7-nitroquinaline-2,3,-dione (CNQX). The EPSP is mediated largely by the non-NMDA, with a small contribution from the NMDA receptors (Turner et al., 1994). The EPSP evokes an action potential from a sub-threshold membrane potential by depolarising the membrane to firing threshold; from a more hyperpolarised membrane potential a low threshold calcium spike can be evoked that triggers a burst of fast spikes (Jahnsen and Llinas, 1984a; Crunelli et al., 1987b; Turner et al., 1994).

*2.6.2 Corticogeniculate projections*

Axons from the visual cortex which, retinotopically, innervate the rat dLGN (Montero and Guillery, 1968) arise from the small pyramidal cells in cortical layer 6 (Sefton and Swindburn, 1981). Cortical axons display immunoreactivity for glutamate (Giuffreda and Rustioni, 1988) and removal of the cortex results in a significant reduction in levels of glutamate in the dLGN (Fosse et al., 1986). Stimulation of corticothalamic afferents in the rat thalamus *in vivo* evokes short latency EPSP's in thalamic relay cells (Deschenes et al., 1984) and similar responses evoked in the cat are mediated by both NMDA and non-NMDA glutamate receptor subtypes (Deschenes and Hu, 1990). Therefore glutamate is thought also to be the transmitter released by corticothalamic axon terminals.

Golgi-impregnation studies in the rat have established that corticothalamic axons emit collaterals that innervate the nucleus reticularis (Scheibel and Scheibel, 1966; Sefton and Swindburn, 1981); stimulation of corticothalamic axons evokes both NMDA and non-NMDA mediated excitatory responses in neurones of the reticular nucleus (de Curtis et al., 1989).

*2.6.3 Brainstem nuclei*

Neuroanatomical and pharmacological investigations have demonstrated four main neurotransmitter systems converge on thalamic nuclei; these form serotoninergic, histaminergic, cholinergic and noradrenergic inputs to relay cells.

Serotonin immunoreactive fibres are found in the rat dLGN (Cropper et al., 1984) and stimulation of the serotoninergic dorsal raphe nucleus results in a slow and prolonged inhibition in rat dLGN relay cells *in vivo* (Kayama, 1989). The effects of serotonin in rat cells *in vitro* have not been studied however inhibitory responses to serotonin are not observed in guinea-pig cells *in vitro*; instead a small depolarisation is evoked due to a

positive shift in the activation kinetics of the mixed cation current, $I_H$ (McCormick and Pape, 1990b). In the absence of an *in vitro* study of serotoninergic responses in the rat it is not possible to discern if this represents a species difference, but it is possible the inhibitory response is due to the indirect excitation of neighbouring GABAergic reticular neurones (McCormick and Wang, 1991).

Thalamic axons immunoreactive for histamine originate in the tuberomammillary nucleus of the hypothalamus (Airakinson and Panula, 1988). A high density of $H_1$ and $H_2$ receptors in the guineas-pig thalamus has been reported (Bouthenet et al., 1988) and the application of histamine to relay cells *in vitro* results in a slow depolarisation due to suppression of a leak potassium conductance. Specific activation of $H_2$ receptors evokes a slow depolarising response due to a shift in the activation of $I_H$ to more depolarised levels (McCormick and Williamson, 1991).

In the rat cholinergic innervation of relay cells in the thalamus arises mainly from the pedunculopontine and lateral dorsal tegmental nuclei of the brainstem (Sofroniew et al., 1985). Autoradiography studies have identified nicotinic (Clarke et al., 1985) and muscarinic (Rotter et al., 1979) receptors in the dLGN of the rat; immunolabelling for nicotinic receptors has identified these receptors in the murine dLGN (Swanson et al., 1987). Acetylcholine, via muscarinic receptors, suppresses a resting leak potassium conductance in guinea-pig and rat relay cells resulting in a slow depolarisation (McCormick and Prince, 1986).

Retrograde labeling studies have shown that catecholaminergic fibres in the dLGN arise from the noradrenergic cells of the locus coerlus (Kromer and Moore, 1980). Excitatory inputs evoked in the rat *in vivo* are prolonged during locus Coerlus stimulation through the activation of $\alpha_1$ adrenoreceptors; $\alpha_1$ receptors are specifically antagonised by prazosin (Rogowski and Aghajanian, 1982; Kayama, 1985). The noradrenaline-induced slow depolarisation *in vitro* is mediated by suppression of a resting leak potassium conductance and the enhanced activation of the mixed cation current $I_H$ (McCormick and Prince, 1988; McCormick and Pape, 1990b; McCormick, 1992).

### *2.6.4 Intrinsic interneurones of the dLGN*

GAD is the synthesising enzyme for the inhibitory neurotransmitter GABA and the presence of GAD-immunoreactivity is an agreed marker for GABAergic neurones (Otterson and Storm-Mathison, 1984b). In the rat dLGN, both GABA- and GAD-immunoreactive

perikarya and cell processes are identified which are morphologically similar to Golgi-impregnated intrinsic interneurones of the mouse and rat (e.g. Grossman et al., 1973; Iwahora and Mazuni, 1984). GABAergic terminals of the intrinsic interneurones make synaptic contacts with relay cells and quantitative analysis of immunolabelling in the rat dLGN demonstrates that interneurones constitute approximately 20 % of the neuronal population (Gabbott et al., 1986; Ohara et al., 1983). In the rodent the dLGN is the exception in that all other dorsal thalamic nuclei lack intrinsic GABAergic interneurones (Ohara et al., 1983; Otterson and Storm-Mathison, 1984a; Benson et al., 1992)

The direct synaptic activation of interneurones via optic tract stimulation can evoke both an early and late phase of hyperpolarisation in rat dLGN relay cells (Crunelli et al., 1987b; Crunelli et al., 1988; Hirsch and Bernod, 1987). The early phase is mediated by chloride ions through the activation of $GABA_A$ receptors, and is blocked by bicuculline (Crunelli et al., 1988). The late phase of hyperpolarisation is blocked by phaclofen and mediated by potassium through the activation of $GABA_B$ receptors (Crunelli et al., 1988; Hirsch and Burnod, 1987).

There are only two published studies of the membrane properties of dLGN intrinsic interneurones (McCormick and Prince, 1988; Pape et al., 1994), although there is a brief description of a sample of interneurones recorded in Leresche et al., (1991). In current clamp, interneurones either lack a low threshold calcium spike or display only a small rebound response that fails to evoke action potentials, after a large hyperpolarisation. Pape et al., (1994) established that interneurones possess both an $I_T$-like and $I_A$-like conductance. Unlike in relay cells, where $I_T$ activates at more hyperpolarised levels than $I_A$ (conferring on $I_A$ the ability to shape the low threshold potential), the activation range of the $I_T$-like and $I_A$-like conductance in the interneurones overlap. The A-conductance is also larger in interneurones than in relay cells and these properties in combination prevent the generation of the low threshold calcium spike in these cells. The application of 4-AP (which at millimolar concentrations blocks $I_A$) reveals a low threshold spike in these cells. Interneurones also lack a delay to the onset to firing during depolarisation and display more linear membrane voltage versus injected current (current-voltage) profiles Intrinsic interneurones and relay cells clearly possess distinct electroresponsive properties.

*2.6.5 Reticular nucleus*

The reticular nucleus of the thalamus is a sheet-like structure encasing much of the dorsal thalamus (Scheibel and Scheibel, 1966). Each thalamic nucleus is associated with a subdivision of the reticular nucleus with which it forms reciprocal synaptic connections (see Jones, 1985). The majority of cell bodies in the reticular nucleus are GABAergic and reticular axons project to the dLGN where their terminals form GABAergic inputs to relay cells (Houser et al., 1980; Ohara et al., 1983; Ohara and Lieberman, 1985). Within the reticular nucleus some GAD-positive axon terminals synapse with GAD-positive cell bodies, substantiating the suggestion that axons projecting to the thalamus give rise to collaterals within the reticular nucleus itself (Ohara and Lieberman, 1985; Montero and Scott, 1981). The IPSP's evoked in rat thalamic relay cells by stimulation of the reticular nucleus are mediated by $GABA_A$ receptors and repolarisation during recovery from a reticular-evoked IPSP evokes a low threshold calcium spike in thalamic relay cells (Thomson, 1988). In this context, the ability of GABAergic reticular neurones to evoke barrages of IPSP's is thought to underlie their role in the synchronous burst firing in relay cells (Steriade et al., 1987; Warren et al., 1994).

**2.7 Efferent projections dLGN relay cells**

The axons of dLGN relay cells project principally to the visual cortex and the reticular nucleus. Following cortical ablation in the rat, the majority of dLGN cells degenerate rapidly indicating that the cortex receives a major input from dLGN cells (Matthews, 1973). Extensive knowledge of the connectivity and distribution of inputs to the rat visual cortex has been gained through the employment of ultrastructural labeling and degeneration techniques which are reviewed in Sefton and Dreher, (1985): In layer 4 and the lower part of layer 3 approximately 80 % of thalamic axons contact: dendritic spines and collaterals of layer 5 and 6 pyramidal cells, dendritic spines of layer 3 pyramidal neurones, sparsely spiny stellate cells, nonpyramidal cell dendrites with perikarya in layers adjacent to 4 and dendritic spines of cells with perikarya in layer 4. A further 15 % of thalamic terminals synapse on dendritic shafts of later 3 and 5 pyramidal cells and the remainder contact perikarya of sparsely spiny or smooth stellate cells. In the cat, activation of thalamocortical afferents can evoke monosynaptic EPSP's in all cortical cells with dendritic processes in layer 4 (cells in cortical layers 3, 4, 5 and 6); similar to the rat, layer 4 is a

major target of thalamocortical axons (Ferster and Lindstrom, 1983). In the cat EAA antagonists block the excitation of cortical cells evoked by electrical stimulation of retinal inputs (Tsumoto et al., 1978). Both glutamate and aspartate are released in the cortex in response to visual stimuli (Kaneko and Mizuno, 1988) and the NMDA and non-NMDA glutamate receptor sub-types are widespread in this area (Monaghan and Cotman, 1982; Monaghen and Cotman, 1985) supporting the suggestion that glutamate, or a related neurotransmitter is released by thalamocortical terminals.

### 2.8 Membrane response properties of dLGN relay cells

During sleep and awakening or conscious states, dLGN relay neurones of the cat recorded *in vivo* display distinctive firing patterns in response to excitatory inputs from retinal ganglion cells; these are termed the "oscillatory" and "transfer" modes of relay cell activity (see Livingstone and Hubel, 1981; Deschenes et al., 1984; Steriade and Llinas, 1988; Steriade et al., 1990b; Steriade et al., 1993). These firing patterns of relay cells arise from the integrated activity of neurotransmitter systems afferent to relay cells (see 2.6 and Steriade et al., 1990a, c; Steriade and McCarley, 1990; Kayama, 1985) and the ionic currents intrinsic to relay cells (see 2.5). In this section the mechanisms underlying the generation of the oscillatory and transfer modes observed *in vivo* are summarised, and the *in vitro* approach to studying the membrane response properties intrinsic to relay cells is described.

Consciousness and the awakening from sleep or anaesthesia is associated with depolarisation of relay cell membrane potentials (Hirsch et al., 1983). During these states there is an accurate transmission of visual information to the cortex as the incoming visual signals from the retinal ganglion cells, in the form of individual EPSP's, are transformed with unitary gain into action potentials in the dLGN relay cells. This tonic activity is then transferred by relay cells axons to the visual cortex. During this behavioural state the tonic firing of action potentials in relay cells is known as the "transfer mode" of activity.

Drowsiness, anaesthesia or deep sleep are associated with hyperpolarised membrane potentials (Hirsch et al., 1983). Incoming EPSP's during these states do not evoke action potentials but promote a burst of between 2 and 8 action potentials due to the activation of a low threshold calcium spike. Due to the kinetics properties of $I_T$, the frequency of this burst response is limited to between 1 and 12 Hz; this rhythmic bursting is termed the

"oscillatory" mode of relay cell activity. Thus, during drowsiness and sleep, the burst response that is evoked in response to visual inputs prevents relay cells from accurately transmitting visual information to the cortex. In this manner relay cells act as a gateway to the cortex, filtering visual information in order that an unconscious state is maintained.

The transition from an unconscious to conscious states is associated with increased activation of the neurotransmitter systems afferent to relay cells, situated in the brainstem, hypothalamus and basal forebrain (Steriade et al., 1990c; Steriade and McCarley, 1990). The findings of neurotransmitter modulation of relay cell ionic conductances *in vitro* (see 2.6) substantiates the suggestion that during awakening afferent neurotransmitter systems promote the depolarisation of the membrane potential. Hyperpolarised membrane potentials in relay cells during the unconscious state facilitates rhythmic burst firing and it is thought that inhibitory episodes from the reticular nucleus assist in maintenance of this oscillatory activity (Steriade et al., 1986; Steriade et al, 1987; Bal et al., 1995). The ability of dLGN relay cells to differentially respond during unconscious and conscious states is therefore a product of their intrinsic membrane conductances and synaptic connectivity.

Relay cells recorded in brain slices in the guinea-pig and rat are silent at rest (e.g. Jahnsen and Llinas, 1984a; Crunelli et al., 1987a; McCormick and Prince, 1990a; Leresche et al., 1991). Constant and episodic current injection of thalamic relay cells *in vitro* can be employed to manipulate the membrane potential and thus monitor the membrane response properties underlying the modes of activity observed *in vivo*; electrical stimulation of the optic tract fibres allows the integrity of the synaptic transmission between retinal ganglion and dLGN relay cells to be monitored *in vitro* (e.g. Jahnsen and Llinas, 1984a; Crunelli et al., 1987b; Turner et al., 1994).

In this study, direct current injection and optic tract stimulation were employed to monitor the functional properties of dLGN relay cells in brain slice preparations from normal and scrapie-infected mice.

# Chapter 3

# Materials and Methods

## 3.1 Experimental mice

### *3.1.1 Normal mouse experiments*

Male Balb\c mice of between 40 and 70 days of age were used in the experiments investigating normal dLGN function. The mice were bred, housed and attended to by the staff in the Faculty Animal Area of the Medical School.

### *3.1.2 Scrapie infected mice experiments*

All procedures relating to the breeding, inoculation and husbandry of the mice for the scrapie experiments were performed by staff in the Neuropathogenesis unit, Edinburgh. The experimental model investigated in this project is used routinely in pathological studies at the Neuropathogenesis Unit. Male mice of the VM/Dk strain (abbreviated to SV) which are homozygous for the s7 allele of the *Sinc* gene (see 1.3.2), were used in this study. The mice were housed in cages of six and all mice were ear punched at weaning for identification. The mice were inoculated with the ME7 strain of scrapie which was originally isolated in 1962 from a Suffolk sheep with natural scrapie; this strain has been passaged in generations of C57Bl mice.

## 3.2 Design of the scrapie experiments

### *3.2.1 Scrapie and control inoculation procedure*

Samples of brain tissue from clinically ill scrapie-infected mice were homogenised in saline at a dilution of $10^{-2}$ (by wet weight) in a glass tube fitted with a plunger (Griffiths tube). Under halothane anaesthesia, 1 μl of homogenate was injected into the scleral margin of one eye using a syringe with a 27 gauge needle; the inoculation procedure took approximately 4 seconds. The retina is not damaged during this procedure however any mice receiving an unsatisfactory inoculation were replaced. The mice behaved normally after recovery from the anaesthetic and an obvious increased intraocular pressure returned to normal within 24 hours. An identical inoculation procedure was undertaken for the mice employed as controls in this study; these mice were injected with a 1 % dilution of homogenized brain from uninfected SV mice. In this thesis, the infected mice are designated "scrapie-inoculated" and the normal brain-inoculated mice "control", to distinguish them from the population of normal (untreated) mice studied.

*3.2.2 Determination of the scrapie incubation period*

Each week from 30 - 50 days prior to the predicted end of the incubation period, staff at the Neuropathogenesis Unit scored the mice for clinical signs of scrapie; lack of grooming, appetite loss and a general lethargy and inattentiveness. There are three scoring grades based on the severity of clinical signs according to the protocol introduced by Dickinson et al., (1968):- "unaffected", "possibly affected" or "definitely affected". The day upon which there was a third consecutive "definite" score or fourth "definite" score in 5 weeks or the day on which the mouse was found dead having scored the previous week, was defined as the end of the incubation period for that mouse.

*3.2.3 Serial data collection throughout the incubation period*

On the first day of each week of experimentation, mice were transferred to, and housed in the Faculty Animal Area at the Medical School, Edinburgh University, according to Home Office requirements. Mice scoring for clinical signs were examined at the Neuropathogenesis unit by a vet before permission was granted for transportation to the Medical School.

The normal brain-inoculated (control) and scrapie-inoculated groups of mice in the two experimental series set up for this study, were injected intraocularly on a single day exactly one week apart. The numbers of mice inoculated took into allowance unexpected death during the incubation period. Electrophysiological experiments commenced at approximately 56 days post-inoculation and were performed over a two week period, at approximately 28 day intervals. At each interval the experiments in the different groups were performed over a five day period; control in the first week and scrapie-inoculated mice during the second week. Cells were recorded from one brain slice preparation per animal sacrificed.

## 3.3 Preparation of the brain slice material for intracellular recording

In the present study an identical protocol was employed in the preparation of brain slices from untreated, control and scrapie-inoculated mice. A lab coat, scientific goggles, surgical gloves and surgical mask were worn during brain slice preparation. All surgical instruments and non-disposable materials used in the preparation of scrapie-infected slices

were sterilised for 40 minutes in 35 % sodium hypochlorite, prepared fresh from a stock solution each day. All disposable materials were incinerated.

*3.3.1 Anaesthesia*

Prior to decapitation, mice were anaesthetized with halothane (May and Baker Ltd., UK). A piece of cotton wool soaked in 2 mls of halothane was placed inside a 20 ml beaker which was secured with its open end against the interior wall of a plastic box. The animal was placed in the box which was sealed by a lid with a small hole for ventilation. The animal was judged to be sufficiently anaesthetised to permit surgery when a reflex responses to a hindlimb or tail-tip pinch was lacking.

*3.3.2 Trans-cardiac perfusion*

In a number of experiments in slices from control and scrapie-inoculated mice, cells were labeled with biocytin (Sigma Chemicals Ltd.). Biocytin is an ideal marker for studying neuronal morphology as it diffuses rapidly within the cell; it is injected, by iontophoresis, from the electrode with relative ease and biocytin-containing electrodes do not possess excessively high resistances (resistance 70 -150 MΩ: Horikawa and Armstrong, 1988). Erythrocytes react with reagents used to visualise biocytin and therefore can obscure labeled parts of the cell. It was therefore necessary to perform a trans-cardiac perfusion, prior to decapitation, to clear the tissue of erythrocytes.

Following the anaesthetic in 3.3.1, the animal was placed in a supine position on a polystyrene board; anaesthesia was maintained by inserting the nose of the animal into the end of a plastic tube connected to a small bell jar housing cotton wool soaked in 2 mls of halothane. The limbs of the animal were pinned to the board, and the skin overlying the chest area removed to expose the ribcage and xiphisternum. An incision was made beneath the xiphisternum, and the rib cage was cut on either side and pinned back to expose the heart which remained beating during the surgery. The cardiac perfusate was a solution of oxygenated artificial cerebrospinal fluid (aCSF: see 3.6) containing 1% heparin (CP Pharmaceuticals, UK), cooled to 4°C on ice. The heparin was incorporated into the solution to prevent the erythrocyte coagulation. A 20 ml syringe was used to draw up the perfusate and the 23 gauge needle of the syringe was then inserted into the left ventricle of the heart. A slight pressure was exerted on the syringe plunger before the right atrium was incised, creating an outlet for the perfusate. The perfusion lasted approximately one minute.

*3.3.3 Preparation of the brain slice*

In this study the animal was decapitated using a small animal guillotine and a rapid craniotomy was performed: The scalp and muscles of the neck were removed and the occipital bones and underlying cerebellum trimmed with fine scissors. The parietal and frontal bones were cut sagitally along the midline and prised to the side using blunt-ended fine tweezers. During this procedure care was taken to ensure minimal damage to the cortex and underlying structures. The dura was cut and peeled to the edges of the skull with a fine spatula and the brain removed with a spatula after which a scalpel was used to cut the cranial nerves. The brain was placed on a cold dissecting stage which comprised ice-cold aCSF-soaked filter paper placed on the surface of an upturned petri dish on ice. Using a disposable pipette the tissue was kept moist by periodic bathing with aCSF which was stored also on ice and continually oxygenated with 95%$O_2$/5%$CO_2$ (cold oxygenated aCSF). During the preparation of slices from control and scrapie-inoculated mice, at this stage one side of the thalamic block (ipsilateral to the infected eye) was trimmed for the purposes of identification. Using cyanoacrylate glue the block was secured by its rostral surface to the stage of a Vibroslice (Campden Instruments Ltd.) opposed to a piece of agar which supported the tissue during sectioning. The stage was then placed in the vibroslice reservoir which contained cold oxygenated aCSF. Coronal sections containing the dLGN were cut at 400 μm thickness and bisected at the midline; the sections containing the dLGN were easily identified by the border created by optic tract fibres. Both sides of the slice was checked to ensure that the dLGN was present for the whole depth of the slice. The slice was then transferred to a recording chamber. One half-coronal brain slice preparation was used from each mouse sacrificed.

*3.3.4 Maintenance of brain slice preparation in the recording chamber*

The design of chamber used to record from brain slices is illustrated in fig.7 and the following description relates to part 1 - 10 of the diagram. The coronal brain slice (1) was placed on the nylon mesh on the ramp surface (2) of an interface-type recording chamber. The slice was continuously perfused with aCSF (3) which was transported within the chamber by a perfusion inlet tube (4). The chamber contains distilled water (5) maintained at $35 \pm 2\ ^0C$ by the combined action of the heating element (6) and the thermistor probe (7). The heated water in the chamber is aerated with a gas mixture of 95% $O_2$/ 5 % $CO_2$ (8 and 9); the water vapour saturated with gas accesses the slice on the ramp of the interface

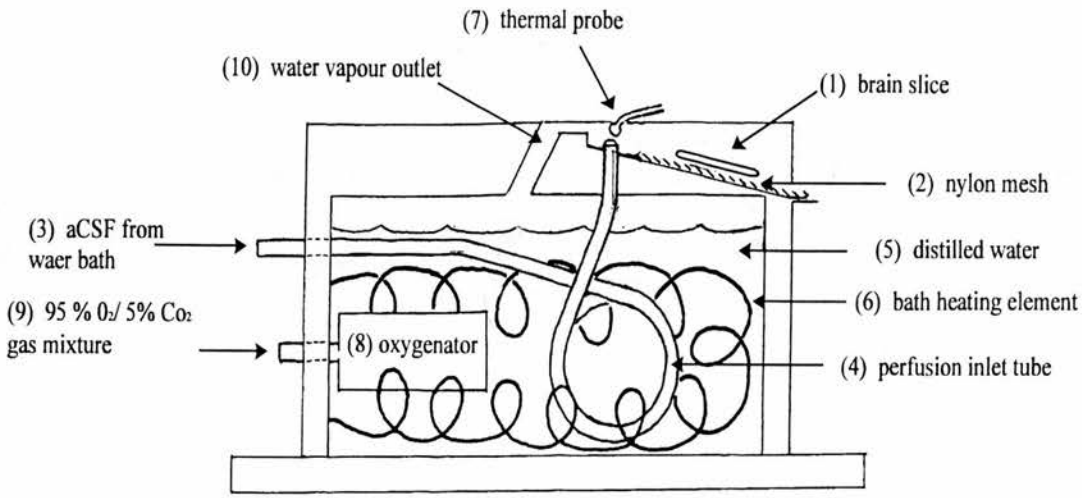


**Fig. 7.** Schematic diagram of the interface recording chamber. The coronal slice preparation, containing the dLGN, is maintained in a humid, oxygen-rich environment and continually perfused with artificial cerebrospinal fluid (aCSF) warmed to 35°C. See 3.3.4 for a description of the functional role of components 1 - 10 in this diagram.

chamber through an outlet in the ceiling of the chamber (10). The slice was therefore maintained in a humid, oxygen rich atmosphere and bathed with aCSF at $35^0$C. Each slice was incubated in the recording chamber for a minimum of one hour prior to intracellular recording. The recording chamber was situated on an antivibration chamber for stability (see fig. 8).

### 3.4 Intracellular recording from dLGN neurones in vitro

*3.4.1. Recording apparatus*

The flow diagram in fig.8 illustrates the main signal pathways between the recording apparatus involved in the collection, storage and analysis of electrophysiological data. Electrodes for intracellular recording were prepared from cylinders of standard wall (1.5mm outer and 0.86 inner diameter) borosilicate glass (Clark Electromedical Instruments Ltd., UK) using a Flaming Brown P87 Microelectrode puller (Sutter Instruments, UK). Electrodes were backfilled with 3 Molar potassium chloride (3M KCl) and resistances ranged from 40 - 90 MΩ. Filled microelectrodes were inserted into a perspex microelectrode holder which contained a silver/silver chloride pellet (Clark Electromedical Instruments Ltd., UK). The electrode holder was attached to the unity gain headstage of a high impedance Axoclamp 2A amplifier (Axon Instruments, USA) connected to a Scat D301 motorised step control (Digitimer, UK). The recording electrode was positioned manually within the confines of the dLGN by visualisation with a Wild M5 binocular dissecting microscope (Heerbrug, Switzerland). The border of the dLGN could be clearly identified. The Scat motorised step control was used to advance the recording electrode into the dLGN in 2 μm steps. Signals from the headstage entered the Axoclamp 2A amplifier and current and voltage (x10) ouputs (band with filter upper limit = 3 kHz) were sent from the amplifier to a Gould 1602 storage oscilloscope where they were monitored continuously. The voltage output was sent to a D130 audio amplifier (Digitimer, UK), and both the current and voltage outputs to an analogue-to-digital (A/D) TL1 DMA interface (Axon Instruments, USA) connected to a 486sx33 microcomputer (Viglen, UK). Enroute to the interface, the signals were boosted at a gain of 5 by a Cyberamp 320 signal conditioning amplifier (Axon Instruments, USA) for optimal use of the A/D range in the microcomputer. Current commands were generated from the computer using pClamp software (Axon Instruments, UK) and were initiated via a Digitimer D4030 pulse generator (Digitimer, UK). All data

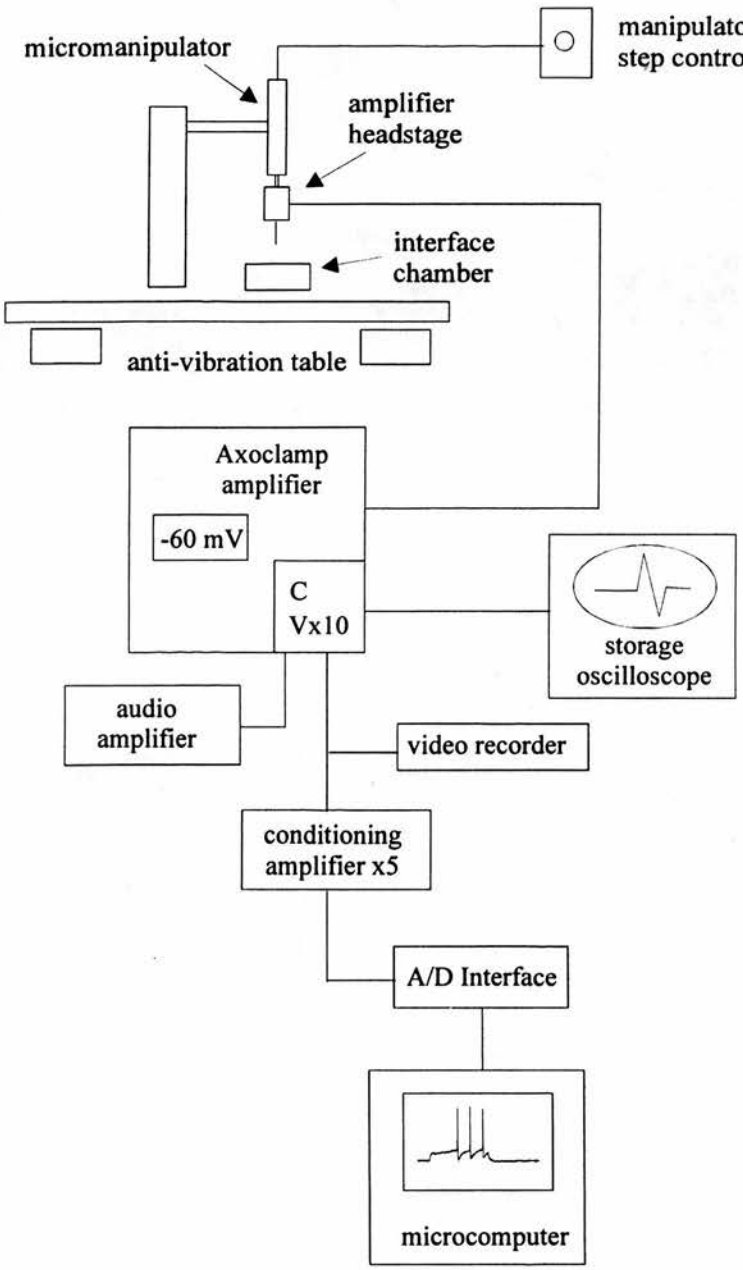


**Fig.8**. Simplified representation of the apparatus for intracellular recording. See 3.4.1.

recordings were stored on the microcomputer hard disk also recorded on video tape (VR-10BCRC Digital data recorder; Instrotech, USA) for back-up in case of computer failure.

*3.4.2. Intracellular impalement of dLGN neurones in vitro*

Microelectrodes for impalement of dLGN neurones were lowered manually into the surface of the slice (approximately 50 μm). Extracellular potentials recorded in the circuit between the microelectrode and bath reference electrode were compensated for using an offset potentiometer. Square DC pulses of -0.2 nA in amplitude (120ms; 2 Hz) were injected continuously through the microelectrode and the bridge created by the current pulse was balanced by a potentiometer. The electrode was advanced using the micromanipulator until a negative deflection of the oscilloscope voltage trace indicated the electrode was opposed to the neuronal membrane. Then using the remote buzz control of the Axoclamp 2A amplifier, brief electrode injection of a high amperage oscillatory current was used to 'buzz' the electrode tip, causing it penetrate the cell. This "buzz" of high intensity current localised at the electrode tip is thought to compromise the integrity of the membrane, allowing the tip to enter the cell (Silinsky, 1992); the precise mechanism by which the cell is impaled is not known. Following impalement, the oscilloscope trace hyperpolarised by the number of millivolts (mV) corresponding to the cell's resting membrane The membrane potential was displayed on the digital voltmeter of the Axoclamp 2A amplifier. For the first few minutes of impalement, each cell was injected with constant hyperpolarising current, -0.1 - 0.4 nA in amplitude, in order to allow the membrane potential to stabilise.

**3.5 Data collection and analysis**

This section details the methods of data collection and quantification employed in this study of dGN neurones in normal (Balb/c), control and scrapie-inoculated mice. All electrophysiological data was sampled in discontinuous current clamp at a rate of 3 - 5 kHz and analysed using pClamp software (Axon Instruments, UK).

*3.5.1.Membrane response properties of dLGN cells*

Voltage activated membrane conductances in dLGN relay cells were studied by injecting of a series of incrementing square current pulses (120 ms; 0.5 Hz) from different membrane potential levels. The first current pulse injected was -1.0 nA in amplitude and

subsequent pulses incremented by 0.1 nA; the fourteenth and final pulse was therefore 0.4 nA in amplitude. Current voltage profiles were constructed by calculating the membrane voltage obtained 100 ms after the onset of the current pulse, and plotting it against the amplitude of current injection (-0.1 to 0.4 nA).

*3.5.2. The basic membrane properties*

The basic membrane properties of dLGN cells are defined as: the resting membrane potential, input resistance, membrane time constant and action potential threshold. The resting membrane potential was defined as the somatic electrical potential recorded intracellularly, relative to a zero extracellular potential. For several minutes following impalement holding current was used to stabilise the membrane potential; the holding current was switched off and the potential measured by the electrode (read from the digital voltmeter on the Axoclamp 2A amplifier) was the membrane potential of the cell. The input resistance was calculated as follows: the amplitude of the voltage deflection from the holding potential of -60 mV was measured 100ms after the injection of a -0.2 nA current pulse; the amplitude of this voltage drop was divided by the amplitude of the current to give the membrane resistance. The membrane time constant (the time taken for the membrane voltage to decay to 63 % of its steady state) was calculated from the voltage response to an identical protocol as use to calculate the input resistance; this value was calculated using pClamp software. The action potential threshold was defined as the membrane voltage at which action potential firing was initiated at 1-2 Hz by the injection from rest of constant amplitude current. This voltage was read from the digital voltmeter on the Axoclamp 2A amplifier.

*3.5.3.The properties of average action potential shapes*

Two methods used in published studies (e.g. Johnston et al., 1994; Storm, 1987) were employed to collect, in each cell, a train of action potentials for quantititative analysis of the averaged action potential shape. Firstly, the membrane potential of the cell was depolarised by constant current injection until the cell fired tonically (i.e. action potentials were initiated) at 1 - 2 Hz.; the membrane potential at which this firing frequency was achieved was termed the action potential threshold for that cell. Secondly, after returning the membrane to rest for one minute the membrane was depolarised to 2 mV below firing threshold and single action potentials were "evoked" by 1 ms current pulses (0.1 - 0.3 nA; 1-

2 Hz). Between 8 and 20 action potentials were sampled by the pClamp (Fetchan) programme to produce the average spike shape; the sweep of the average was triggered by the peak of the action potential. The threshold read from the voltmeter on the Axoclamp 2A amplifier, and the membrane potential 2 mV below this value, were the baselines from which the parameters illustrated in fig. 9A were measured.

The effect of 100 nM apamin on the average action potential shape in dLGN cells was obtained by subtraction of the action potential profile in apamin-containing aCSF, from the spike profile in control aCSF. In order to achieve this the spike waveforms were imported into an Excel spreadsheet (Microsoft Corporation, USA) as a series of {x, y} co-ordinates and the subtraction performed with the peak of the spike as the central reference point. The parameters of the apamin-sensitive component measured are shown in fig. 9B.

*3.5.4. The response of dLGN cells to afferent optic tract stimulation*

The coronal slice preparation of the dLGN contains fibres of the optic tract which are routinely stimulated to monitor the efficacy of the synaptic input between retinal ganglion cell axons and dLGN relay cells (see 2.6.1). A tungsten bipolar electrode (A-M systems Inc., USA) was used to stimulate the retinal ganglion cell axons afferent to neurones in the dLGN. The electrode, placed on the surface of the optic tract, was connected to a voltage stimulator (Digitimer DS2A: Digitimer, UK). Electrical stimulation (1-40 Volts; 50 μs; 1 Hz) evoked a post-synaptic response in the dLGN cells. All responses included in this study were orthodromic in origin as they were not occluded by somatic action potentials, a phenomenon observed when antidromic responses are initiated in dLGN cell axons.

The maximum EPSP ($EPSP_M$) was recorded in dLGN cells using a protocol adopted from Cepeda et al., (1992). The stimulus intensity applied to the optic tract fibres, whilst the membrane potential was held at -60 mV, was increased until the excitatory post-synaptic potential (EPSP) was just sub-threshold for action potential generation. As illustrated in figure 9C, the peak amplitude, 10 to 90 % rise time and 10 to 90 % decay time of single maximum EPSP's were measured.

*3.5.5. Hippocampal field potentials*

It was not possible to record extracellular field potentials in the murine dLGN, and thus a global measure of the functional integrity of the population of cells in this nucleus

**A The average action potential shape**

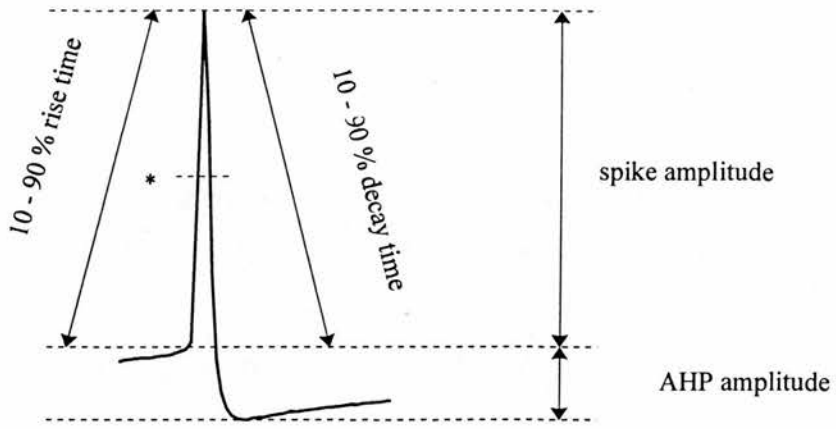


**B The apamin-sensitive component of the slow AHP**

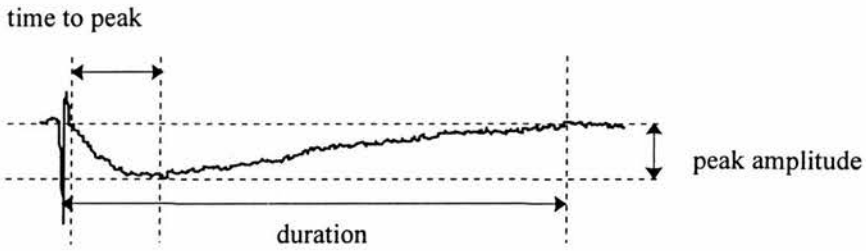


**C The maximum EPSP**

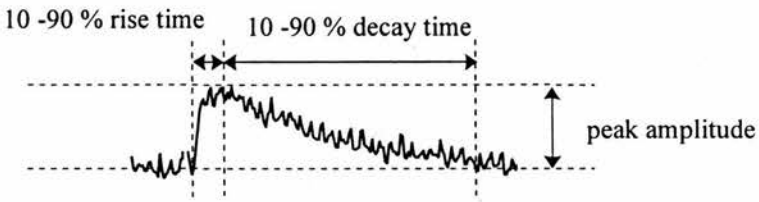


**Fig.9.** Illustrations of the parameters measured in A, the average action potential shape B, the apamin-sensitive component of the action potential and C, the maximum EPSP evoked by optic tract stimulation. In A, * = the point at spike half height where the spike width was measured.

could not be obtained. Therefore in a number of experiments, to control for the general integrity of the brain slice preparation the extracellular field EPSP was recorded in the hippocampal CA1 subfield following stimulation of the Schaffer collateral pathway. The bipolar stimulating electrode was placed on the stratum radiatum at the border of the CA1/CA2 subfields, and the recording electrode was positioned near the middle of the stratum radiatum in the CA1a pyramidal cell subfield. The bipolar electrode was stimulated (0.25 Hz) at increasing intensities until the maximum field potential, in the absence of population spikes, was obtained.

*3.5.6. Criteria for the inclusion of cells for analysis*

The minimum criteria for inclusion of cells in the groups for analysis were similar for the experiments in normal, control and scrapie-infected mice, in order that comparisons could be made between the data obtained in each group. Published studies of neurones recorded in brain slices set minimum criteria for the membrane and action potential properties to distinguish poor impalements from robust cells (e.g. Jahnsen and Llinas, 1984a). Poor impalements in brain slice preparations can be attributed to cells that may have been compromised during the slicing procedure or those that have not been properly impaled by the electrode. In the dLGN of normal mice, apparently poor impalements typically displayed: weak membrane responses to current injection; low amplitude fast spikes (30 to 40 mV); relatively depolarised thresholds (positive to -30 mV); relatively depolarised membrane potentials (positive to -40 mV) and low input resistance resistances (less than 25 MΩ). The criteria in this study were set at the minimum value that allowed discrimination between robust cells and poor impalements: action potential amplitude (spike amplitude + AHP amplitude) of 55 mV; resting membrane potential -45 mV; action potential threshold -35 mV; input resistance 30 MΩ.

**3.6. Solutions and channel blockers**

At the start of each slice experiment aCSF was made up fresh from refrigerated stock solutions. The aCSF composition was modified from the recipe used by Llinas and Sugimori, (1980). The medium was composed of - 124 mM sodium chloride (NaCl); 2.5 mM potassium chloride (KCl); 1.2 mM sodium dihydrogen orthosphosphate ($NaH_2PO_4$); 26 mM sodium hydrogen carbonate ($NaHCO_3$); 10 mM D (+) - Glucose; 1.3 mM magnesium

sulphate heptahydrate ($MgSO_4$); 2.4 mM calcium chloride ($CaCl_2$). Apamin, TTX and the nickel chloride were purchased from Sigma Biochemicals, UK. These channel blockers were made up as stock solutions and stored frozen in aliquots; using a Gilson pipette apamin was added to a final concentration of 100 nM, TTX as 0.5 μM and nickel chloride as 2 mM to the aCSF continually perfusing the brain slice preparation.

### 3.7. Intracellular labeling of dLGN cells by iontophoresis

*3.7.1 Biocytin injection procedure*

For intracellular labeling, recording electrodes were filled with a solution of 1.5 - 2 % biocytin dissolved in 0.05 M Tris (pH 7.4 at $37^0$C). Electrode resistance ranged from 70 - 150MΩ. The electrophysiological properties of the cell were recorded before injecting with biocytin. Depolarising pulses (0.6 - 0.9 nA; 300 ms duration; 0.6 Hz) were used to inject current for between 10 and 15 minutes whilst the cell was recorded in bridge mode. A single cell was injected in the dLGN of each slice at a minimum depth of -70 μm. The injection procedure was halted if the resting membrane potential of the cell was seen to deteriorate.

*3.7.2 Visualisation of neuronal morphology*

Following the iontophoresis of biocytin into dLGN neurones, the slices were incubated for at least two hours in the recording chamber to facilitate diffusion of biocytin throughout the cell (Horikawa and Armstrong, 1988). After this time the flow rate to the interface chamber ramp was increased and the slices floated onto a paintbrush before being transferred to fixative [4% paraformaldehyde made up in 0.05M phosphate buffered saline (PBS, pH 7.4)]. The slices were refrigerated until further processing took place: The 400 μm slice was adhered to a metal block by cyanocryalate glue, and the block secured on the stage of a vibrating microtome (Oxford Instruments, USA). The stage was submersed in 0.05 M PBS containing a sealed ice pack. Serial sections of 70μm in thickness were cut in the horizontal plane. Each section was transferred by paint brush to a mesh basket in 0.05M PBS. The baskets were placed in each of a multi-welled dish. Thus during the subsequent procedures each section-containing basket was transferred to the different solutions entailing minimal structural damage to the slice. Sections were washed for 2 x 5 minutes in 0.05M PBS then bleached (1% hydrogen peroxide in methanol) for 1 minute to remove endogenous peroxidase activity in erythrocytes that were not removed during the trans-

cardiac perfusion (see 3.3.2). Sections were transferred to Triton X-100 (0.4% in 0.05M PBS) which permeabilises the membrane. The sections were then incubated in avidin and biotinylated horseradish peroxidase complex (in 0.05 M PBS) for 40 - 60 minutes (Vectastain Elite ABC kit: Vector Laboratories Ltd., USA). Excess avidin-biotin-peroxidase complex was removed by a 5 minute wash in PBS and the sections reacted with diaminobenzidine (DAB: Vector Laboratories Ltd., USA) for visualisation of the biocytin-labelled cell. After a final wash in PBS (5 minutes) serial sections were floated, with aid of a paintbrush, onto gelatin-coated glass slides. After air-drying, the sections were dehydrated through alcohols (60 to 90 %) and mounted with a coverslip.

### *3.7.3. Camera lucida reconstruction of biocytin-labelled neurones*

The reconstruction and photomicrography of dLGN neurones labeled with biocytin was achieved with the aid of a microscope equipped with camera lucida and photomicrography facilities. Using a Leitz Diaplan microscope equipped with a camera lucida facility, biocytin-filled cells were reconstructed from each 70μm thick section at a magnification of 600x, using a 60x objective and 10x eyepiece. Each section containing a part of the biocytin-filled cell was drawn on tracing-paper and drawings were then overlaid in order to assess where the serial sections of the cell joined. The cell was then reconstructed on A3 paper in pencil using the camera lucida microscope and the complete cell reproduced on tracing-paper in indelible ink. The photographs of cells in this thesis were taken using a (Wild MPS52:Leica, Germany) camera attached to the microscope.

### *3.7.4. Morphometric analysis of biocytin-labelled cells*

The protocol for the morphometric analysis of the reconstructed biocytin-labelled cells was adapted from Snider, (1988). The cells were scored for: dendritic process length, the radius of a circle drawn with its centre the cell body and its radius the tip of the longest dendritic process; the extent of dendritic branching: the number of dendritic processes that crossed the perimeter of circle drawn at half the radius of the previous circle; the number of primary dendrites: each processes emanating from the cell soma a greater distance that the soma width. The longest diameter of the soma was measured and it was also noted if biocytin labeled the axon and/ or dendritic spines.

## 3.8. Statistical analysis

### *3.8.1 Analysis and graphical soft ware*

Excel was used for data manipulation and the construction of graphs. Graphs from Excel, data records from pCLAMP and the drawings of reconstructed cells were imported into Corel Draw (Corel Corporation Inc., USA) for construction of the illustrations. All statistical procedures were performed using Sigma Stat (Jandell Instruments, USA).

### *3.8.2 Statistical tests*

The Students t-test was used for the comparison of paired data groups. The Pearson Product Moment correlation was used to assess for independent and dependent variables. A two way analysis of variance (ANOVA) was used to determine global significant differences where two factors varied between groups (e.g. inoculation type and time point). Where the F ratio was significant, this was followed by post-hoc analysis for individual differences by the Student-Neuman-Keuls test. A one way ANOVA was used to determine the significant differences where a single factor varied between more than two groups. Similarly, the Student-Neuman-Keuls test was employed.

All results in this thesis are expressed as the mean ± the standard error of the mean (SEM). All data values in histograms and graphs are, similarly, expressed as mean ± SEM,

## The aims of this study

The purpose of this investigation was to characterise the effect of intraocular ME7 scrapie on the functional and morphological properties of dLGN relay cells in the mouse. In this experimental model there is an association between the onset of pathological changes and neuronal loss (Jeffrey et al., 1995). However the relationship between infection and dLGN dysfunction that must precede cell death is unknown. Specifically, I aimed to record from cells throughout the disease incubation period and interpret electrophysiological and morphological findings in terms of the published data concerning infectivity levels, and the temporal profile of disease pathology in the dLGN (see 1.3).

Investigations of murine thalamic relay neurones to date are limited to a brief description of whole cell recordings in ventro-posterior thalamic neurones (Warren et al., 1994). The membrane properties of murine relay cells, using sharp electrodes, have not been characterised; a considerable amount is known of the intrinsic properties of relay cells in the rat and guinea-pig which, collectively, function as a homogeneous population. Prior to investigating neuronal function in mice infected with ME7 scrapie it was necessary to establish if the electrophysiological properties of murine relay cells are comparable with those in the rat and guinea-pig, and therefore if the data from this study could be interpreted in the context of available literature. In addition a description of the membrane properties in dLGN cells in the normal mouse was essential as a control for possible adverse effects on neuronal function, attributable to the inoculation procedure.

In the first part of this study the electrophysiological properties of dLGN cells in the normal mouse were investigated; in particular I examined if, in terms of their properties, murine dLGN relay cells constitute a homogeneous population, as they do in the rat and guinea-pig. The primary aim of this study was to control for the parameters investigated in the control and infected mice; the protocols for collection of these parameters are detailed in 3.5. In normal mouse dLGN cells, the effect of several ion channels blockers on the membrane and action potential properties, were also monitored.

In the second part of this study similar parameters were investigated in dLGN cells in scrapie infected (scrapie-inoculated) and age-matched normal brain-inoculated (control) mice. When this project began, there were no published reports of the electrophysiological properties of single cells recorded in brain slice preparations of scrapie-infected models or in other encephalopathy models. In the first experimental series of animals investigated in this study, the aim was to monitor the basic membrane properties and morphological profiles of neurones in the scrapie-infected dLGN. During this project, Jefferys et al., (1994)

published their findings of abnormal synaptic and action potential properties in intracellularly recorded neurones in the scrapie-infected hippocampus (see 1.5). In light of these findings, a specific protocol was adopted to monitor the efficacy of the direct synaptic input from retinal ganglion to relay cells throughout the incubation period (see 3.5.4). This protocol, in which the maximum synaptic input or "maximum EPSP" to dLGN cells was quantified, was adopted from Cepeda et al., (1994); in the published study this method was used to compare the efficacy of synaptic input to human caudate neurones at different stages of development. Given that, in the scrapie experiments, recordings were obtained from cells at different temporal stages, in comparison this seemed a suitable method to employ; the maximum EPSP parameter was therefore quantified in normal mice. In the second experimental series of inoculated animals, the action potential properties were also monitored.

# Chapter 4

## Results:

## The functional properties of dLGN relay cells in normal, control and scrapie-infected mice

## 4.1 The properties of dLGN cells in the normal mouse

**The tables and illustrations relevant to the following description are situated after the text of section 4.1.**

*4.1.1 Voltage-activated membrane responses*

All 42 cells that satisfied the criteria for inclusion in this study possessed a stable resting membrane potential i.e. they did not fire action potentials at rest or show any sign of spontaneous electrical activity. At similar membrane potentials, all cells studied displayed the voltage activated membrane responses to current pulse injection illustrated in fig.10A and B. From a resting potential of -60 mV the injection of large negative current pulses resulted in an inward rectification, seen as a depolarising sag of the membrane potential (fig.10A, arrow 1). With incrementing hyperpolarising current pulses the sag became more pronounced. In response to the injection of positive current pulses of increasing amplitude there was an outward rectification of the membrane i.e. the deflection of the membrane potential was less than that observed with hyperpolarising pulses of equal amplitude (fig.10A, arrow 2). The onset of action potential firing (fig.10A, arrow 3) was delayed during a depolarisation from approximately -60 to -70 mV. Following termination of hyperpolarising pulses, the membrane potential was seen to overshoot rest by 10 - 30 mV; the overshoot response was composed of a slowly rising and decaying triangular shaped potential, approximately 40 to 60 ms in duration, which supported a burst of between four and seven high frequency spikes at its peak (fig.10A, arrows 4 and 5). The triangular response will be termed a low threshold spike.

From a more hyperpolarised level (see fig.10B), the negative current pulse resulted in a depolarising sag of the membrane potential, and a low threshold spike supporting a burst of fast spikes was triggered by the repolarisation of the membrane potential towards rest, identical to the responses in fig.10A. A similar response was evoked by depolarising pulses from the more hyperpolarised membrane potential (fig.10B, arrow B1). The onset of the low threshold spike was delayed and the rising phase prolonged when the response was initiated from membrane potentials between approximately -60 and -75 mV (fig.10B, arrow 2). The current-voltage profiles, in fig.10C, illustrate that the responses of the membrane potential to current injection were highly non-linear.

There were therefore no cells recorded in the dLGN that satisfied the criteria for inclusion in this study, that did not display the robust voltage activated membrane properties detailed above.

4.1.2 *Voltage activated currents: $I_{Na}$, $I_L$, and $I_T$*

Tetrodotoxin (TTX) blocks voltage-activated sodium conductances including $I_{Na}$ which mediates the rapid upstroke of the action potential in mammalian neurones; nickel chloride blocks the T-type and L-type calcium channels which, in thalamic relay cells, mediate low and high threshold spikes respectively (see 2.5.1). The effects of 0.5 μm TTX and 2 mM Nickel Chloride on murine dLGN cells function were investigated (fig.11).

The response of a dLGN cell to TTX (0.5 μM) is shown in fig.11B. TTX selectively abolished the fast spikes evoked both by direct depolarisation and those evoked by the low threshold spike (5 minutes: n = 5 cells in 5 slices). In the presence of TTX, positive pulses from a membrane potential of approximately -20 mV evoked a series of slow spikes of between 20 and 60 ms duration (fig.11D). The application of 2 mM nickel chloride, in the presence of TTX, subjectively reduced the amplitude of the triangular potential (fig.11C). The TTX-insensitive slow spikes evoked at membrane potentials depolarised to -20 mV, were not observed in the presence of nickel chloride (10 minutes: n = 3 cells). The effects of nickel chloride were associated with a decrease in membrane conductance, seen as an increase in the amplitude of the voltage deflection in response to current injection (see panels in fig.11C).

*4.1.3 Basic membrane properties of dLGN cells in the normal mouse*

The mean resting membrane potential, action potential threshold, input resistance and time constant of all 42 murine dLGN cells sampled are detailed in table 1; published values for these parameters are also shown. The distribution of the values for the basic membrane properties studied in murine dLGN cells, are illustrated in figs.12 and 13 (fig.12A, resting membrane potential B, action potential threshold; fig.13A, input resistance B, time constant). The action potentials initiated at threshold by a positive current injection maintained a steady rate of discharge without any evidence of frequency adaptation.

Scatter plots were constructed in order to assess if, in terms of the basic membrane properties, the cells sampled functioned as a homogeneous population. Plots of the input resistance, action potential threshold and membrane time constant against input resistance,

and the membrane time constant against input resistance are shown in fig.14; the correlation coefficient (C) calculated by the Pearson Product Moment correlation, and the associated significance level (p), for each set of variables are shown above each plot in panels A-D. The population spread of the variables plotted appears homogeneous; in terms of these properties in the cells studied, there are not any focal clusters of data points that would suggest the existence of more than one population of cells. The action potential threshold, time constant and input resistance were independent of the resting potential; the input resistant and time constant were clearly dependent (fig.14D).

*4.1.4 Action potential parameters*

Two approaches are used for the collection of action potentials for analysis in published studies (see 3.5.3). In fig15. A-C, for three cells, the average shape of action potentials initiated at threshold are aligned with the average shape of action potentials evoked from 2 mV below threshold. Mean values for the spike and AHP amplitude, spike rise and decay time and spike half width of the initiated and evoked action potentials, obtained in 27 cells, are detailed in table 2. Comparison of the action potential shapes demonstrates that the spike amplitude is significantly larger ($p < 0.001$, Paired t-test), and the fast AHP significantly smaller ($p = 0.04$, Paired t-test) in the action potentials evoked at 2 mV below threshold. The increment in spike amplitude in the evoked action potentials was 5.7 ± 0.8 mV and the reduction in fast AHP amplitude, 0.9 ± 0.2 mV. There was a significant correlation ($C = 0.65$; $p = 0.04$: Pearson Product Moment correlation) between the increment in evoked spike amplitude and threshold in those cells with a firing threshold positive to -45 mV ($n = 10$ cells). This correlation was not significant in cells with thresholds between -46 and -50 mV ($C = 0.52$; $p = 0.28$; $n = 7$)) and negative to -50 mV ($C = -0.22$; $p = 0.53$; $n = 10$).

The average spike shape obtained from firing initiated at threshold is illustrated for three cells in fig.15 D-F. In each cell studied the repolarisation following the peak of the action potential was biphasic. In the examples in fig.15 a rapid hyperpolarising phase of the action potential, lasting several milliseconds (open arrow), is followed by a slower phase (filled arrow) that could delay the return of the membrane potential to threshold (T) by up to 100 ms. The different profiles of the slow after-hyperpolarisation (slow AHP) illustrated in fig.15 D-F (and A-C), were evident in the proportion 13:12:2 in the sample of 27 cells studied.

For the average shapes of action potentials initiated at threshold, the spike and fast AHP amplitude against threshold, and the fast AHP amplitude against spike amplitude are plotted in fig.16A-C. There was a significant inverse relationship between the action potential threshold and spike amplitude ($C = -0.53$; $p = 0.006$, Pearson Product Moment correlation) and between threshold and fast AHP amplitude ($C = -0.57$; $p = 0.002$). The correlation between spike amplitude and AHP amplitude was not significant ($C = 0.366$; $p = 0.066$). The scatter of the plots are consistent with the action potentials behaving as a single population.

*4.1.5 The slow AHP: sensitivity to the SK channel blocker apamin*

The slow AHP in thalamic cells has not been characterised. A similar hyperpolarising potential is mediated by the current $I_{AHP}$ in a number of mammalian neurones (see 2.5.2). In this study the effects of apamin, which selectively blocks the SK calcium-activated potassium channels mediating $I_{AHP}$, were monitored in 6 dLGN cells.

Fig.17A-C illustrates the effect of 100 nM apamin on the average action potential shape in three murine dLGN cells. The spike shapes obtained in control and apamin-containing medium are superimposed. The spike shape parameters measured before and after exposure to apamin are shown in table 3; the parameters measured in control and apamin-containing medium were not significantly different ($p > 0.05$, Paired t-test).

The amplitude of the slow AHP was dramatically reduced in the presence of apamin; the profile of the apamin-sensitive component in each cell (obtained by subtraction of the spike shape in apamin-containing, from that in control medium) is shown in the inset of panels A-C in fig.17. The peak amplitude of the apamin-sensitive component was $3.52 \pm 0.34$ mV, the rise time to peak was $9.72 \pm 1.3$ ms and the duration $65.2 \pm 2.9$ ms ($n = 6$ cells). The effect of apamin on the voltage activated membrane responses of a dLGN relay cell are shown in fig.18. In control medium, the cell exhibited membrane response properties typical of the murine dLGN cells (see 4.1.1). After 15 minutes in apamin-containing aCSF, an identical depolarising pulse protocol initiated action potentials with an apparent increased frequency of discharge. In response to identical hyperpolarising pulses, there appeared to be an increase in the duration of the low threshold spike and a greater number of fast spikes were elicited at the peak of this potential. The arrows in the lower panels of fig.18A and B, indicate the time point at which values were taken to construct the current-voltage profile in fig.18C. This plot illustrates that there was not a discernible

difference in the somatic input resistance of the cell in control and apamin-containing medium.

*4.1.6 The maximum EPSP*

In dLGN relay cells at a membrane potentials of -60 mV, stimulus intensities between 1 and 39 Volts evoked the $EPSP_M$. At similar membrane potentials all five cells studied showed the membrane responses to the $EPSP_M$, illustrated in fig.19A-C. An example of the $EPSP_M$ in a mouse dLGN cell is illustrated in fig.19B. The peak amplitude of the $EPSP_M$ was 5.96 ± 1.72 mV, the rise time of the $EPSP_M$, 2.67 ± 0.33 ms and the decay time, 27 ± 7.0 (n = 5 cells). When the membrane potential was depolarised from rest, the post-synaptic response evoked an action potential (fig,19A) and at hyperpolarised levels, (e.g. -74 mV in fig.19C), a low threshold spike and burst of action potentials was evoked.

| Species | Resting membrane potential (mV) | Time constant (ms) | Input resistance (MΩ) | Action potential threshold (mV) |
|---|---|---|---|---|
| A. Mouse | -59.2 ± 0.82 | 22.3 ± 2.53 | 86.9 ± 6.62 | 64.84 ± 1.5 |
| B. Rat | -60 ± 0.15 | 19.4 ± 0.17 | 59 ± 0.26 | 77 ± 0.15 |
| C. Guinea-pig | -64 ± 0.39 | - | 42 ± 0.74 | - |
| D. Guinea-pig | -65 ± 0.38 | - | 51 ± 0.62 | 79 ± 0.38 |

**Table 1.** Intrinsic properties of thalamic relay cells recorded intracellularly in brain slice preparations in A, mouse dLGN (this study: n = 42) B, rat dLGN (Crunelli et al., 1987a: n = 44) C, guinea-pig thalamic nuclei (Jahnsen and Llinas, 1984a: n = 34) D, guinea-pig dLGN (McCormick and Prince, 1987: n = 50).

| Method | Spike amplitude (mV) | AHP amplitude (mV) | 10 - 90 % rise time (ms) | 10 - 90 % decay time (ms) | half width (ms) |
|---|---|---|---|---|---|
| T | 56.1 ± 0.94 | 8.74 ± 0.40 | 0.53 ± 0.03 | 0.58 ± 0.03 | 0.57 ± 0.02 |
| T - 2 | 61.8 ± 0.91 | 7.82 ± 0.34 | 0.60 ± 0.04 | 0.59 ± 0.02 | 0.56 ± 0.02 |
| | p <0.001 | p = 0.04 | p = 0.14 | p = 0.57 | p = 0.65 |

**Table 2.** Comparison of paramaters in averaged action potentials, in 27 cells, initiated at threshold (T) and 2 mV below threshold (T -2). The significance levels associated with the Paired t-test are shown (p).

| Protocol | Spike amplitude (mV) | AHP amplitude (mV) | 10 - 90 % rise time (ms) | 10 - 90 % decay time (ms) | half width (ms) |
|---|---|---|---|---|---|
| Control | 59.4 ± 2.3 | 10.3 ± 0.94 | 0.52 ± 0.05 | 0.52 ± 0.05 | 0.58 ± 0.05 |
| Apamin | 59.8 ± 1.86 | 9.7 ± 1.1 | 0.51 ± 0.09 | 0.54 ± 0.04 | 0.61 ± 0.05 |
| | p = 0.76 | p = 0.17 | p = 0.90 | p = 0.80 | p = 0.72 |

**Table 3.** Comparison of parameters in average action potential shapes, initiated at threshold, in normal and 100 nM apamin-containing aCSF (n = 6). The significance levels associated with the Paired t-test are shown (p).

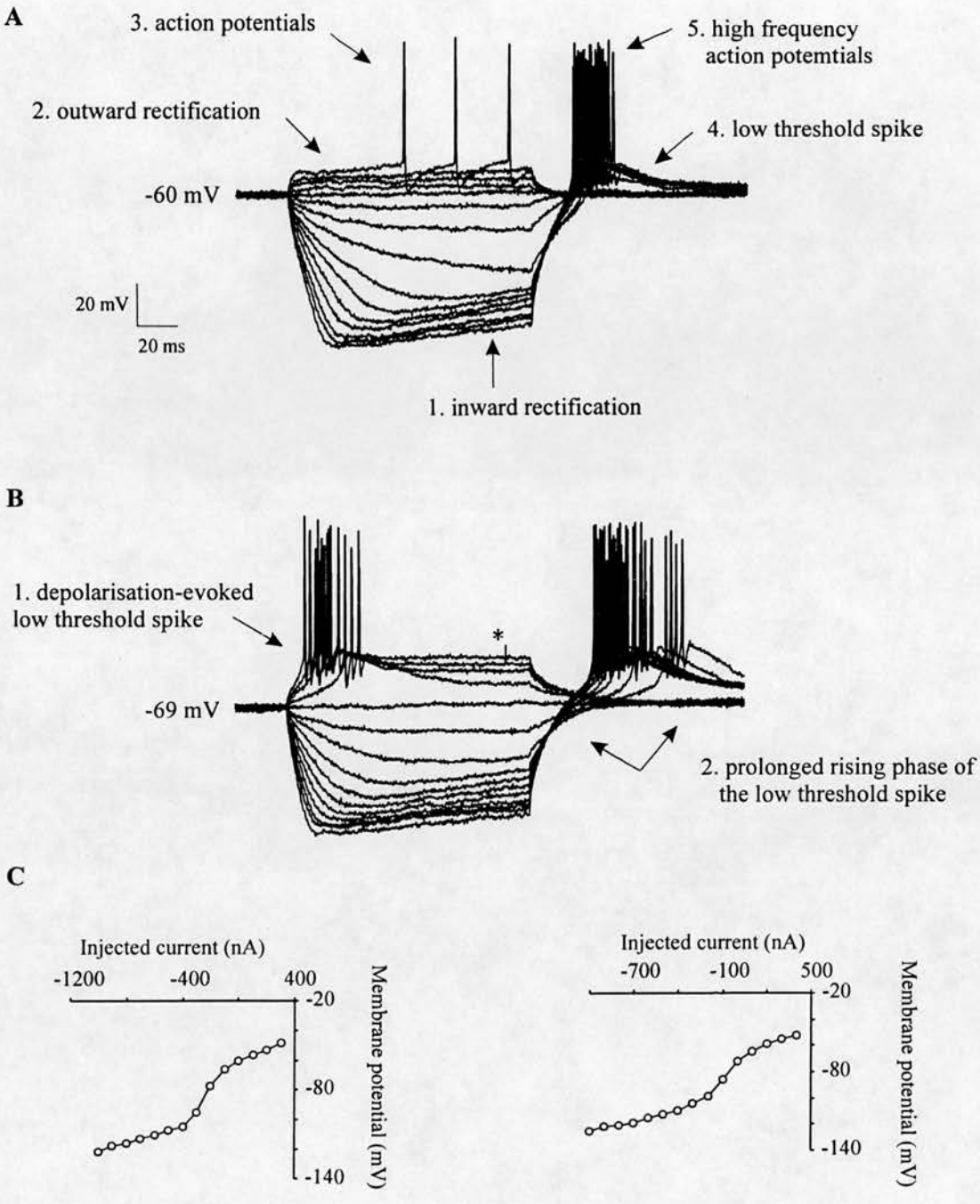


**Fig.10.** Membrane responses of a murine dLGN cell to intracellular current injection. All 42 cells studied displayed the pattern of activity shown in panels A and B, when at similar membrane potentials (profiles generated by 100 ms, -1.0 to 0.4 nA current pulses. A1, large hyperpolarising pulses result in a depolarising sag of the membrane potential (inward rectification). A2, outward rectification and a delay to the onset of spike discharge in respons to depolarising pulses. A3, fast spikes (action potentials) evoked by depolarisation. A4, triangular shaped potential (low threshold spike: LTS) is evoked by repolarisation of the membrane potential at the termination of hyperpolarising pulses. A5, the LTS promotes a burst of action potentials. B1, from a membrane potential negative with respect to resting membrane potential, the LTS is evoked by depolarising and hyperpolarising pulses. B2, the onset of the LTS is delayed when triggered by depolarising and hyperpolarising current from this membrane potential. C, current voltage profiles of the dLGN cell responses illustrated in A and B are shown in the left and right panels, respectively; profiles, calculated from the time indicated by the asterisk in B, show that the cell displays marked non-linear membrane response properties.

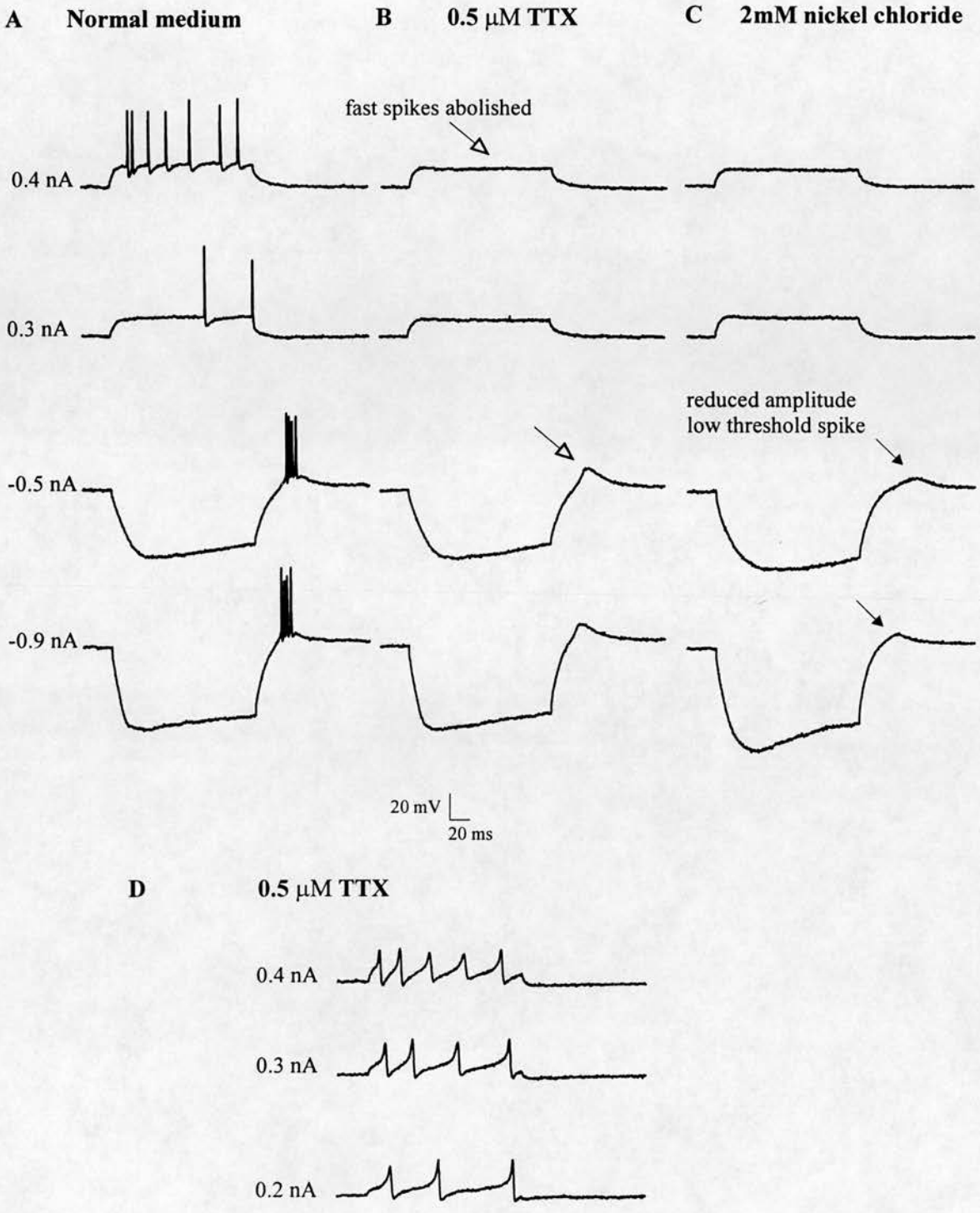


**Fig.11.** The effects of 0.5 mM TTX and 2mM nickel chloride on the membrane response properties of a murine dLGN cell. A, membrane response to current pulses from -53 mV in normal aCSF (normal medium). B, in TTX-containing medium an identical protocol fails to evoke action potentials (open arrows). C, nickel chloride reduces the amplitude of the low threshold spike (filled arrows). In the presence of TTX only, depolarising current pulses from approximately -24 mV reveal the pattern of firing shown in D. This activity was abolished by nickel chloride.

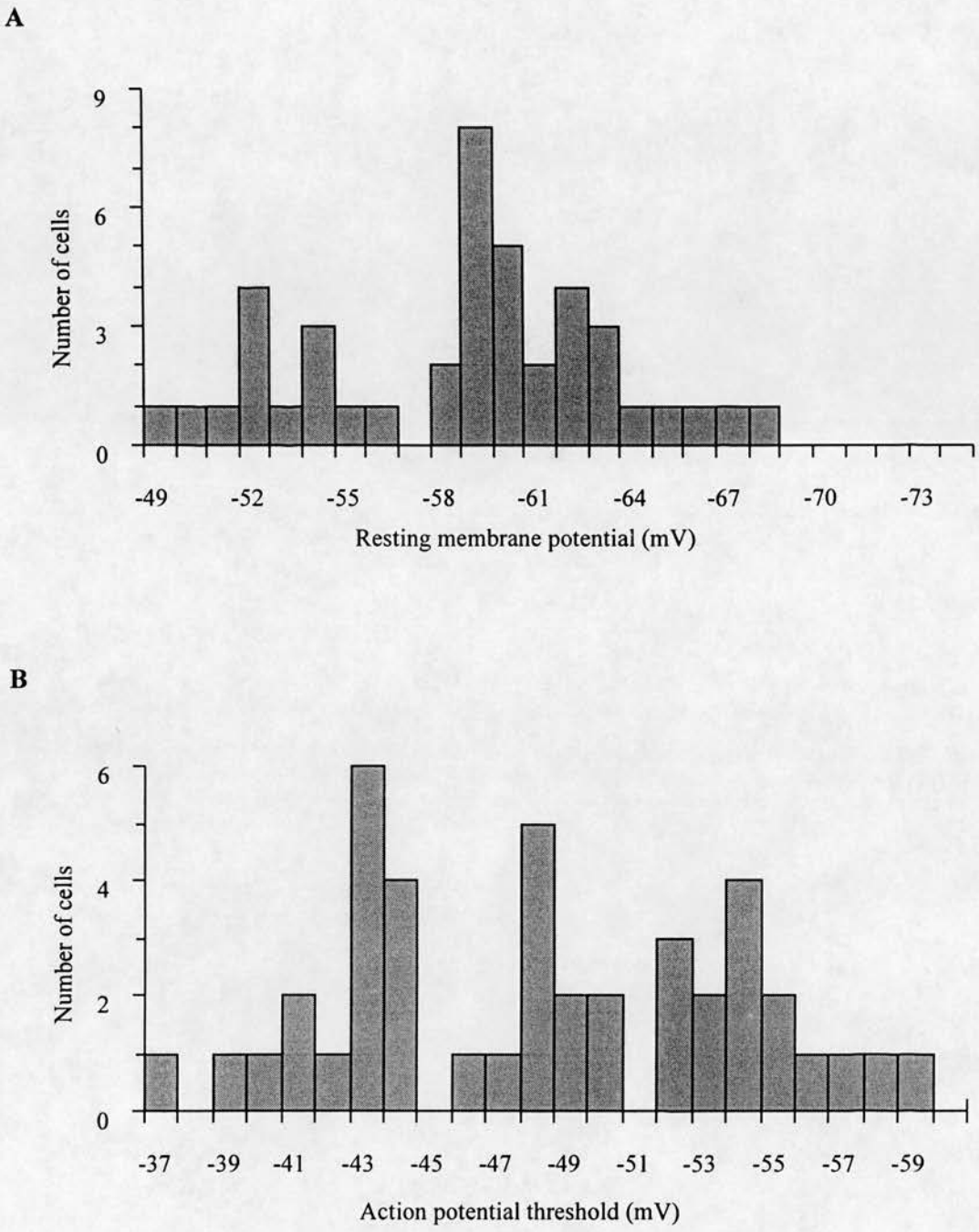


**Fig.12.** For 42 murine dLGN cells, the distribution of A, resting membrane potential and B, action potential threshold. The resting membrane potential is the voltage recorded intracellularly in the absence of injected current. B, action potential threshold is the voltage at which constant amplitude current initiated action potentials at 1-2 Hz. (The action potential thresholdand membrane potential are plotted on a reverse scale.)

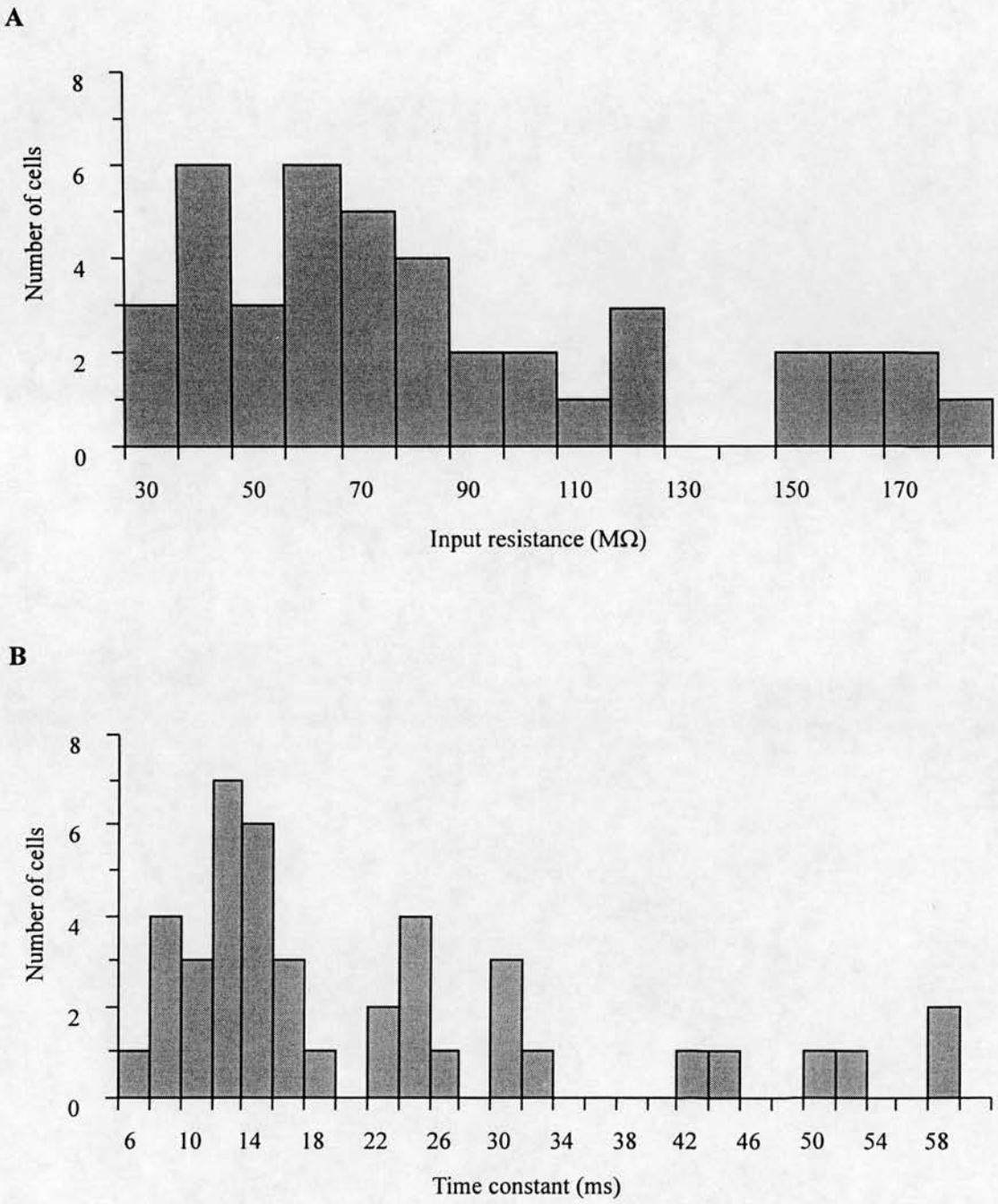


**Fig.13.** For 42 cells the distribution of A, membrane input resistance and B, time constant. Input resistance and time constant measured from the voltage deflection to a -0.2 nA current pulse from a holding potential of -60 mV; input resistance measured 100 ms after onset of the current pulse and time constant, time taken for the membrane to decay to 63 % of steady state.

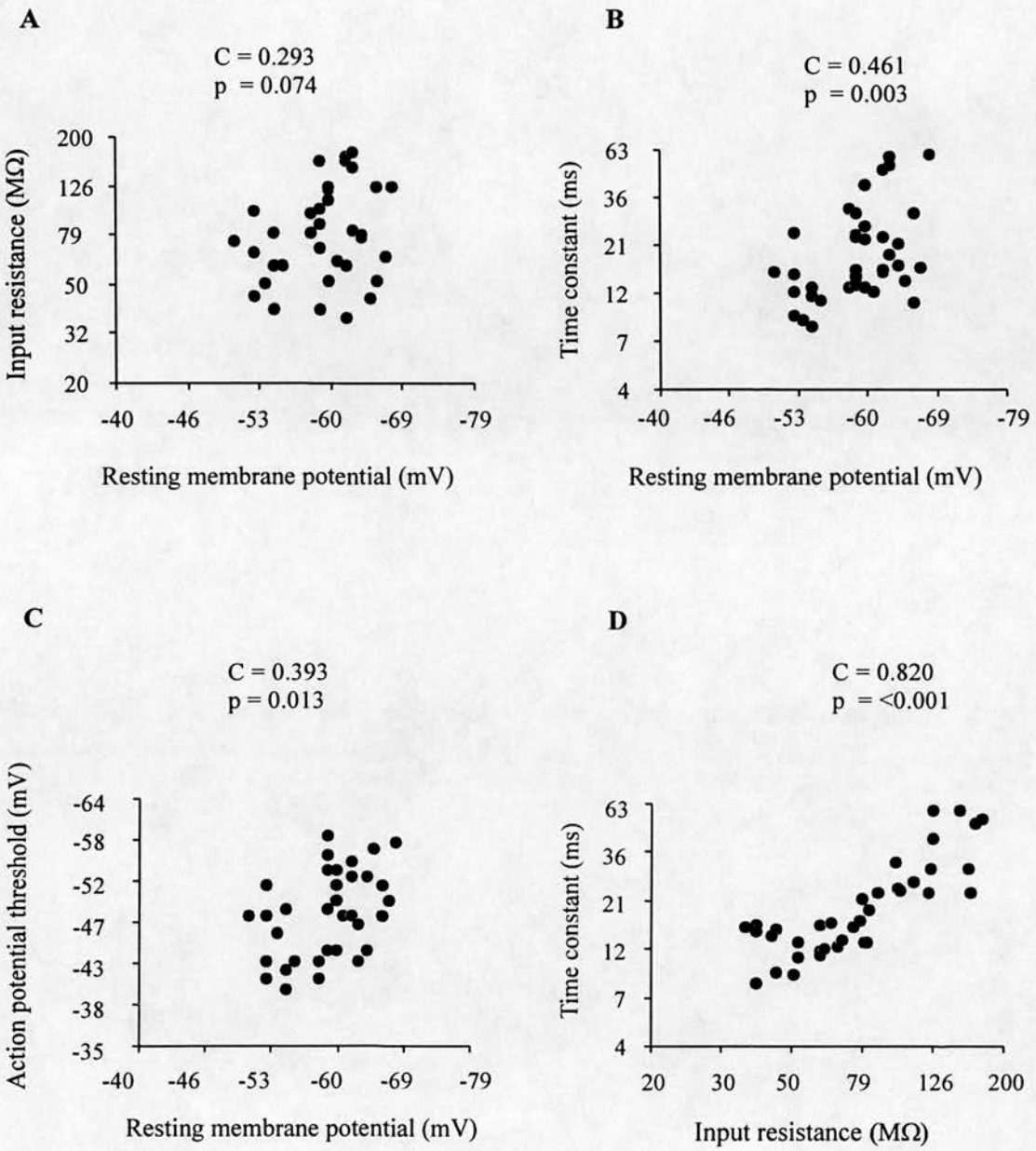


**Fig.14.** For 42 dLGN cells, scatter plots illustrate the relationship between A, resting membrane potential and input resistance B, resting membrane potential and time constant C, resting membrane potential and threshold and D, input resistance and time constant. The correlation coefficient (C) and significance level (p) associated with the Pearson Product Moment correlation are shown above each panel. The values for each parameter have been plotted on a logarithmic (and a reverse scale for resting potential and threshold), scale intervals rounded up to the nearest whole number. The scatter in each of panels A-D appears consistent with a homogeneous sample of murine dLGN cells. There is a significant correlation between the input resistance and time constant in the sample studied (D).

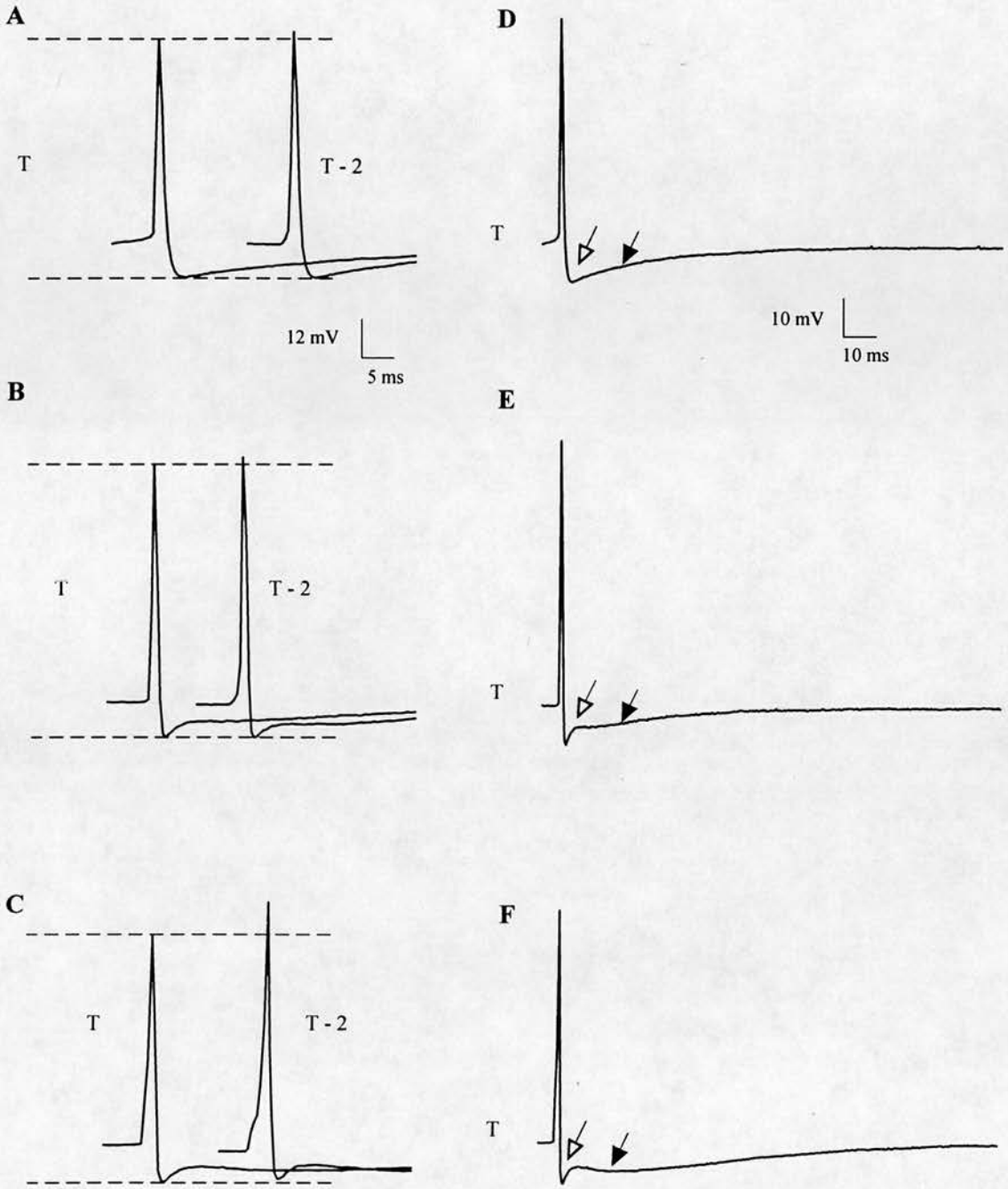


**Fig. 15A-C** (see 4.1.4), comparison of average shapes in action potentials initiated at threshold (T) and evoked at 2 mV below threshold (T-2) in 27 dLGN cells. The spike amplitude in evoked action potentials is significantly larger ($p < 0.001$, Paired t-test) and the fast AHP amplitude significantly smaller ($p = 0.04$, Paired t-test) than in initiated action potentials. D-F, average shapes of action potentials initiated at threshold showing a fast (open arrow) and slow (filled arrow) AHP; slow AHP profiles in D, E and F were found in the proportion 13:12:2 in the population studied.

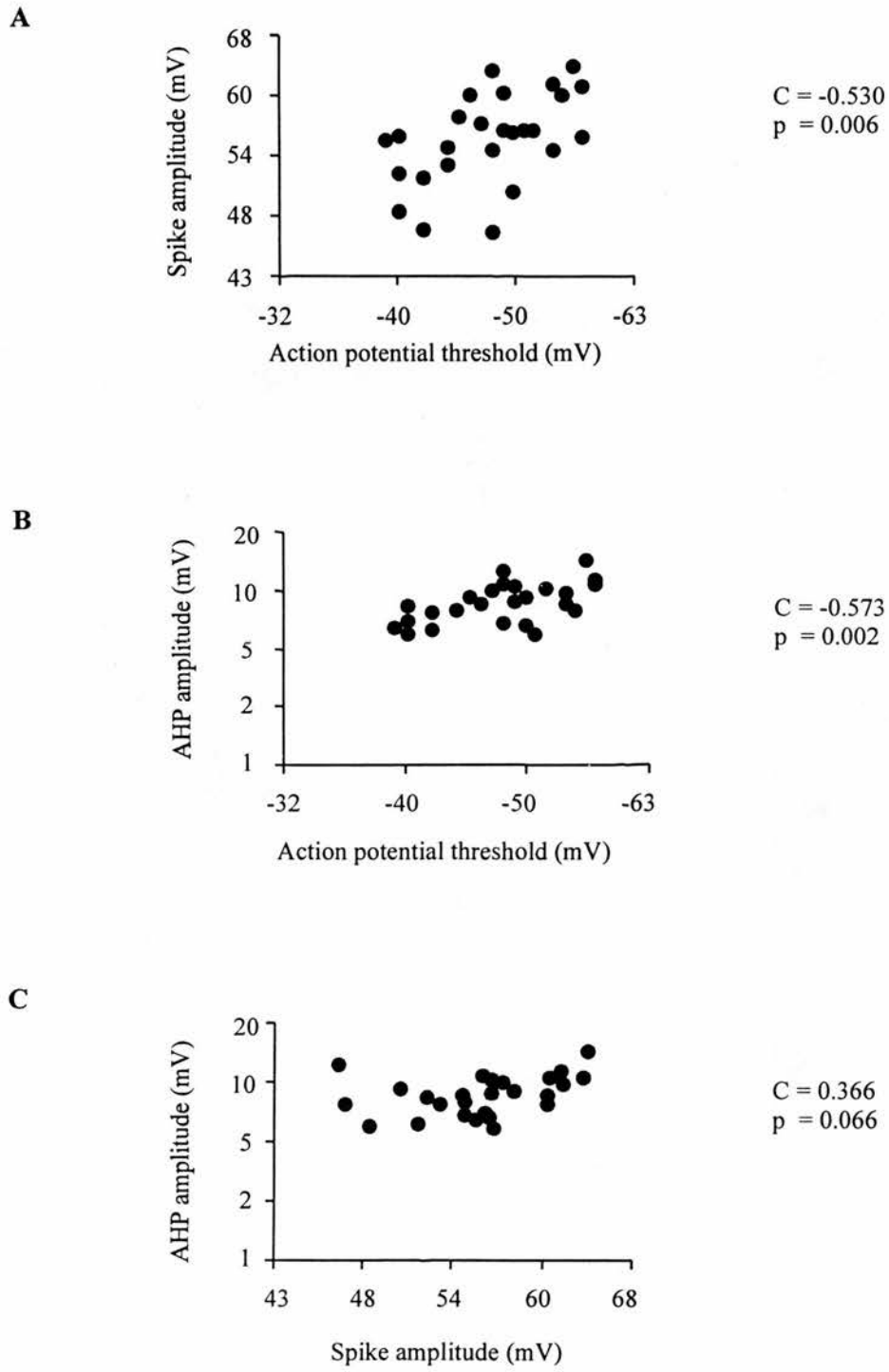


**Fig.16.** Scatter plots illustrating, for 27 cells, the relationship between A, spike amplitude and threshold B, AHP amplitude and threshold and C, spike and AHP amplitude. The correlation coefficient (C) and the significance level (p) associated with the Pearson Producr Moment correlation are shown beside each panel. The values for each parameter are plotted on a logarithmic scale (and for threshold on a reverse scale), the scale intervals rounded up to the nearest whole number. The scatter of the action potential parameters in A- C is consistent with a homogeneous population. As expected from the respective scatter plots, the correlation between threshold and both AHP and spike amplitude is significant.

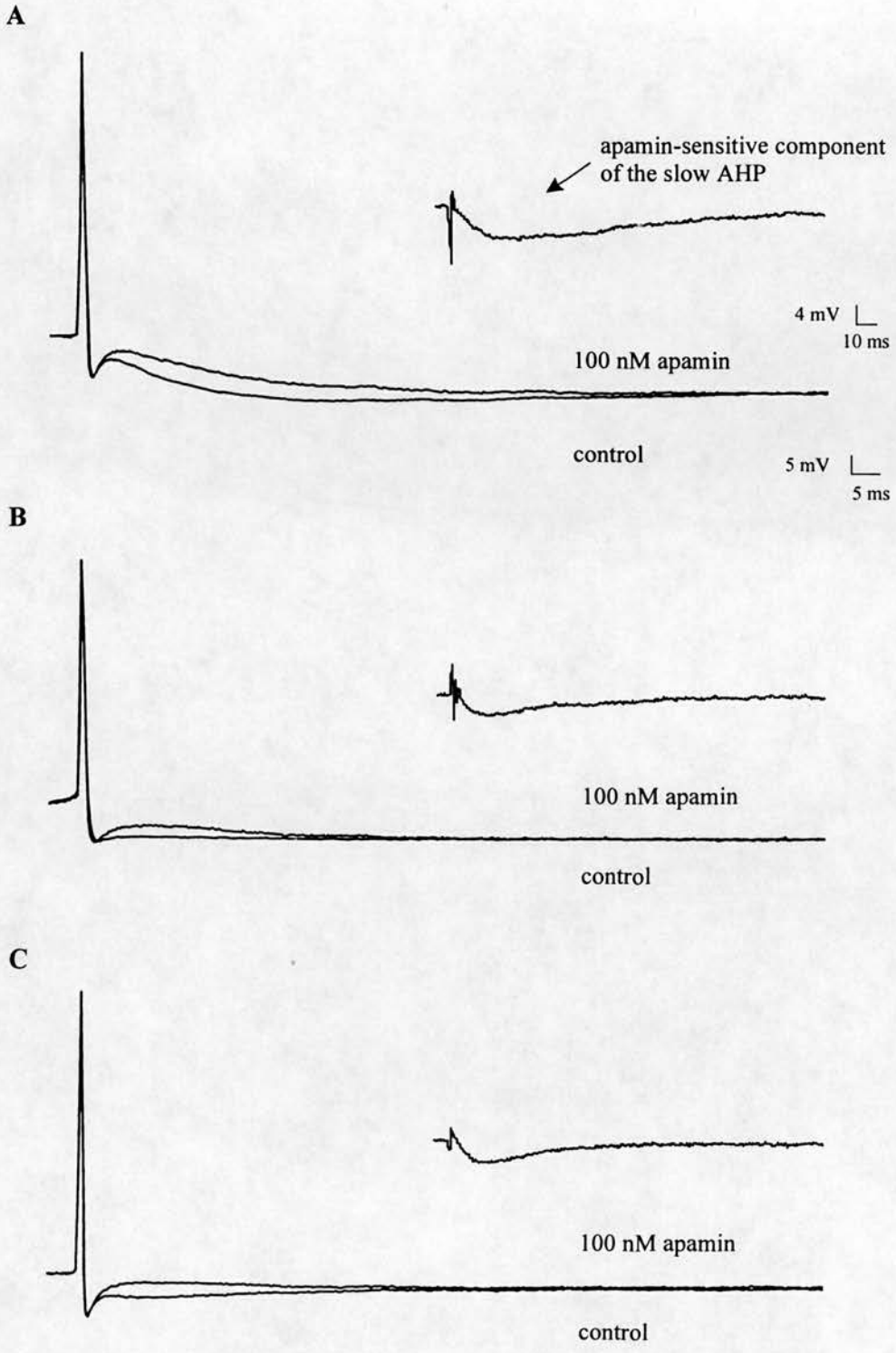


**Fig.17.** Apamin (100nM) selectively abolished a component of the slow AHP following the action potentials in murine dLGN cells. A-C, the average shapes in control (normal aCSF) and apamin-containing medium are superimposed. Panels A-C *inset;* the apamin-sensitive component of dLGN cells, obtained by subtraction of the spike shapes (with the peak of the spike as the central reference point), is shown. Apamin did not significantly alter the action potential parameters quantified ($p > 0.05$; see 4.1.5).

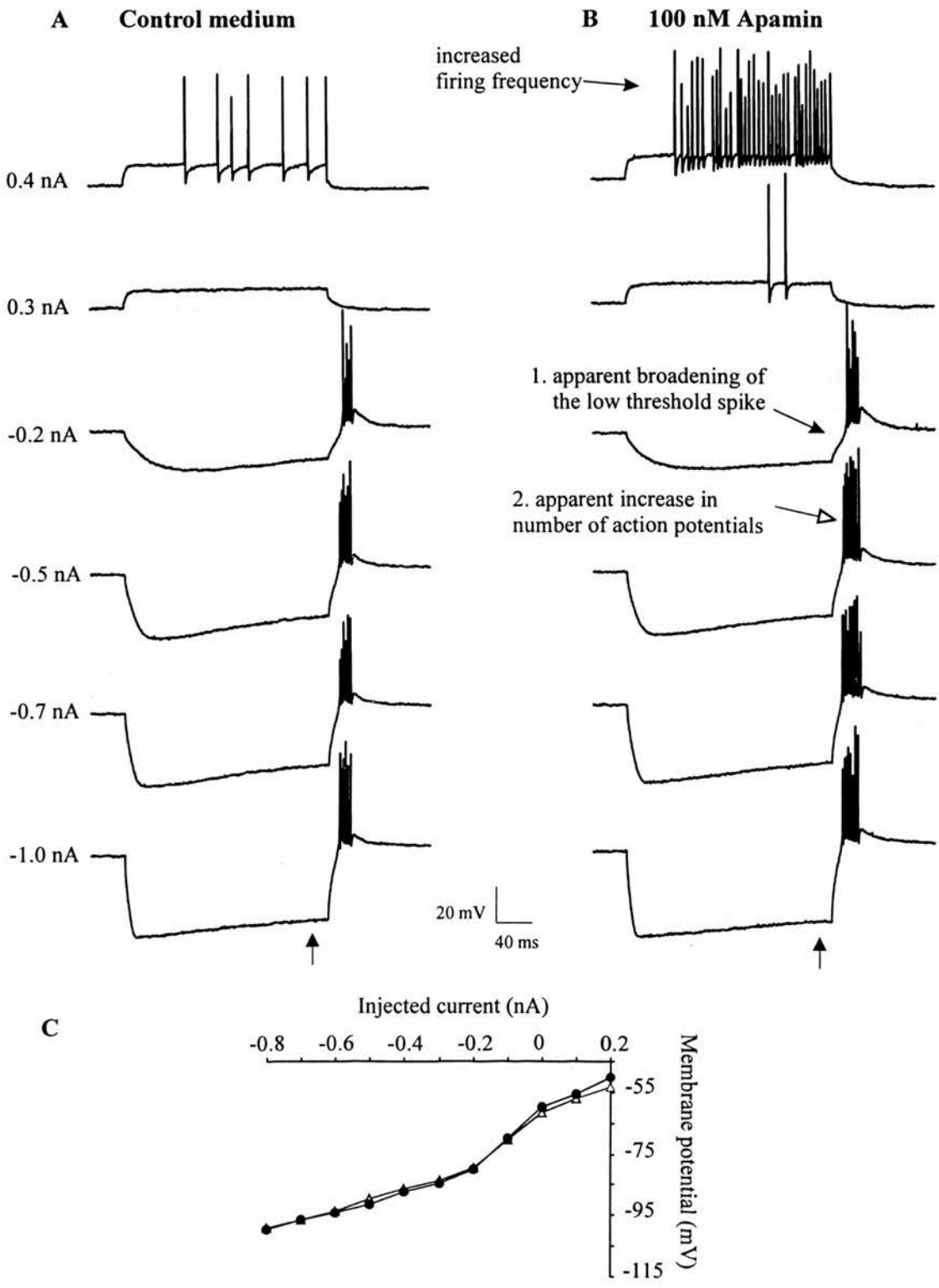


**Fig.18.** A, response of a dLGN cell to current pulse injection in control (normal aCSF) and B, apamin-containing medium. B *top panel*; action potentials are evoked at a higher frequency in the presence of apamin. Subjective comparison of the panels in A and B reveals that, in the presence of apamin, the low threshold spike is broadened (B1) and this response evokes an increased number of fast spikes (B2). C, the current-voltage profile of the cell in control (filled circles) and apamin-containing (open triangles) medium; profile calculated for the time point illustrated by the asterisk in the lower panels of A and B. The 6 cells tested exhibited a similar pattern of activity in the presence of 100 nM apamin, indicating that this component has a role in regulating the action potential discharge.

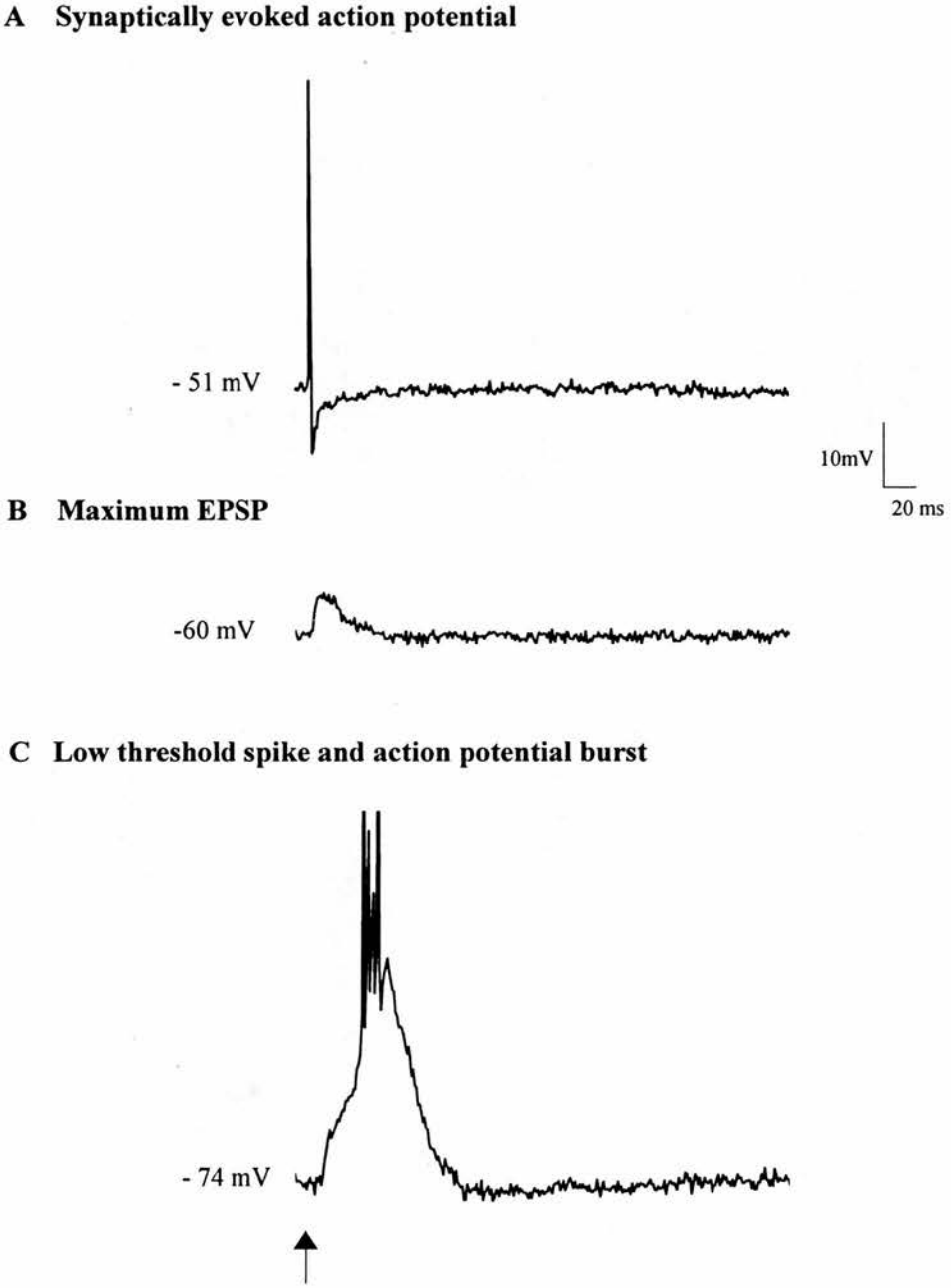


**Fig 19**.Response of murine dLGN cell to afferent optic tract stimulation. A, action potential evoked by the EPSP. B, the maximum $EPSP_M$ (the maximum amplitude EPSP that is subthreshold to action potential firing when evoked at -60 mV). C, with hyperpolarisation of the membrane the post-synaptic response evoked a triangular potential (a low threshold spike) which depolarised the cell to the firing threshold for action potentials (action potentials are truncated in panel C). The filled arrow in C indicates the time point of optic tract stimulation.

## 4.2 The properties of dLGN cells in control and scrapie-infected mice

Despite the expectation of a progressive deterioration in the electrophysiological properties of neurones in the dLGN, this study revealed that only cells with normal action potential, basic membrane, optic tract-evoked and morphological properties were recorded in scrapie-infected mice:

### *4.2.1 Behavioural observations*

Until approximately 240 - 250 days post-inoculation in both experiments, control and scrapie-infected mice appeared healthy and were physically active in their cages. The mice appeared alert and their coats well groomed. Mice became progressively inactive during the last 4 weeks of the incubation period, neglected grooming and became indifferent to handling.

### *4.2.2 Recordings from brain slice preparations in control and scrapie-inoculated mice*

Five control and five scrapie-inoculated mice in each series were studied at the incubation period intervals: 57 - 63, 85 -90, 110 - 115, 138 - 143, 166 - 171, 195 - 200 and 220 - 230 days post-inoculation. The intervals are abbreviated to 60, 88, 112, 140, 168, 198 and 225. The mean incubation period in the two experimental series of mice was 277 ± 3 (n = 12 mice) and 274 ± 4 (n = 10 mice) days. The similarity of the incubation period lengths justified the combination of data collected from each experiment.

In the first experiment, recordings from dLGN relay cells in scrapie-inoculated mice were achieved during the intervals up to, and including, 225 days post-inoculation; no cells (not even poor impalements) could be recorded in the dLGN of scrapie-infected slices at 250 days post-inoculation (n = 4 slices from 4 animals). In the second experiment, a lack of cells was noted at the earlier stage of 225 days post-inoculation. In order to determine if this inactivity at the earlier stage was due to scrapie infection in the dLGN, or due to external insult during slice preparation, an extracellular field EPSP was recorded in the hippocampal CA1 subfield of control and scrapie-infected slices. Qualitatively, similar maximum field potentials were obtained in control and scrapie-infected mice (fig. 20), but cells were impaled in the dLGN of the control but not the scrapie-inoculated slices. This suggests that the inactivity in the dLGN was not due to compromise during slice preparation and may be disease specific.

The border of the dLGN is easily identifiable in the coronal brain slice preparation. An observation made during these experiments was that the dLGN appeared to occupy a reduced area of the brain slice in infected mice from 200 days post-inoculation.

In the following description the basic membrane, action potential, optic-tract evoked and morphological properties of dLGN cells in control and scrapie-inoculated mice, are reported. As stated in the aims preceding this chapter, the first experiment (in which cells were recorded until 225 days post-inoculation in the infected mice) concentrated on studying the basic membrane and morphological properties of dLGN cells. In the second experimental series of animals (in which cells were recorded in infected animals until 200 days post-inoculation) the action potential and synaptic properties of these cells were investigated. Therefore the basic membrane and morphological properties in infected and control animals are reported for up until 225 days in the incubation period, and for the action potential and synaptic properties, until 200 days in the incubation period.

*4.2.3 Voltage-activated membrane responses in control and scrapie-inoculated mice*

The 71 cells in control, and 88 in scrapie-inoculated mice that satisfied the criteria for inclusion in this study (see 3.5.6) were recorded throughout the spatial extent of the dLGN. The cells detailed in this study possessed a stable resting membrane potential i.e. there was no sign of spontaneous electrical activity. All cells recorded at each incubation period interval in control and scrapie-infected mice displayed similar membrane responses to current injection to those in normal mouse dLGN cells (see 4.1.1 and fig. 10). The population of current voltage profiles in dLGN cells in control and scrapie-inoculated also were similar to those seen in normal mouse dLGN cells. Membrane responses to current injection profiles observed in control and scrapie-inoculated mice at 68, 140 and 220 days post-inoculation, are shown in the left panels of figs. 21 - 23 respectively. In each figure the right hand panel illustrates the current-voltage profiles of each cell; the data is shown in association with records from normal mouse dLGN cells.

The response properties of the 29 cells from control, and the 22 from scrapie-inoculated mice that did not satisfy the criteria were indistinguishable from the results of poor impalements in slices from normal mice. From a subjective assessment, these cells were recorded spatially throughout the extent of the dLGN; poor impalements were recorded during all incubation period intervals.

*4.2.4 The analysis of dLGN cell properties in control and scrapie-infected mice*

The analysis protocol detailed below refers to the comparisons between the basic membrane properties (4.2.5), action potential properties (4.2.6) and maximum EPSP ($EPSP_M$) properties (4.2.7) in dLGN cells of normal, control and scrapie-inoculated mice:-

(*i*) *Inoculation procedure test.* The values in normal mice were compared with the data at each incubation period interval in control mice to assess the effects of the inoculation procedure (one way ANOVA).

(*ii*) *Age-related test.* The values at all intervals within the control and the scrapie groups were compared to assess for age-related changes in membrane properties (incorporated in the two way ANOVA).

(*iii*) *Treatment test.* At each incubation period interval the data in the control and scrapie groups was compared to assess for an effect due to scrapie infection (incorporated in the two way ANOVA).

(*iv*) *Pooled test.* In both the control and scrapie groups the values from all incubation period intervals was pooled; the pooled data in control and scrapie groups were compared (Paired t-test).

(*v*) *Regrouped test.* The data in the incubation period intervals from the scrapie-infected mice was regrouped: 60 - 112 days, 140 - 168 days, 198 - 225 days; the data in the regrouped intervals were compared with the pooled infection test group data *(iv)* in control mice (one way ANOVA).

The number of cells in which each dLGN cell parameter was studied are detailed in table 4. In each of the analysis groups (*i* - *iv*) detailed above, the data collected for the $EPSP_M$ at 60 days, and the action potentials at 88 days is discounted. This is due to a sample number of one in the respective data groups. Tables containing the mean values for analysis groups *i* - *v* and the significance levels associated with the tests are situated at the end of the text. The illustrations referred to in the text are placed after the tabulated data.

*4.2.5 Basic membrane properties in dLGN cells of control and scrapie-infected mice*

The mean resting membrane potential, action potential threshold, input resistance and time constant in control and scrapie-inoculated mice at each interval, are detailed in table 5 and the pooled and regrouped values in table 6. The significance values associated

with the analysis of these parameters (see *i* - *v* in 4.2.4) are detailed in table 7. The only significant difference found between the basic membrane properties was revealed by the *regrouped data test*. The firing threshold in the data group 198 - 225 days in scrapie-inoculated mice, was significantly lower than the threshold in the pooled data group (60 - 230 days) in the control mice ($p = 0.02$, one way ANOVA). The temporal profile of the mean resting membrane potential (fig.24A), action potential threshold (fig.25A), input resistance (fig.26A) and time constant (fig.27A) are shown. Panel B in each figure illustrates the mean values associated with the *regrouped* data.

Scatter plots were constructed to assess the homogeneity of the cells sampled, and assess the population spread of the basic membrane properties in dLGN cells of control and scrapie-inoculated mice. Plots of the input resistance, time constant and action potential threshold against resting membrane potential, and the time constant against input resistance are shown in figs.28 - 31. In each figure, the variables in control and scrapie-inoculated mice at 68, 140 and 230 days post-inoculation are shown in association with the data obtained in the study of normal mouse dLGN cells (see 4.1.3). The scatter of the relationships between resting membrane potential and input resistance, time constant and action potential threshold and also input resistance and time constant for both control and scrapie-inoculated groups appear homogenous with the population of normal mouse cells.

*4.2.6 The action potential properties in dLGN cells in control and scrapie-inoculated mice*

The action potential properties in the dLGN cells of control and scrapie-inoculated mice at 60, 112, 140, 168 and 198 days post-inoculation are detailed in table 8. The mean values for the *pooled* and *regrouped* data are shown in table 9 and the significance values associated with analysis (*i* -*v*) in 4.2.4 are shown in table 10. The parameters of the averaged action potentials shapes measured were the spike and AHP amplitude, the spike rise and decay time and the spike half width. Of the parameters investigated the only significant difference was found using the *age-related change test*: the spike rise time at 112 days ($n = 2$ cells) was significantly greater in duration than the values in action potentials at 140, 168 and 198 days ($p < 0.05$, two way ANOVA); the rise time at 56, 140, 168 and 198 were not significantly different. The average shapes of action potentials initiated at threshold in control and scrapie-inoculated mice at 198 days post-inoculation are shown in fig.32. The average spike shapes were from a train of spikes attained at threshold. The average spike shapes in both inoculated groups exhibited both a fast and slow phases of after-

hyperpolarisation. The mean values of the spike parameters at each interval, in control and scrapie-inoculated mice, are shown in panel A of figs, 33 -37. In panel B of these figures the mean values of the regrouped data groups used in analysis (*v*) detailed in 4.2.4, are shown.

Scatter plots illustrating the different relationships between the spike amplitude, AHP amplitude and threshold, at three incubation period intervals (60, 140 and 198 days post-inoculation), in control and scrapie-inoculated mice are shown in figs.38, 39 and 40. For comparison, the data in the control and scrapie-inoculated groups is shown in association with the data in the normal mouse. The sample sizes obtained in control and scrapie inoculated mice were insufficient to consistently perform correlations on the data at each interval. However in plotting the variables in association with the normal mouse data (figs.38, 39 and 40) it can be seen that population spread of the relationships between action potential properties appeared consistent with scatter of these variables in the normal mouse population.

*4.2.7. The maximum EPSP in control and scrapie-inoculated mice*

The properties of the maximum EPSP in the dLGN cells of control and scrapie-inoculated mice at 88, 112, 140, 168 and 198 days post-inoculation are detailed in table 11. The mean values for the pooled and regrouped data are shown in table 12 and the significance levels associated with the statistical comparisons (4.2.4:*i* - *v*) are shown in table 13. A similar voltage range required to evoke the maximum EPSP of dLGN cells in control (1.3 - 40 V) and scrapie-inoculated (2 - 36 V) mice; this range was similar to that in the population of normal mouse dLGN cells (1 - 39 V). In fig.41., the maximum EPSP ($EPSP_M$) in two cells in control and scrapie-inoculated mice at 198 days post-inoculation is shown together with the action potentials evoked at depolarised levels.

The results of the analyses protocols performed on the peak amplitude, rise time and decay time of the synaptic response did not reveal any significant differences between groups for the parameters measured. The values for these parameters across the time intervals studied are shown in figs. 42, 43 and 44A together with the regrouped and pooled data means for the scrapie-inoculated and control mice respectively.

*4.2.8 Morphology of dLGN cells recorded in control and scrapie-inoculated mice*

The morphology of three cells in control mice at 114, 196 and 230 days post-inoculation, respectively are shown in fig.45. The suspected labeled axon of these cells is identified. The morphology of the cells labeled in scrapie-inoculated mice is shown in figs. 46, 47 and 48. Subjectively the morphology of cells labeled in the control and scrapie-inoculated mice was similar. The even radiation of the dendrites from the soma, the secondary branching points and the presence of dense swellings, especially at branch points on the proximal dendrites was similar in both groups at the different incubation period stages. In the control cells at 114, 196 and 230 days post-inoculation, the dimensions of the cell body (longest diameter) were 25, 23 and 20 μm, respectively.

In the cells at 85, 164, 165, 197 and 199 days post-inoculation in scrapie-infected mice, the dimensions of the cell somas were 16, 22, 28, 31, 17 and 28 μm. There was no evidence of dendritic enlargements other than those observed in control cells and in Golgi-impregnated mouse cells (Rafols and Valverde, 1973). Table 14 details the results of a morphometric analysis (adapted from Snider, 1988) of the camera-lucida reconstructions of the labeled cells. The cells were scored for dendritic process length, the extent of dendritic branching, and the number of primary dendrites (see 3.7.4). Also shown in the table is whether biocytin successfully labeled the axon and/or dendritic spines on these cells; possible axons were identified according to their description in Golgi-impregnated murine relay neurones (see 2.2). It was possible to identify a candidate cell process as the dLGN cell axon in all cells, but dendritic spines were inconsistently labeled in neurones from both control and scrapie-inoculated groups; those spines identified were sparsely and irregularly distributed at random sites on the dendritic arbor. Statistical analysis was not performed due to the limited sample size. However, from observation of the raw data it can be seen that within the control and scrapie-inoculated groups the values for each parameter are within a relatively small range; also there is a large amount of overlap in the range of values for each parameter when compared between control and scrapie-inoculated groups.

Figs. 49 and 50 are photographic examples of biocytin labeled cell processes in 70 μm sections of the 400 μm brain slice. In each figure the primary dendrites emanating from the polygonal cell bodies can clearly be seen. The processes in each cell were drawn separately and reconstructed to form two dimensional image, typical examples of which are seen in figs. 45 - 48.

| *days post-inoculation* | membrane properties | | action potential properties | | $EPSP_M$ properties | |
|---|---|---|---|---|---|---|
| | *control* | *scrapie* | *control* | *scrapie* | *control* | *scrapie* |
| 60 | 9 | 4 | 7 | 2 | 2 | 1 |
| 88 | 5 | 18 | 1 | 4 | 4 | 4 |
| 112 | 10 | 10 | 2 | 6 | 4 | 6 |
| 140 | 10 | 25 | 6 | 5 | 4 | 5 |
| 168 | 16 | 15 | 6 | 5 | 2 | 5 |
| 198 | 12 | 14 | 3 | 6 | 7 | 6 |
| 225 | 9 | 4 | - | - | - | - |

**Table 4.** Cell numbers in which dLGN cell parameters were recorded at each incubation period interval i.e. number of *days post-inoculation*. The action potential and $EPSP_M$ properties were studied in the second experiment, during which cells were not recorded at 225 days post-inoculation in scrapie-infected mice.

| Days | Resting potential (mV) | | Action potential threshold (mV) | | Input resistance (MΩ) | | Time constant (ms) | |
|---|---|---|---|---|---|---|---|---|
| | Cont. | Scrapie | Cont. | Scrapie | Cont. | Scrapie | Cont. | Scrapie |
| 60 | 60.8 ± 2.4 | 59.5 ±3.6 | 49.2 ± 2.0 | 49.0 ± 3.0 | 92.2 ± 17.0 | 112.0 ± 11.4 | 18.0 ± 2.1 | 23.7 ± 3.1 |
| 88 | 58.0 ± 3.2 | 59.1 ± 1.7 | 43.4 ± 2.7 | 45.4 ± 1.4 | 66.2 ± 8.0 | 107.1 ± 15.2 | 10.8 ± 2.8 | 19.9 ± 1.5 |
| 112 | 60.9 ± 2.3 | 57.8 ± 2.3 | 48.9 ± 1.9 | 46.0 ± 1.9 | 101.0 ± 10.8 | 77.1 ± 10.8 | 14.8 ± 2.0 | 14.9 ± 2.0 |
| 140 | 58.9 ± 1.8 | 58.1 ± 1.4 | 45.7 ± 1.9 | 47.4 ± 1.2 | 92.7 ± 6.8 | 91.1 ± 10.8 | 17.9 ± 2.0 | 16.4 ± 1.2 |
| 168 | 58.1 ± 1.8 | 58.7 ± 1.8 | 45.4 ± 1.5 | 45.2 ± 1.6 | 106.0 ± 8.8 | 101.1 ± 8.5 | 17.2 ± 1.6 | 16.7 ± 1.6 |
| 198 | 62.3 ± 2.1 | 62.4 ± 1.9 | 44.7 ± 1.5 | 51.4 ± 1.6 | 84.4 ± 9.1 | 93.9 ± 9.8 | 14.4 ± 1.8 | 17.0 ± 1.7 |
| 225 | 65.6 ± 2.4 | 66.5 ± 3.6 | 50.3 ± 2.0 | 56.5 ± 3.0 | 100.0 ± 17.0 | 128.0 ± 11.4 | 20.9 ± 2.1 | 18.2 ± 3.1 |

**Table 5.** The basic membrane properties of dLGN cells in control (Cont.) and scrapie-inoculated mice at 60, 88, 112, 140, 168, 198 and 225 days post-inoculation, all results expressed as mean ± SEM. For sample numbers in each group at each interval, see table 4.

| Group | Resting potential (mV) | Action potential threshold (mV) | Input resistance (MΩ) | Time constant (ms) |
|---|---|---|---|---|
| Control | | | | |
| 60 - 225 days | -60.7 ± 0.87 | -46.8 ± 0.70 | 94.5 ± 4.1 | 16.6 ± 0.80 |
| Scrapie | | | | |
| 60 - 225 days | -60.3 ± 0.93 | -48.7 ± 0.78 | 101.0 ± 4.44 | 18.1 ± 0.82 |
| Scrapie | | | | |
| 60 - 112 days | -58.8 ± 1.3 | -46.1 ± 1.03 | 98.1 ± 6.6 | 18.8 ± 1.2 |
| Scrapie | | | | |
| 140 - 168 days | -58.4 ± -0.96 | -46.6 ± -1.04 | 94.7 ± 5.2 | 16.5 ± 0.90 |
| Scrapie | | | | |
| 198 - 225 days | -63.3 ± 1.9 | -52.6 ± -1.46 | 101.4 ± 8.5 | 17.3 ± 1.43 |

**Table 6.** The mean of the pooled and regrouped values of the basic membrane properties of dLGN cells in control and scrapie-inoculated mice as detailed in 4.2.4. All values expressed as mean ± SEM.

| Analysis type | Resting membrane potential | Action potential threshold | Input resistance | Time constant |
|---|---|---|---|---|
| Inoculation procedure test | 0.21 | 0.05 | 0.35 | 0.1 |
| Age-related test | 0.05 | 0.05 | 0.22 | 0.12 |
| Treatment test | 0.95 | 0.13 | 0.11 | 0.09 |
| Pooled test | 0.7 | 0.08 | 0.12 | 0.11 |
| Regrouped test | 0.05 | 0.002 | 0.09 | 0.38 |

**Table 7.** The significance levels associated with the statistical comparisons of the basic membrane properties of normal, control and scrapie-inoculated mice, detailed in 4.2.4.

| | Spike amplitude (mV) | | AHP amplitude (mV) | | Rise time (ms) | | Decay time (ms) | | Half width (ms) | |
|---|---|---|---|---|---|---|---|---|---|---|
| Days | Cont. | Scrapie | Cont. | Scrapie | Cont | Scrapie | Cont. | Scrapie | Cont. | Scrapie |
| 60 | 56.7 ± 1.9 | 54.1 ± 3.6 | 10.3 ± 0.7 | 10.4 ± 1.3 | 0.51 ± 0.02 | 0.51 ± 0.03 | 0.54 ± 0.05 | 0.38 ± 0.09 | 0.60 ± 0.05 | 0.64 ± 0.09 |
| 112 | 59.5 ± 3.6 | 54.7 ± 3.0 | 9.8 ± 1.3 | 11.3 ± 1.1 | 0.62 ± 0.03 | 0.58 ± 0.02 | 0.50 ± 0.09 | 0.58 ± 0.07 | 0.50 ± 0.09 | 0.75 ± 0.07 |
| 140 | 56.1 ± 1.5 | 58.4 ± 1.7 | 8.6 ± 0.8 | 10.1 ± 0.6 | 0.50 ± 0.01 | 0.54 ± 0.01 | 0.58 ± 0.04 | 0.51 ± 0.04 | 0.58 ± 0.03 | 0.58 ± 0.04 |
| 168 | 57.1 ± 2.1 | 57.4 ± 2.1 | 8.6 ± 0.6 | 10.0 ± 0.8 | 0.50 ± 0.02 | 0.50 ± 0.02 | 0.58 ± 0.05 | 0.58 ± 0.04 | 0.54 ± 0.05 | 0.62 ± 0.05 |
| 198 | 55.7 ± 3.0 | 59.0 ± 3.0 | 9.7 ± 1.1 | 7.5 ± 1.1 | 0.47 ± 0.02 | 0.50 ± 0.03 | 0.56 ± 0.06 | 0.59 ± 0.04 | 0.62 ± 0.07 | 0.58 ± 0.07 |

**Table 8.** **A**, the action potential parameters of the average spike shapes in dLGN cells in control (Cont.) and scrapie-inoculated mice at 60, 88, 112, 140, 168, and 225 days post-inoculation. All values are mean ± SEM. Sample numbers for each interval can be found in table 4.

| Group | Spike (mV) | AHP (mV) | Rise time (ms) | Decay time (ms) | Half width (ms) |
|---|---|---|---|---|---|
| Control | | | | | |
| 60 - 198 days | 56.4 ± 0.66 | 9.07 ± 0.20 | 0.50 ± 0.02 | 0.56 ± 0.02 | 0.50 ± 0.02 |
| Scrapie | | | | | |
| 60 - 198 days | 56.7 ± 1.23 | 9.86 ± 0.46 | 0.52 ± 0.01 | 0.53 ± 0.03 | 0.64 ± 0.03 |
| Scrapie | | | | | |
| 60 - 112 days | 54.1 ± 1.3 | 10.4 ± 1.8 | 0.51 ± 0.01 | 0.38 ± 0.13 | 0.64 ± 0.11 |
| Scrapie | | | | | |
| 140 - 168 days | 57.5 ± 1.78 | 10.3 ± 0.4 | 0.52 ± 0.02 | 0.52 ± 0.04 | 0.62 ± 0.04 |
| Scrapie | | | | | |
| 198 days | 58.0 ± 1.4 | 9.2 ± 0.7 | 0.50 ± 0.0 | 0.51 ± 0.03 | 0.61 ± 0.04 |

**Table 9.** The mean of the pooled and regrouped values of the action potential parameters in dLGN cells in control and scrapie-inoculated mice as detailed in 4.2.4. All values expressed as mean ± SEM.

| Analysis type | Spike amplitude | AHP amplitude | Rise time | Decay time | Half width |
|---|---|---|---|---|---|
| Inoculation procedure test | 0.57 | 0.08 | 0.72 | 0.7 | 0.78 |
| Age-related test | 0.95 | 0.36 | < 0.05 | 0.36 | 0.92 |
| Treatment test | 0.57 | 0.32 | 0.74 | 0.41 | 0.30 |
| Pooled test | 0.86 | 0.46 | 0.92 | 0.53 | 0.11 |
| Regrouped test | 0.73 | 0.19 | 0.81 | 0.12 | 0.68 |

**Table 10.** The significance levels associated with the statistical comparisons of action potential properties of normal, control and scrapie-inoculated mice, as detailed in 4.2.4.

| | $EPSP_M$ amplitude (mV) | | $EPSP_M$ rise time (ms) | | $EPSP_M$ decay time (ms) | |
|---|---|---|---|---|---|---|
| Days | Control | Scrapie | Control | Scrapie | Control | Scrapie |
| 88 | 6.28 ± 0.23 | 6.75 ± 1.6 | 2.15 ± 0.38 | 2.55 ± 1.2 | 36.4 ± 8.6 | 39.25 ± 2.8 |
| 112 | 6.62 ± 0.9 | 6.78 ±. 0.74 | 2.45 ± 0.74 | 2.3 ± 0.6 | 26.0 ± 8.4 | 25.9 ± 6.9 |
| 140 | 5.48 ± 0.91 | 5.8 ± 0.71 | 2.35 ± 0.72 | 2.1 ± 0.61 | 37.4 ± 8.2 | 37.0 ± 6.5 |
| 168 | 5.85 ± 1.27 | 6.83 ± 0.81 | 1.20 ± 0.9 | 2.7 ± 0.66 | 33.6 ± 11.9 | 29.7 ± 7.5 |
| 198 | 5.99 ± 0.68 | 6.71 ± 0.68 | 3.23 ± 0.60 | 2.4 ± 0.56 | 26.1 ± 6.4 | 37.9 ± 6.4 |

**Table 11.** the maximum EPSP ($EPSP_M$) parameters of the average spike shapes in dLGN cells in control and scrapie-inoculated mice at 60, 88, 112, 140, 168, and 225 days post-inoculation. The sample numbers associated with each interval for both experimental groups are detailed in table 4.

| Group | $EPSP_M$ amplitude (mV) | $EPSP_M$ rise time (mV) | $EPSP_M$ decay time (ms) |
|---|---|---|---|
| Control 88 - 198 days | 6.7 ± 0.91 | 2.37 ± 0.50 | 37.9 ± 7.5 |
| Scrapie 88 - 198 days | 6.53 ± 0.37 | 2.38 ± 00.3 | 32.6 ± 3.46 |
| Scrapie 88 - 112 days | 6.05 ± 0.36 | 2.51 ± 0.33 | 30.9 ± 3.3 |
| Scrapie 140 - 168 days | 6.77 ± 0.71 | 2.4 ± 0.50 | 31.3 ± 4.9 |
| Scrapie 198 - 198 days | 6.27 ± 0.35 | 2.39 ± 0.38 | 33.7 ± 4.4 |

**Table 12.** the mean values of the maximum EPSP ($EPSP_M$) properties in dLGN cells in pooled control (60 -225 days) and scrapie- (88 - 112, 140 - 168 and 198 days) inoculated mice, as detailed in 4.2.4.

| Analysis type | $EPSP_M$ amplitude (mV) | $EPSP_M$ rise time (mV) | $EPSP_M$ decay time (ms) |
|---|---|---|---|
| Inoculation procedure test | 0.9 | 0.81 | 0.45 |
| Age-related test | 0.62 | 0.65 | 0.55 |
| Treatment test | 0.97 | 0.46 | 0.72 |
| Pooled test | 0.38 | 0.89 | 0.74 |
| Regrouped test | 0.79 | 0.81 | 0.77 |

**Table 13.** The significance levels associated with the statistical comparisons of maximum EPSP ($EPSP_M$) properties of normal, control and scrapie-inoculated mice, as detailed in 4.2.4.

**A Control mice**

| Days post-inoculation | Dendritic process length (mm) | Number of primary dendrites | Extent of dendritic branching | Labelling of axon ? | Labelling of spines ? |
|---|---|---|---|---|---|
| 114 | 8.7 | 12 | 34 | + | + |
| 194 | 10.8 | 10 | 52 | + | - |
| 230 | 9.8 | 9 | 24 | + | - |

**B Scrapie-inoculated mice**

| Days post-inoculation | Dendritic process length (mm) | Number of primary dendrites | Extent of dendritic branching | Possible labelling of axon ? | Labelling of spines ? |
|---|---|---|---|---|---|
| 85 | 9.7 | 10 | 42 | + | - |
| 164 | 9.6 | 8 | 46 | + | + |
| 165 | 9.8 | 10 | 40 | + | + |
| 197 | 8 | 13 | 40 | + | - |
| 199 | 10.9 | 9 | 29 | + | + |
| 225 | 11.2 | 11 | 36 | + | - |

**Table 14.** Morphometric analysis of dLGN cells labelled with biocytin in (A) control and (B) scrapie-inoculated mice. The dendritic process length was measured as the radius of the circle drawn around the dendritic process radiating the greatest distance from the centre point, the soma. A circle was then drawn with a radius half that distance and the number of dendritic processes traversing that line was a measure of the dendritic branching. A primary dendrite was termed as a process extending from the soma for a distance greater than the soma diameter.

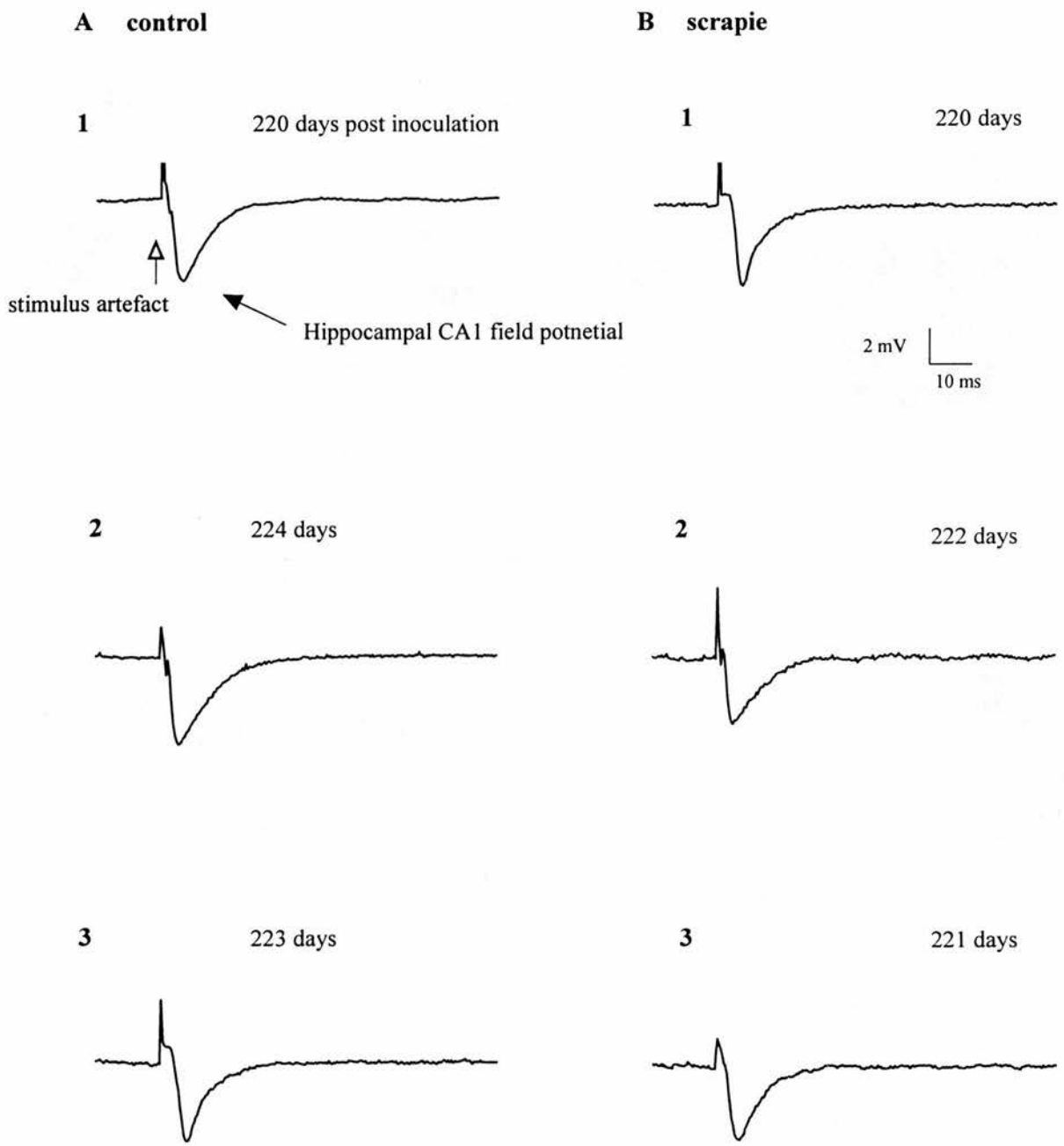


**Fig. 20.** Extracellular field potentials in the hippocampal CA1 area recorded in slices from A, three control and B, three scrapie-inoculated mice at 200-225 days post inoculation. Recordings in A and B1-3, are the average of 4 potentials evoked by stimulation of the afferent Schaffer collateral pathway at 0.25 Hz. The time point of stimulation is indicated by the open arrow in A1. Intracellular recordings in the dLGN were obtained in the slices from control but not scrapie-inoculated mice.

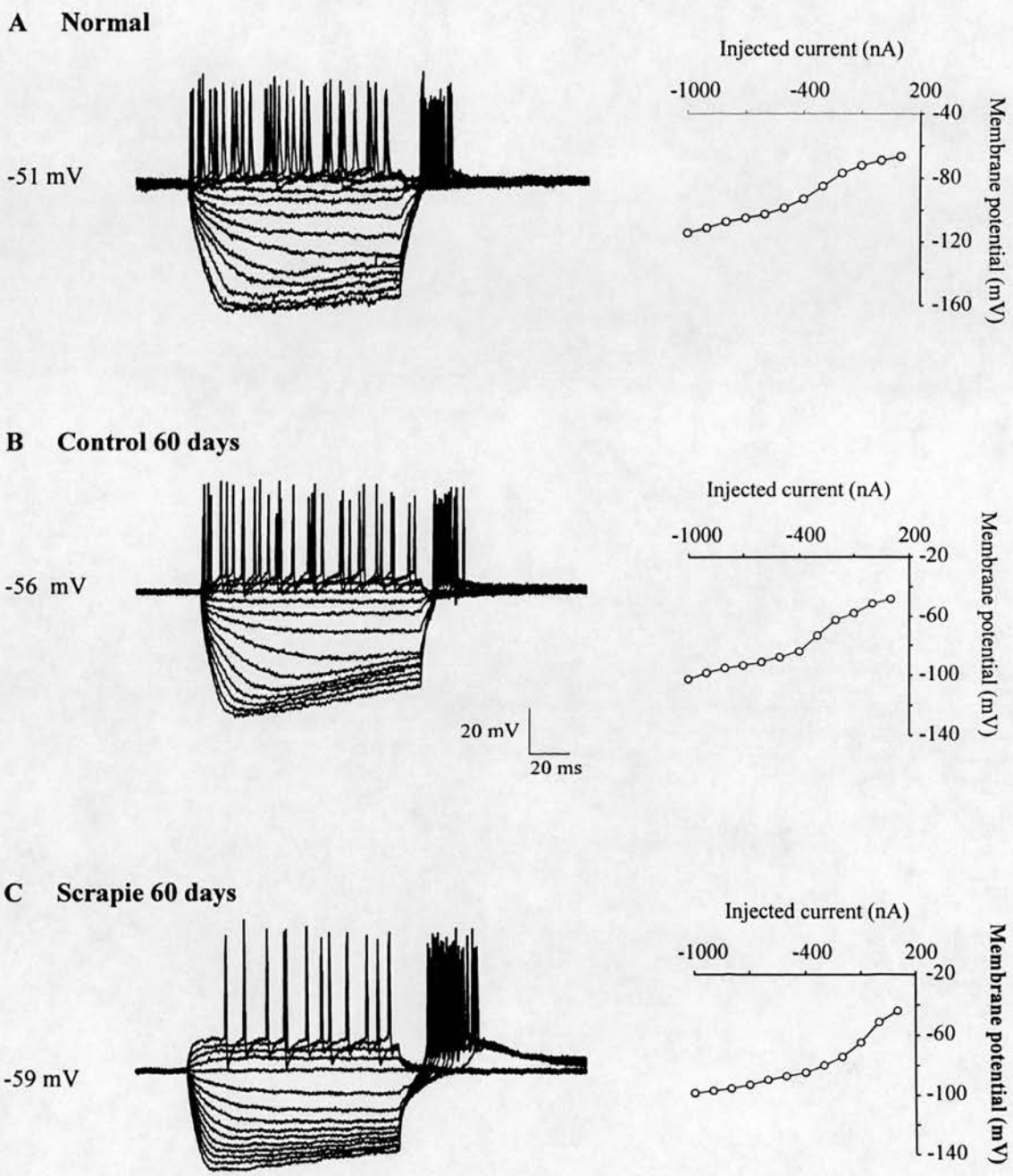


**Fig.21.** A *left panel*, membrane responses to intracellular current injection of dLGN cells in normal mouse and similarly in B and C, responses in control and scrapie-inoculated mice at 60 days post-inoculation. A-C *right panel*, the current voltage profile of each cell. Figs. 2 and 3 (overleaf) illustrate a similar pattern of activity in normal and experimental mice, at 140 and 225 days respectively. In each figure dLGN cells exhibit patterns voltage - activated membrane response properties similar to in the population of normal dLGN cells studied. The non-linear current voltage profiles demonstrate the inward and outward rectification in each cell.

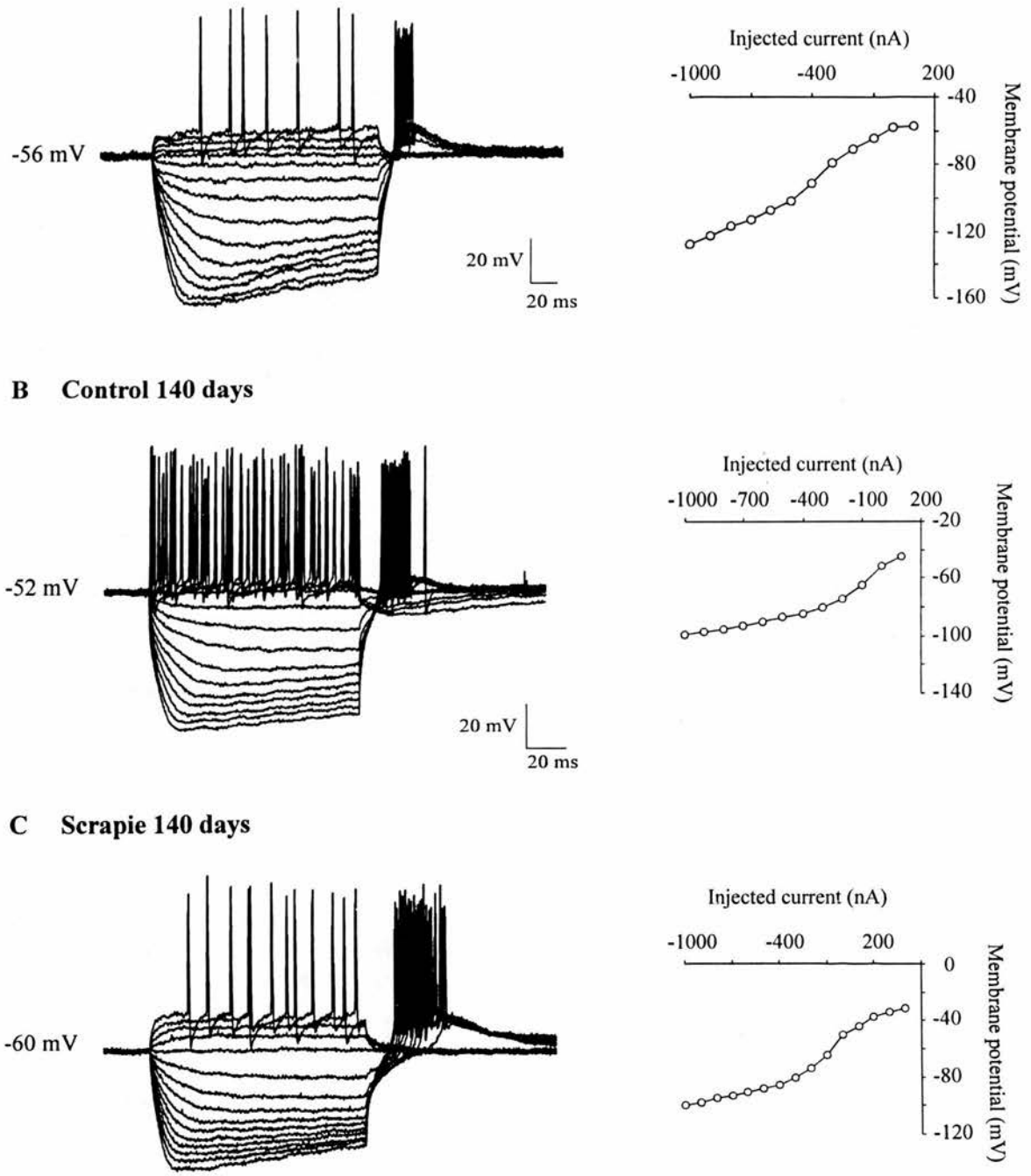


**Fig.22.** A *left panel*, membrane responses to intracellular current injection of dLGN cells in normal mouse and similarly in B and C, responses in control and scrapie-inoculated mice at 140 days post-inoculation. A-C *right panel*, the current voltage profile of each cell.

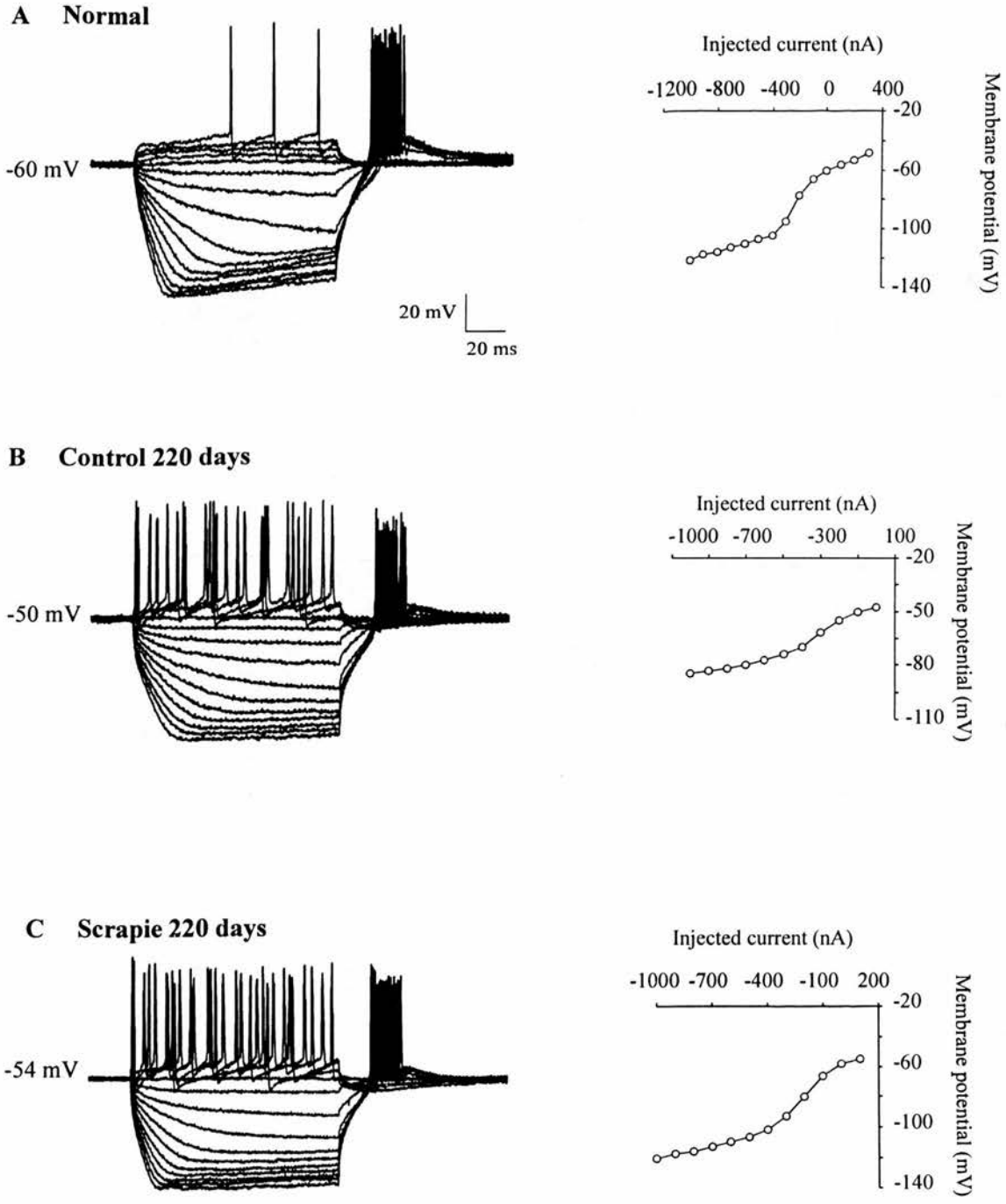


**Fig.23.** A *left panel*, membrane responses to intracellular current injection of dLGN cells in normal mouse and similarly in B and C, responses in control and scrapie-inoculated mice at 220 days post-inoculation. A-C *right panel,* the current voltage profile of each cell.

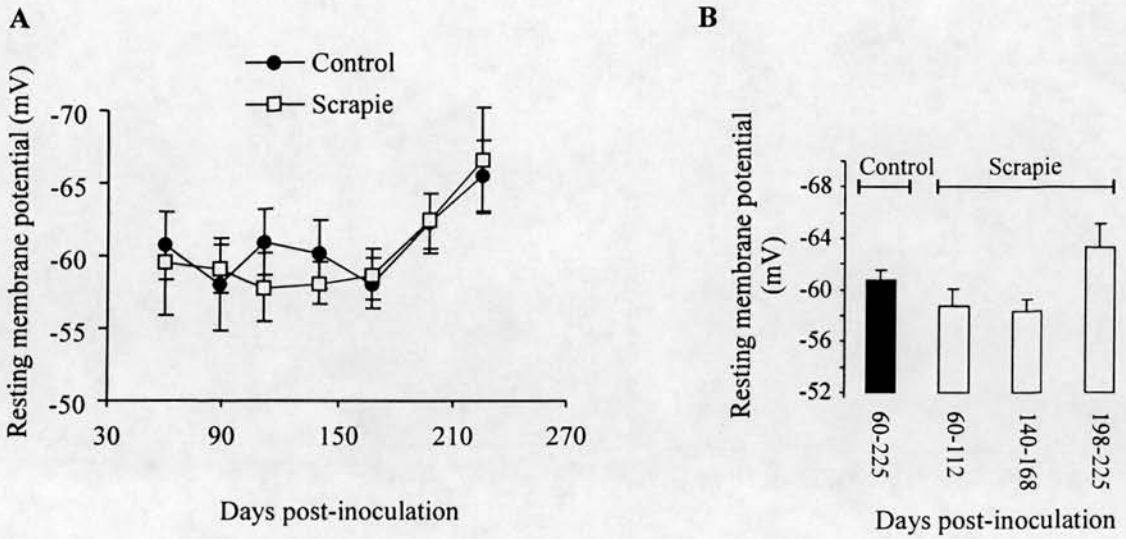


**Fig.24** The mean resting membrane potential in dLGN cells at 60, 88, 112, 140, 168, 198 and 225 days post inoculation in control and scrapie-inoculated mice. A, resting potential between groups at each time point and within groups across time is not significantly different ($p > 0.05$, two way ANOVA). B, the mean resting membrane potenial of pooled and regrouped data as shown. The resting membrane potential is plotted on a reverse scale. See table 4 for sample numbers at each time interval

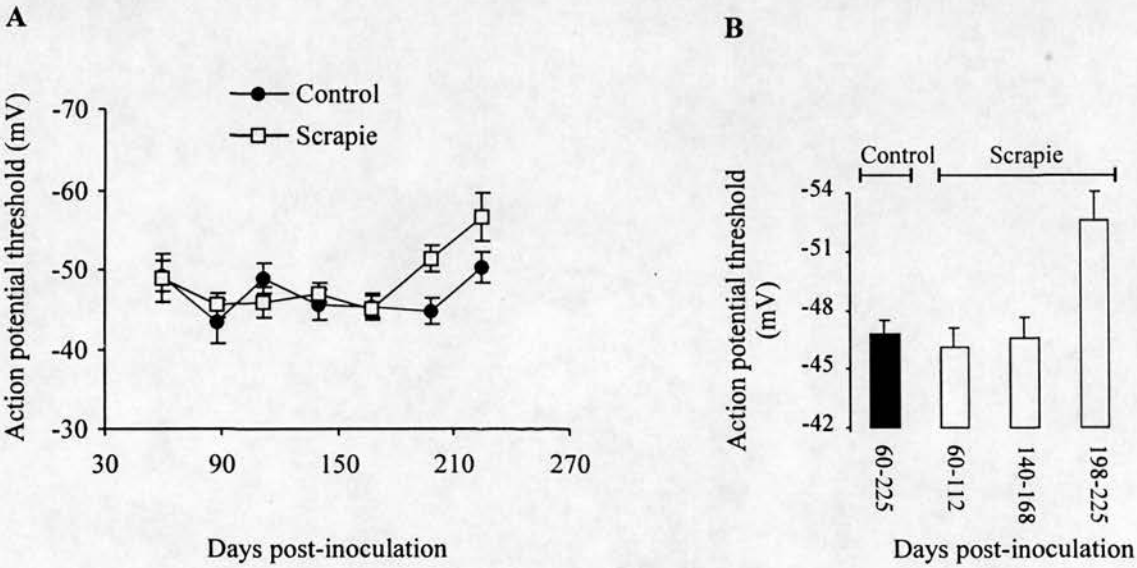


**Fig. 25.** The mean action potential threshold in dLGN cells at 60, 88, 112, 140, 168, 198 and 225 days in control and scrapie-inoculated mice. A, threshold between groups at each time point and within groups across time is not significantly different ($p > 0.05$, two way ANOVA). B, the mean action potential threshold of pooled and regrouped data as shown. The mean value of the control (60-225 days) and scrapie-inoculated (198-225 days) groups is significantly different ($p = <0.05$, one way ANOVA). The firing threshold is plotted on a reverse scale. For sample numbers at each time interval see table 4.

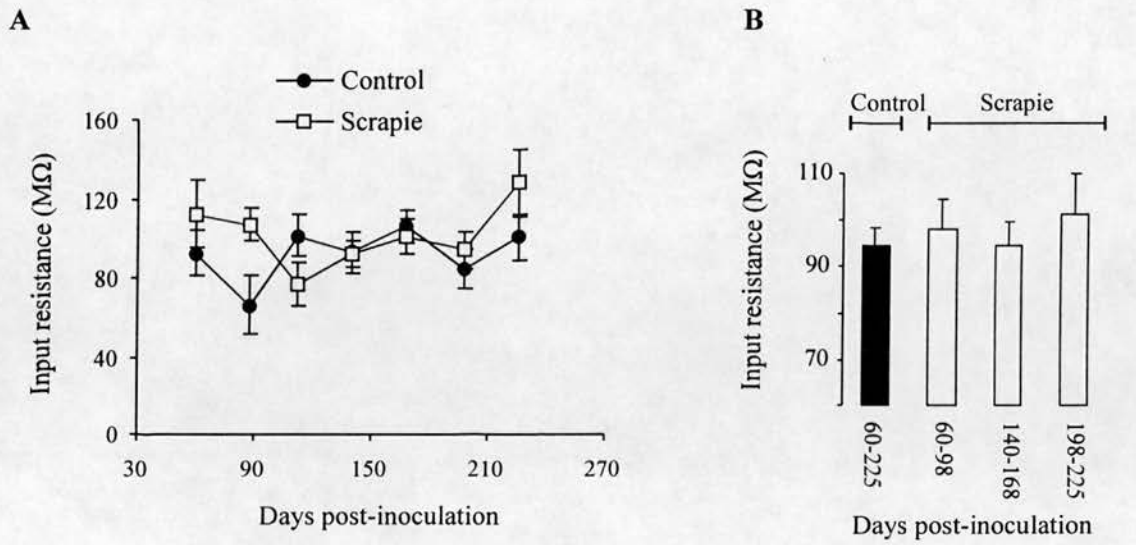


**Fig. 26.** The mean input resistance of dLGN cells at 60, 88, 112, 140, 168, 198 and 225 days post-inoculation in control and scrapie-inoculated mice. A, the input resistance between groups at each time point and within groups across time is not significantly different ($p>0.05$, two way ANOVA). B, the mean input resistance of pooled and regrouped data groups as shown. For sample numbers at each interval, see table 4.

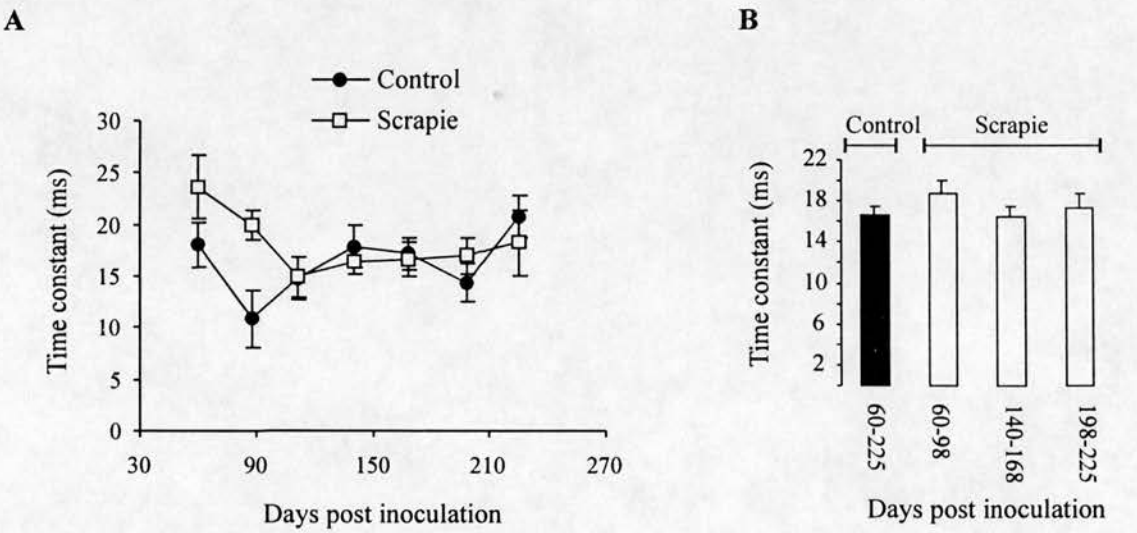


**Fig. 27.** The mean time constant in dLGN cells at 60, 88, 112, 140, 168, 198 and 225 days post-inoculation in control and scrapie-inoculated mice. A, the time constant between groups at each time point and within groups across time is not significantly different ($p>0.05$, two way ANOVA). B, the mean time constant in pooled and regrouped data as shown. See table 4 for sample numbers at each interval.

**A 60 days**

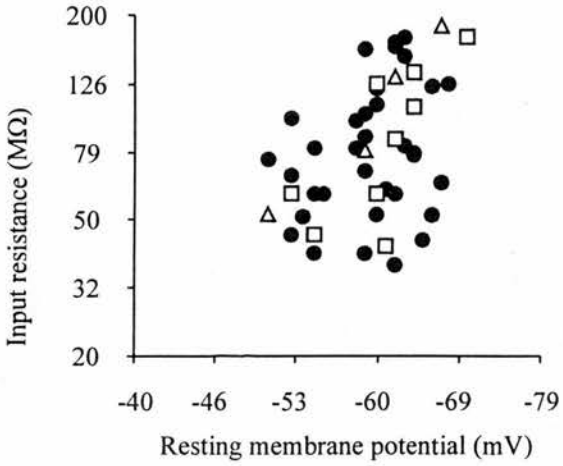


**B 140 days**

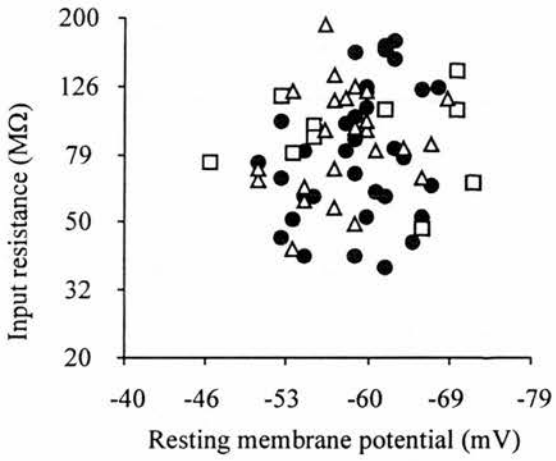


**C 225 days**

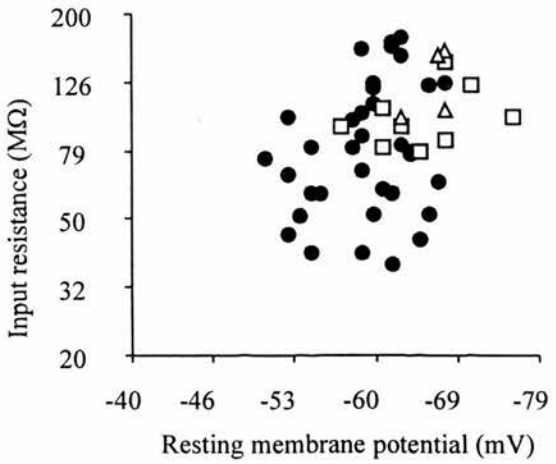


**Fig. 28.** Relationship between resting membrane potential and input resistance in dLGN cells in normal (filled circles), control (open triangles) and scrapie inoculated (open squares) mice. Measurements from control and scrapie inoculated mice at 60, 140 and 225 days post-inoculation are shown in association with the normal mouse data in panels A-C, respectively. The values for each parameter have been plotted on a logarithmic scale (and on a reverse scale for the resting membrane potential), scale intervals rounded up to the nearest whole number. A-C, the scatter of input resistance and resting membrane potential in dLGN cells is consistent with normal, control and scrapie-inoculated groups behaving as a single population.

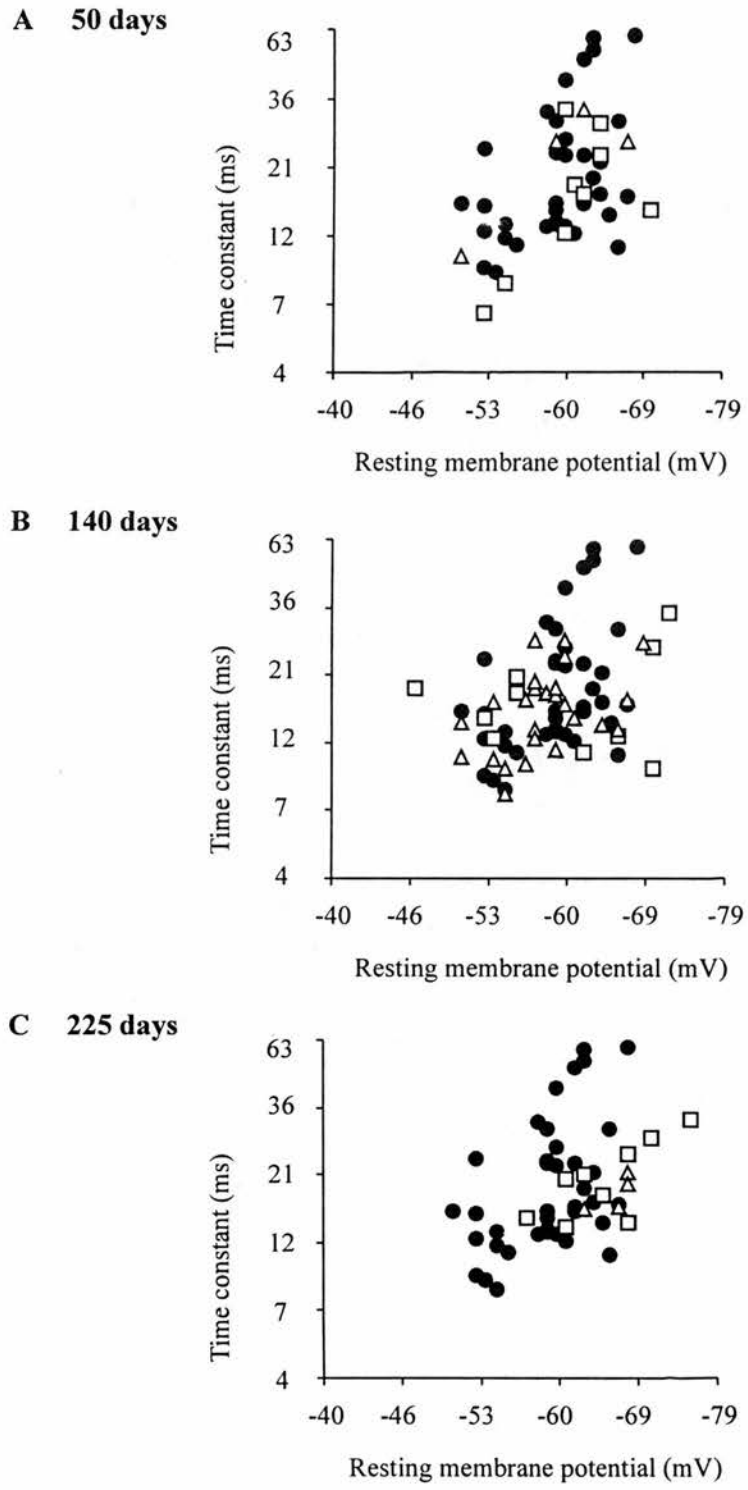


**Fig29.** Relationship between resting membrane potential and time constant in dLGN cells in normal (filled circles), control (open triangles) and scrapie inoculated (open squares) mice. Measurements from control and scrapie inoculated mice at 60, 140 and 225 days post-inoculation are shown in association with the normal mouse data in panels A-C, respectively. The values for each parameter have been plotted on a logarithmic scale (and for resting membrane potential on a reverse scale), scale intervals rounded up to the nearest whole number. A-C, the scatter is consistent with normal, control and scrapie-inoculated groups behaving as a single population.

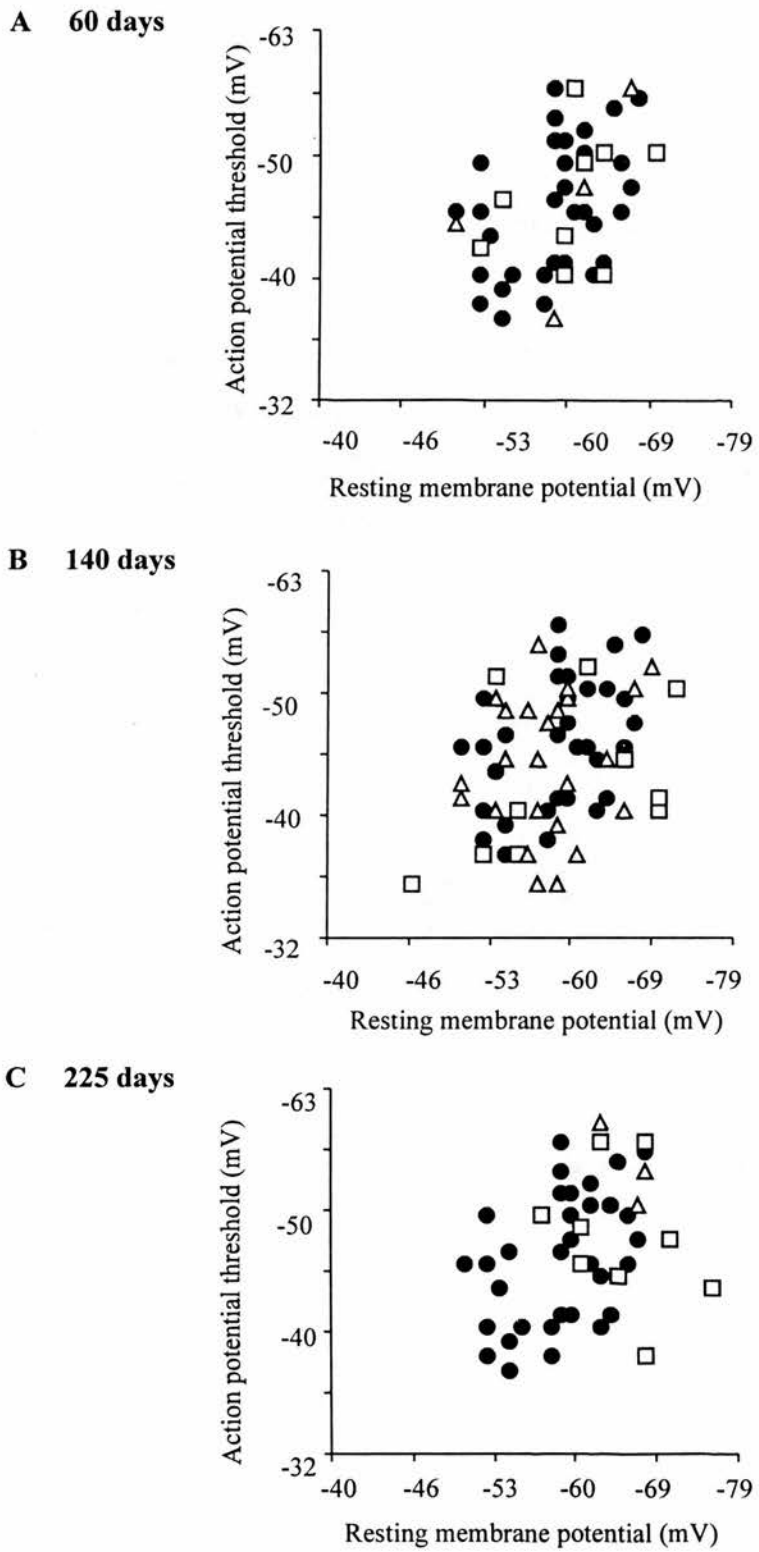


**Fig.30.** Relationship between resting membrane potential and action potential threshold in dLGN cells in normal (filled circles), control (open triangles) and scrapie inoculated (open squares) mice. Measurements from control and scrapie inoculated mice at 60, 140 and 225 days post-inoculation are shown in association with the normal mouse data in panels A-C, respectively. The values for each parameter have been plotted on a logarithmic scale (and for resting membrane potential on a reverse scale), scale intervals rounded up to the nearest whole number. A-C, the scatter threshold and resting membrane potential is consistent with normal, control and scrapie-inoculated groups behaving as a single population.

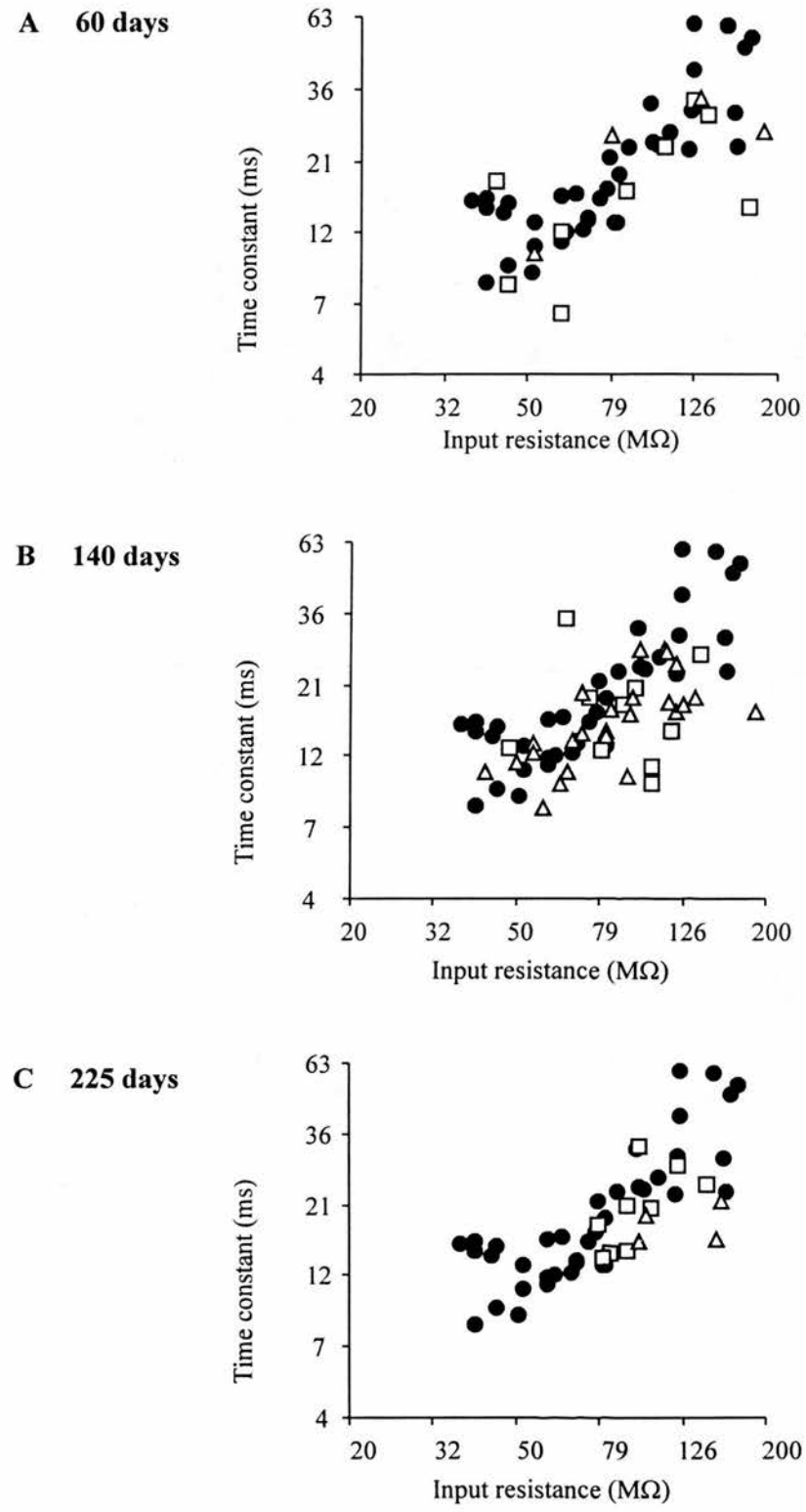


**Fig.31**. Relationship between input resistance and time constant in dLGN cells in normal, control and scrapie inoculated mice. Measurements from control and scrapie inoculated mice at 60, 140 and 225 days post-inoculation are shown in association with the normal mouse data in panels A-C, respectively. The values for each parameter are plotted on a logarithmic scale, scale intervals rounded up to the nearest whole number. A-C, at each time interval studied the scatter of the relationship between input resistance and time constant is consistent with the normal and experimental groups behaving as a single population.

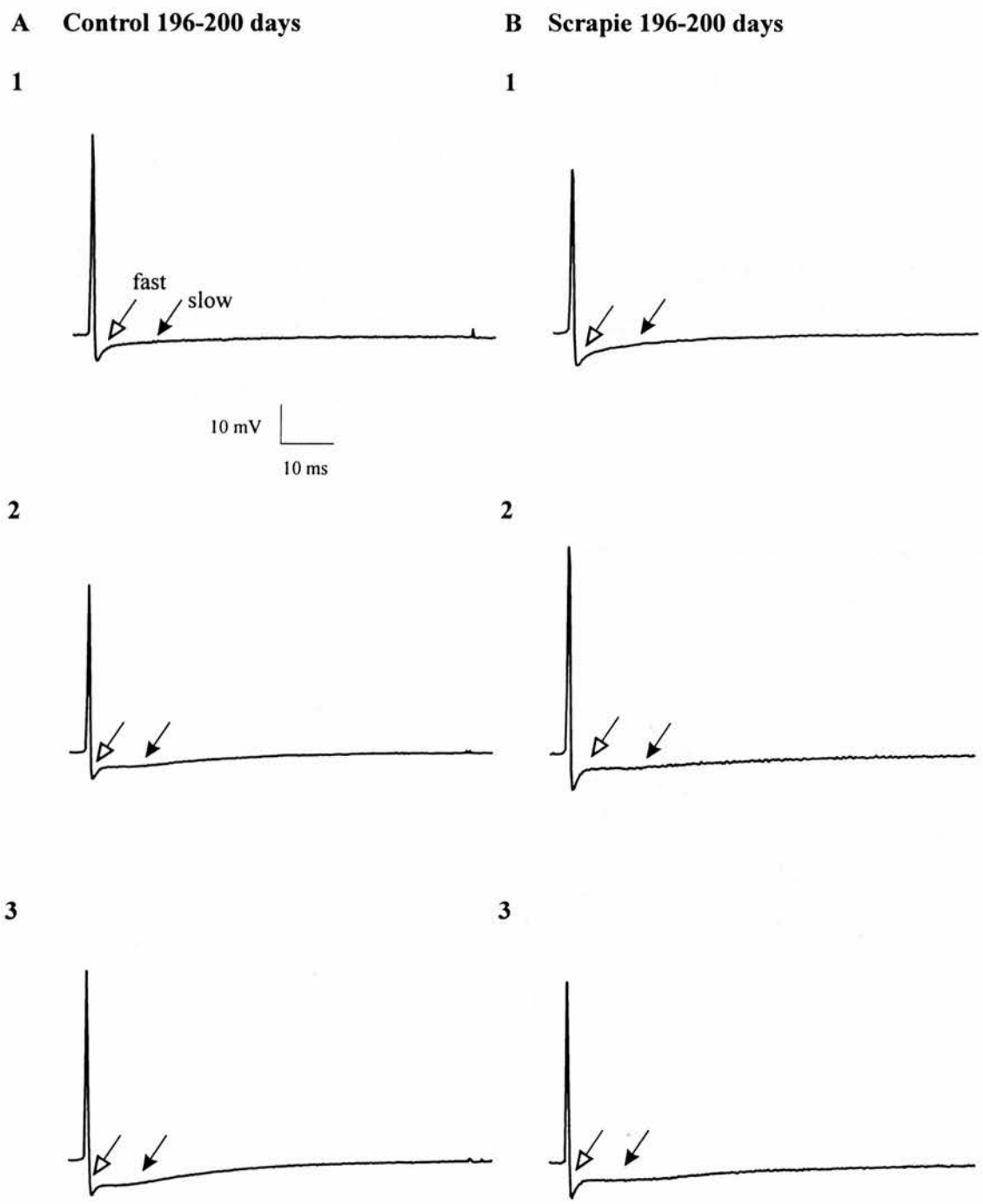


**Fig32.** Average action potential shapes in dLGN cells in control and scrapie-inoculated mice at 196-200 days post-inoculation. A and B1-3, examples of the different action potential shapes initiated by depolarisation to firing theshold. There is not a significant difference between the action potential parameters measured in both experimental groups ($p > 0.05$, two way ANOVA). The dLGN cell spike shapes in both control and scrapie-inoculated mice display both a fast (open arrow) and slow (filled arrow) phase of after-hyperpolarisation.

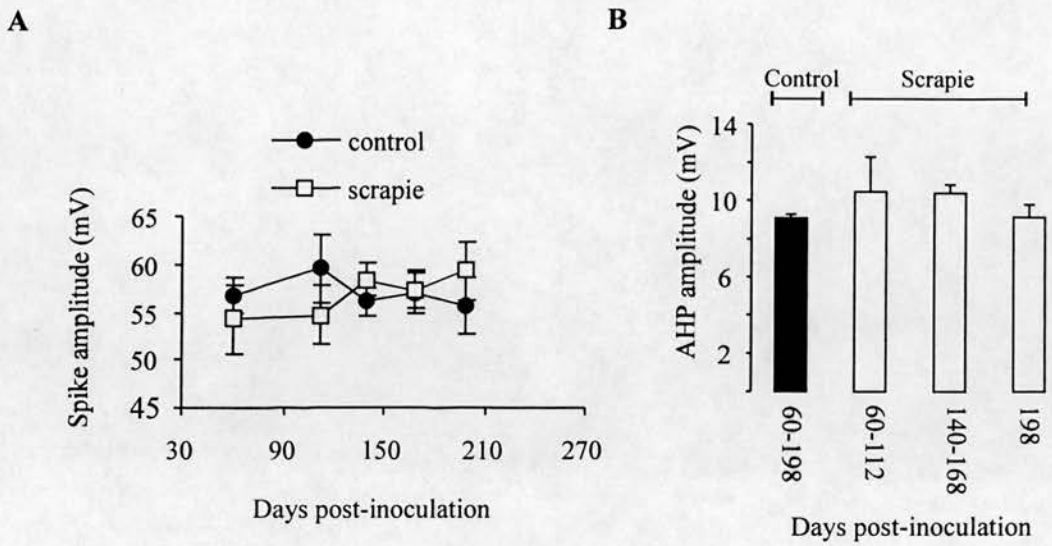


**Fig33.** The mean spike amplitude in dLGN cells at 60, 112, 140, 168 and 198 days post-inoculation in control and scrapie-inoculated mice. A, spike amplitude between groups at each time point and within groups across time is not significantly different ($p > 0.05$, two way ANOVA). B, the mean spike amplitude of pooled and regrouped data as shown. For sample numbers at each interval see table 4.

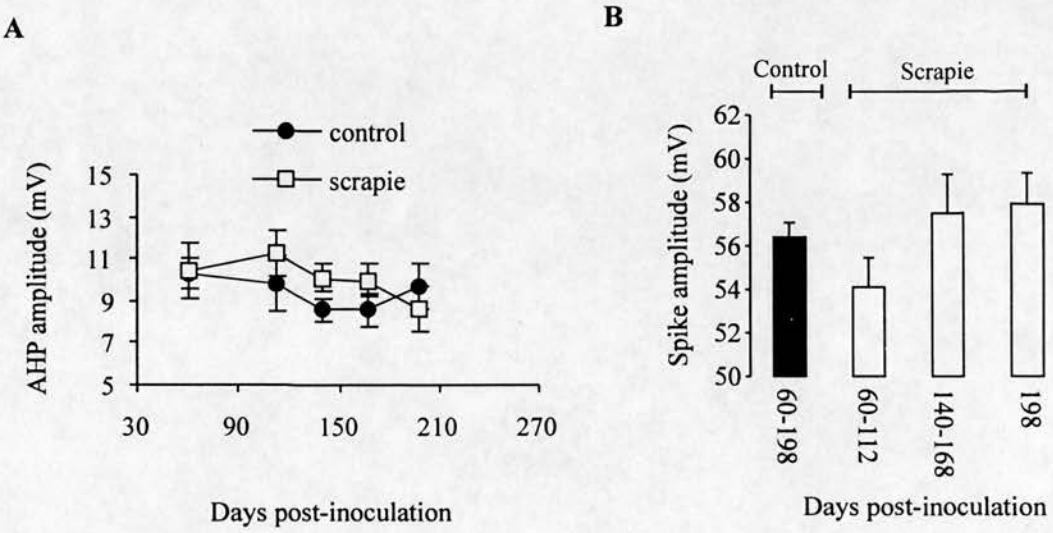


**Fig34.** The mean after-hyperpolarisation (AHP) amplitude in dLGN cells at 60, 112, 140, 168 and 198 days post-inoculation in control and scrapie-inoculated mice. A, AHP amplitude between groups at each time point and within groups across time is not significantly different ($p > 0.05$, two way ANOVA). B, the mean AHP amplitude of pooled and regrouped data as shown. The sample size for each interval is detailed in table 4.

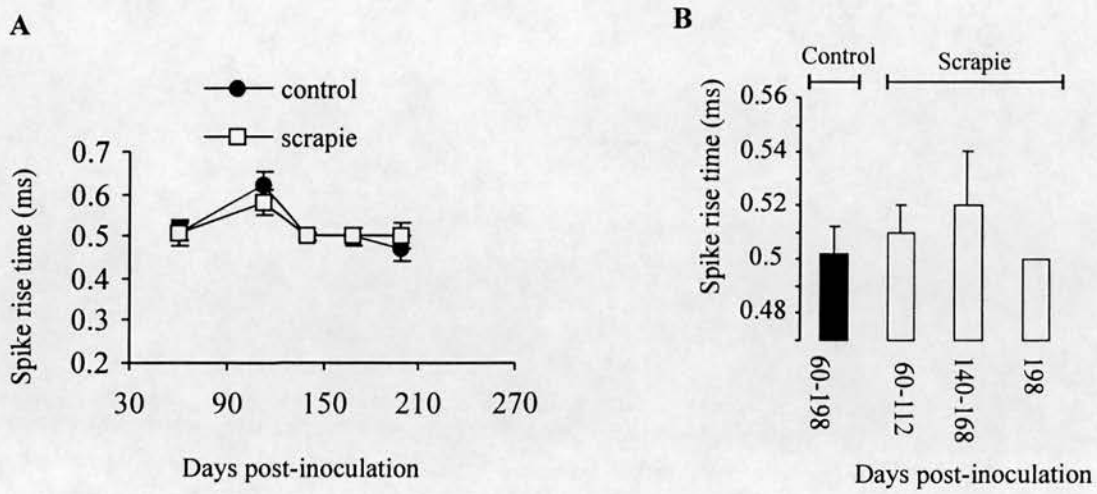


**Fig35.** The mean spike rise time in dLGN cells at 60, 112, 140, 168 and 198 days post-inoculation in control and scrapie-inoculated mice. A, spike rise time between groups at each time point is not significantly different ($p > 0.05$, two way ANOVA) but the rise time in the control group at 112 days was significantly different from the values in that group at 60, 140 and 198 days ($p < 0.05$, two way ANOVA) B, the mean spike rise time of pooled and regrouped data as shown.The sample numbers at each interval are detailed in table 4.

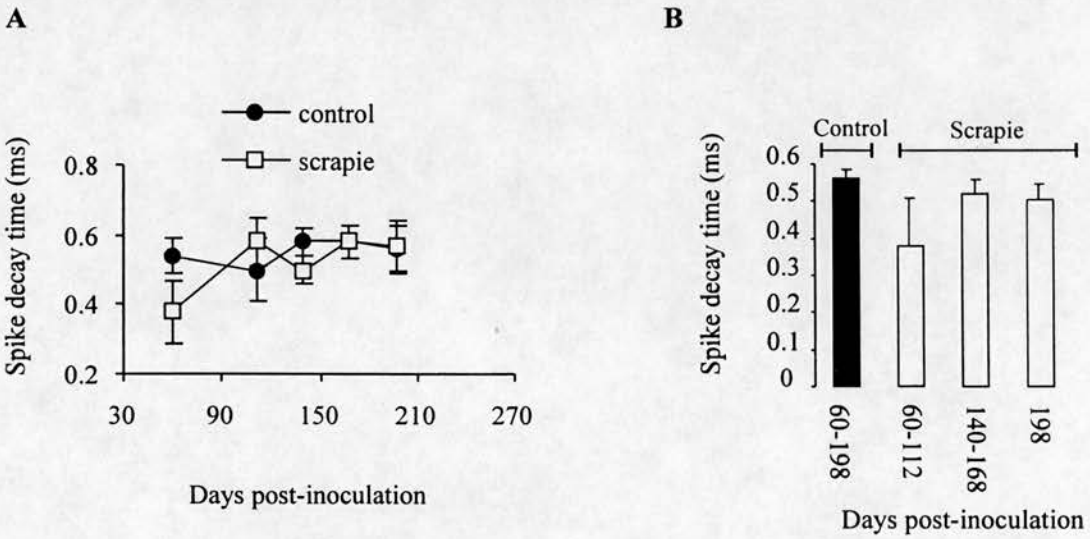


**Fig36.** The mean spike decay time in dLGN cells at 60, 112, 140, 168 and 198 days post-inoculation in control and scrapie-inoculated mice. A, spike decay time between groups at each time point and within groups across time is not significantly different ($p > 0.05$, two way ANOVA). B, the mean spike decay time of pooled and regrouped data as shown.

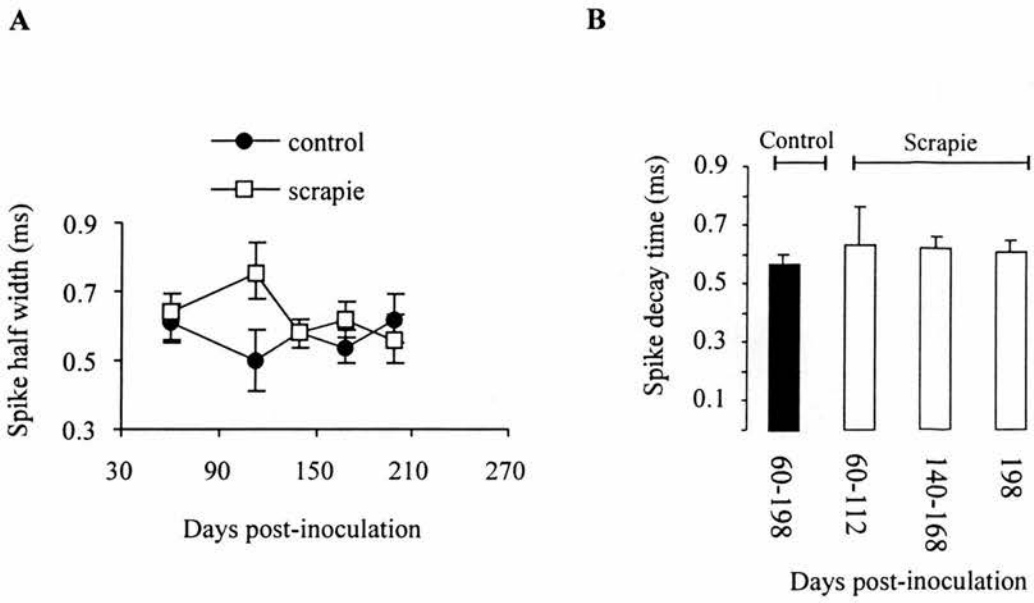


**Fig.37.** The mean spike half width in dLGN cells at 60, 112, 140, 168 and 198 days post-inoculation in control and scrapie-inoculated mice. A, spike half width between groups and within groups at each time point is not significantly different ($p > 0.05$, two way ANOVA). B, the mean spike half width of pooled and regrouped data as shown; sample numbers for incubation period intervals are found in table 4.

**A 60 days**

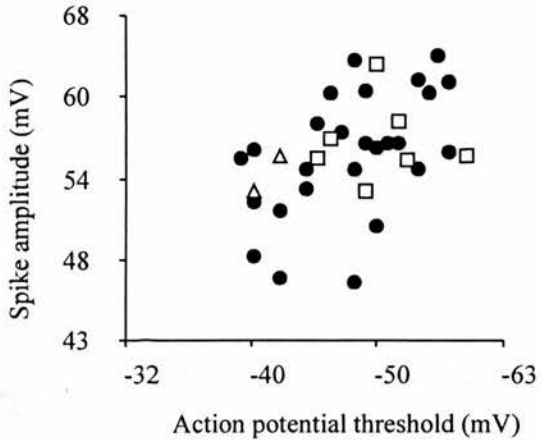


**B 140 days**

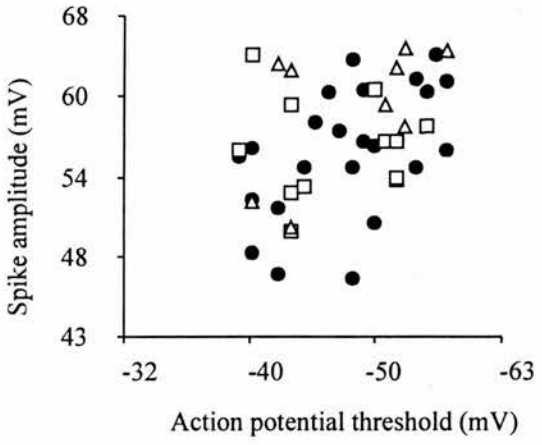


**C 198 days**

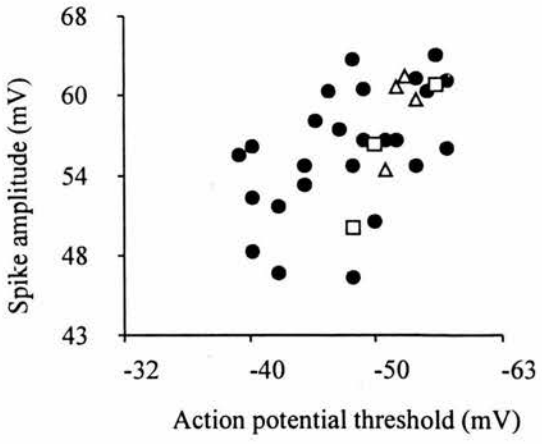


**Fig.38.** Relationship between action potential threshold and spike amplitude in dLGN cells in normal (filled circles), control (open triangles) and scrapie-inoculated (open squares) mice. Measurements from control and scrapie-inoculated mice at 60, 140 and 198 days post-inoculation are shown in association with the normal mouse data in panels A-C, respectively. The values for each parameter are plotted on a logarithmic scale (and for threshold on a reverse scale), scale intervals rounded up to the nearest whole number. A-C, at the time intervals shown the scatter of the relationship between threshold and spike amplitude is consistent with the normal and experimental groups behaving as a single population

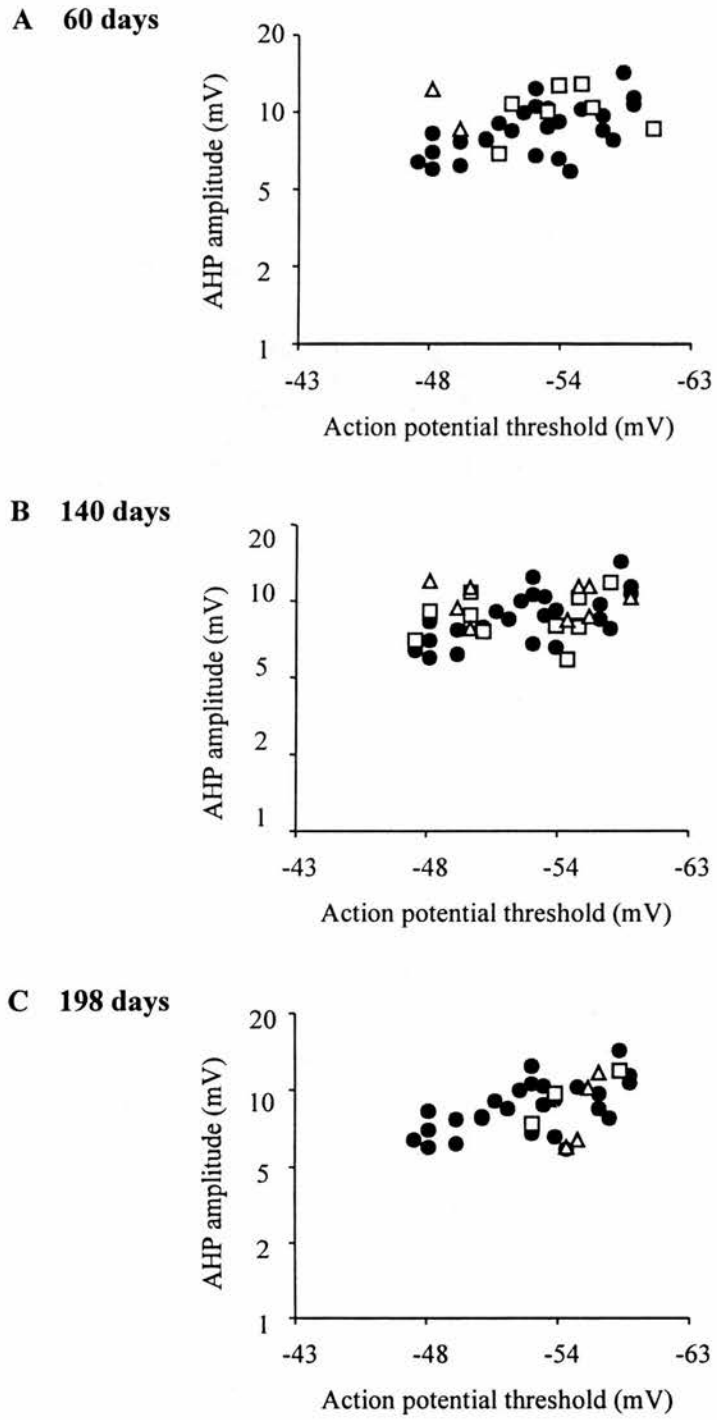


**Fig.39.** Relationship between action potential threshold and afterhyperpolarisation (AHP) amplitude in dLGN cells in normal (filled circles), control (open triangles) and scrapie-inoculated (open squares) mice. Meaurements from control and scrapie-inoculated mice at 60, 140 and 198 days post-inoculation are shown in association with normal mouse data in panels A-C, respectively. The values for each parameter are plotted on a logarithmic scale (and for firing threshold on a reverse scale), scale intervals rounded up to the nearest whole number. A-C, at the time intervals shown the scatter of the relationship between threshold and AHP amplitude is consistent with the normal and experimental groups behaving as a single population.

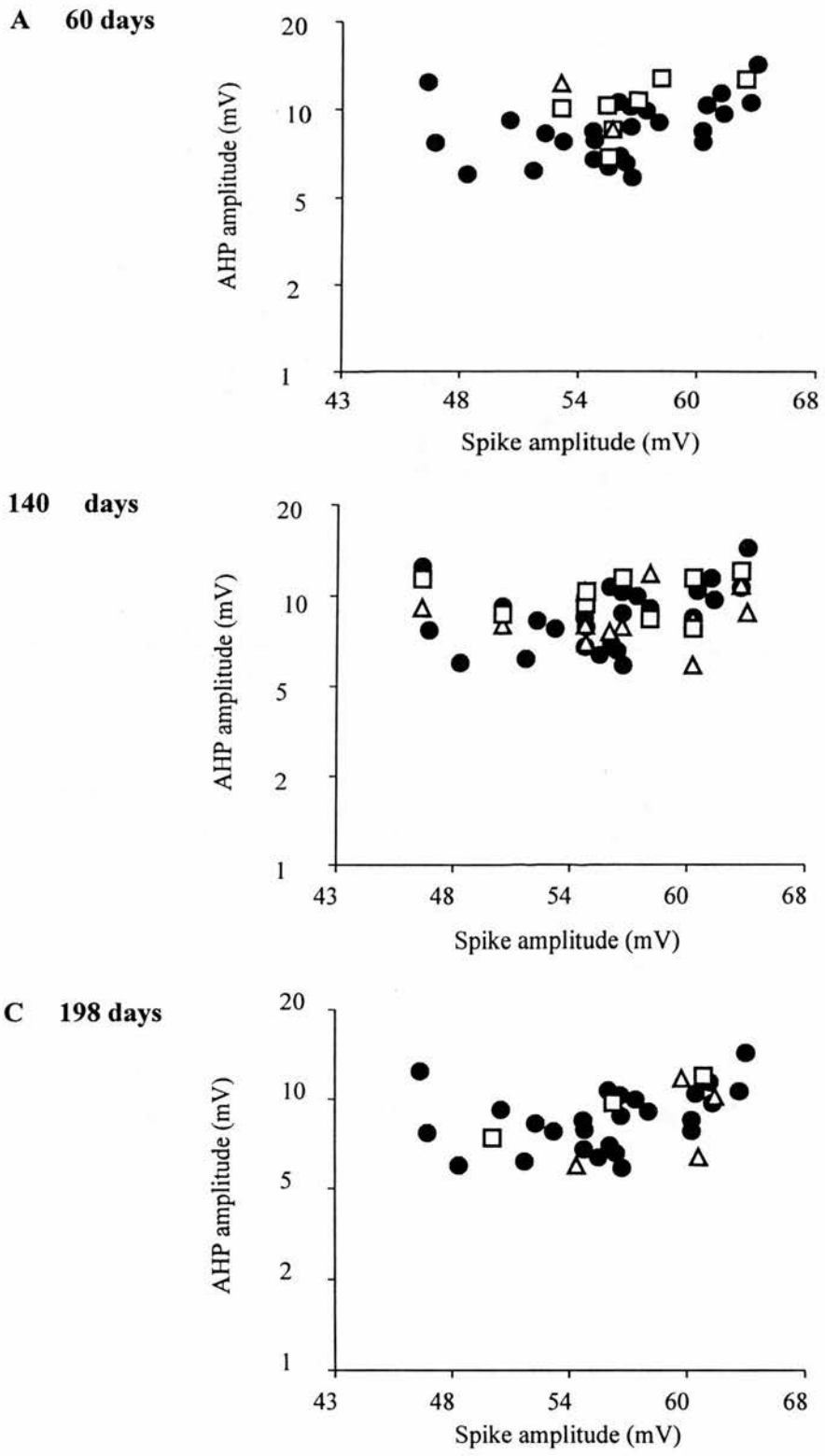


**Fig.40.** Relationship between spike amplitude and afterhyperpolarisation (AHP) amplitude in dLGN cells in normal (filled circles), control (open triangles) and scrapie-inoculated (open squares) mice. Measurements from control and scrapie-inoculated mice at 60, 140 and 198 days post-inoculation are shown in association with normal mouse data in panels A-C, respectively. The values for each parameter are plotted on a logarithmic scale, scale intervals rounded up to the nearest whole number. A-C, at the time intervals shown the scatter of the relationship between spike and AHP amplitude is consistent with the normal and experimental groups behaving as a single population.

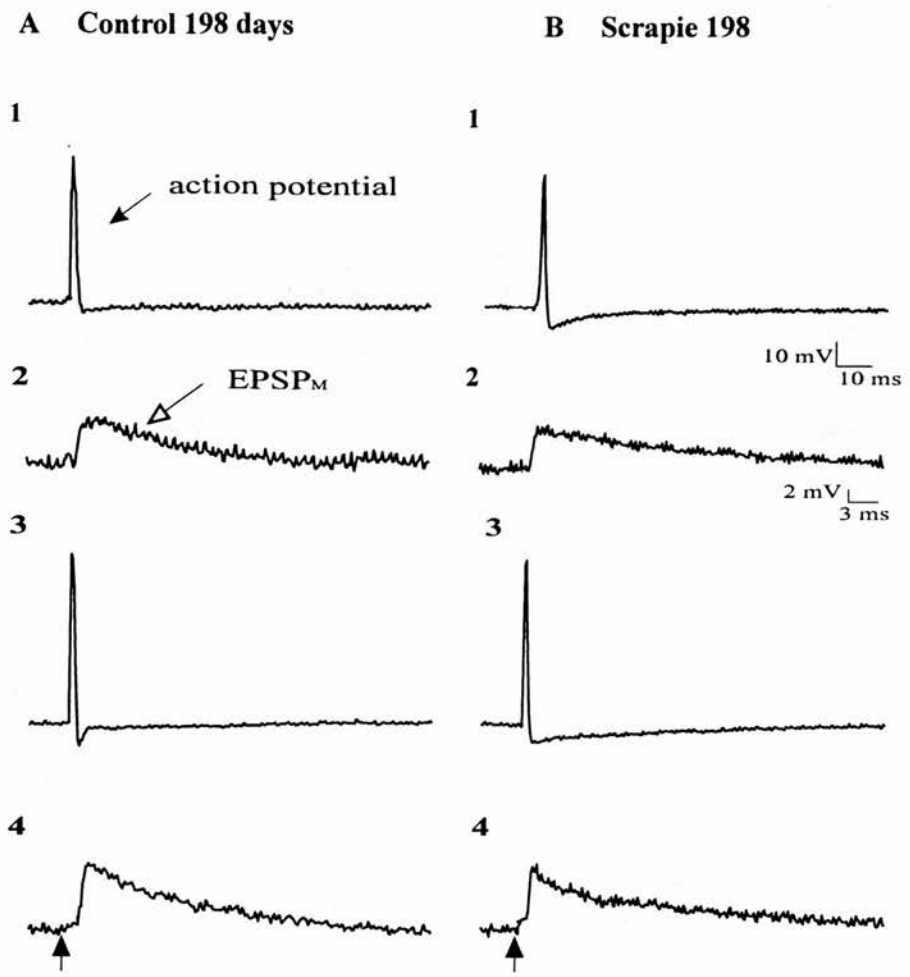


**Fig.41.** The maximum EPSP ($EPSP_M$) in dLGN cells in (A) control and (B) scrapie-inoculated mice at 198 days post-inoculation. A and B panels 1 and 3, action potentials evoked by the maximum EPSP at depolarised membrane potentials. Panels 2 and 4, the maximum EPSP in each cell. The peak, rise time and decay time of the maximum EPSP within the experimental groups studied and between groups at each of the time intervals, were not significantly different ($p > 0.05$, two way ANOVA). The arrow indicates the time of the optic tract stimulation.

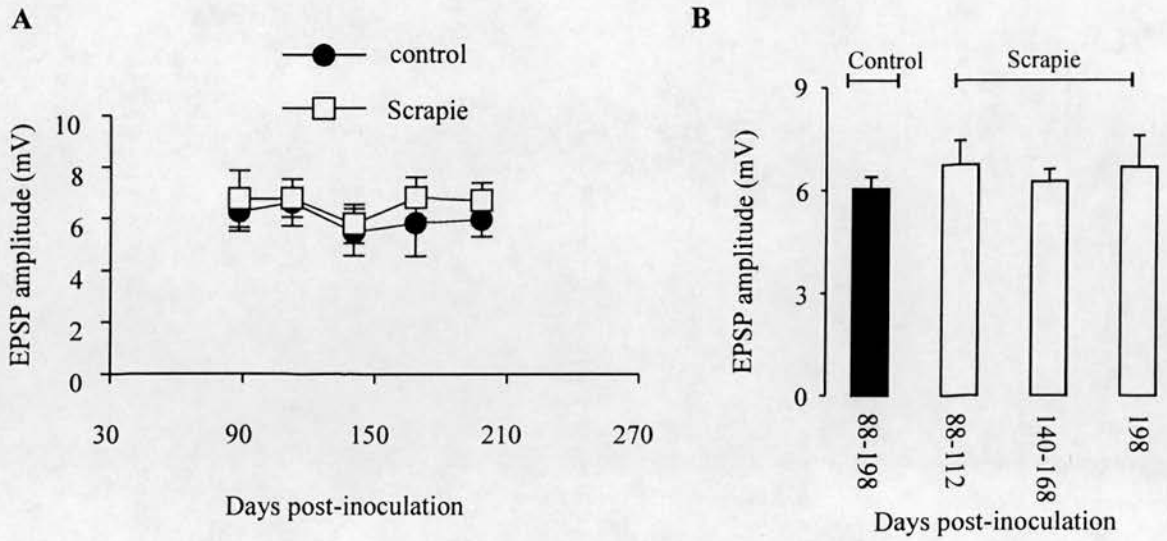


**Fig.42.** The mean maximum EPSP amplitude in dLGN cells at 88, 112, 140, 168 and 198 days post-inoculation in control and scrapie-inoculated mice. A, EPSP amplitude between groups at each time point and within groups across time is not significantly different ($p > 0.05$,two way ANOVA ). B, the mean EPSP amplitude of pooled and regrouped data as shown. The sample numbers for each interval are in table 4.

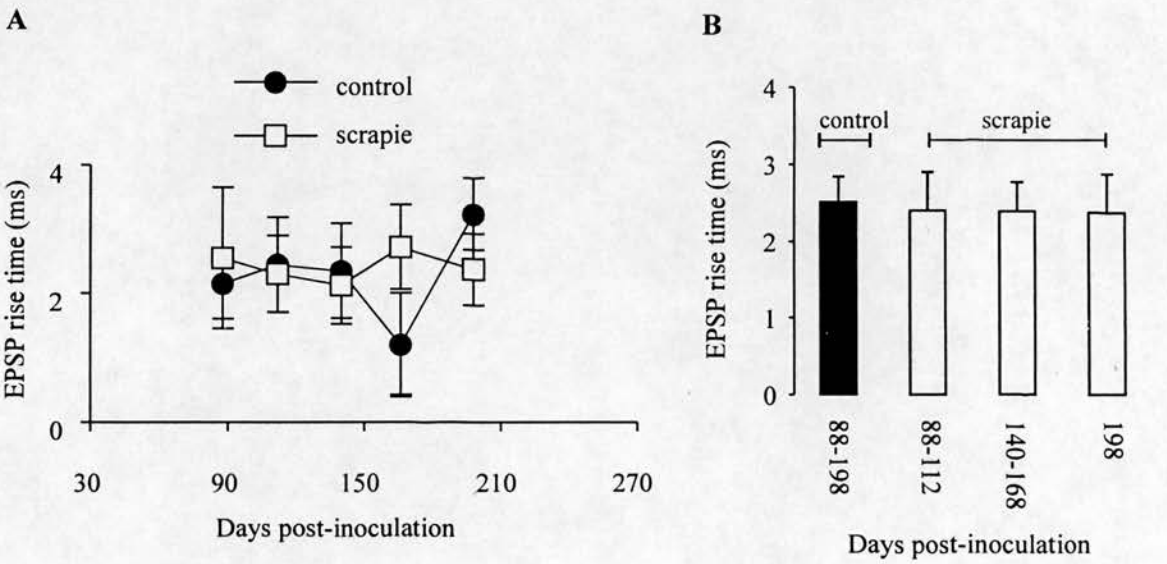


**Fig.43.** The mean maximum EPSP rise time in dLGN cells at 80, 112, 140, 168 and 198 days post-inoculation in control and scrapie-inoculated mice. A, EPSP rise time between groups at each time point and within groups across time is not significantly different ($p > 0.05$, two way ANOVA) B, the mean EPSP rise time of pooled and regrouped data as shown. The number of cells in the samples at each interval are shown in table 4.

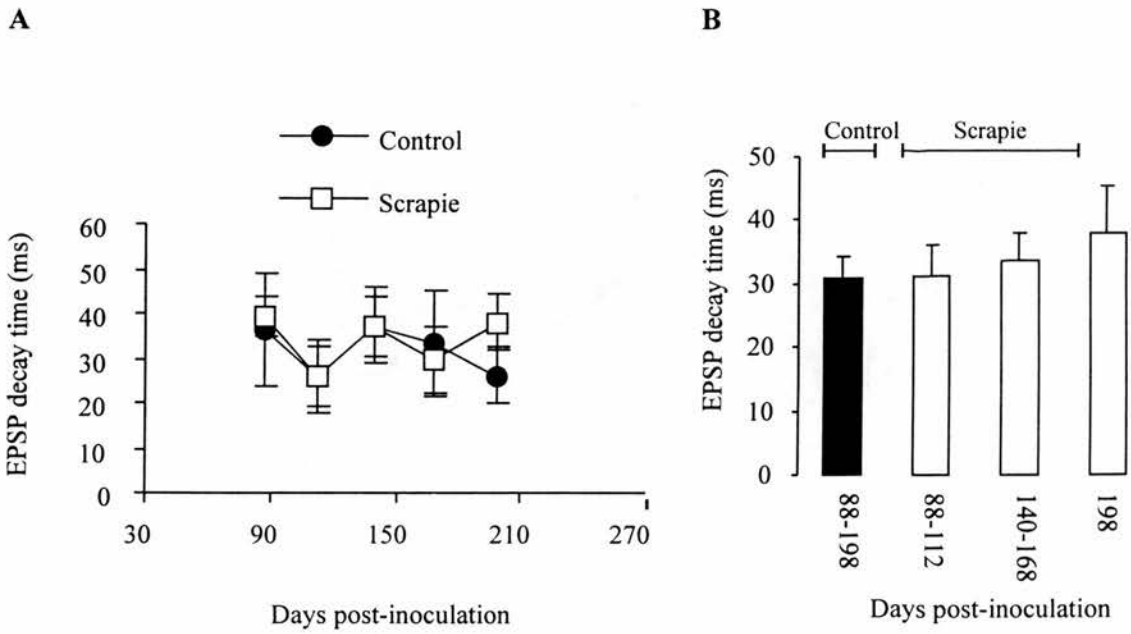


**Fig.44.** The mean maximum EPSP amplitude in dLGN cells at 88, 112, 140, 168 and 198 days post-inoculation in control and scrapie-inoculated mice. A, EPSP amplitude between groups at each time point and within groups across time is not significantly different ($p > 0.05$, two way ANOVA). B, the mean EPSP amplitude of pooled and regrouped data as shown. The sample numbers for each interval are shown in table 4.

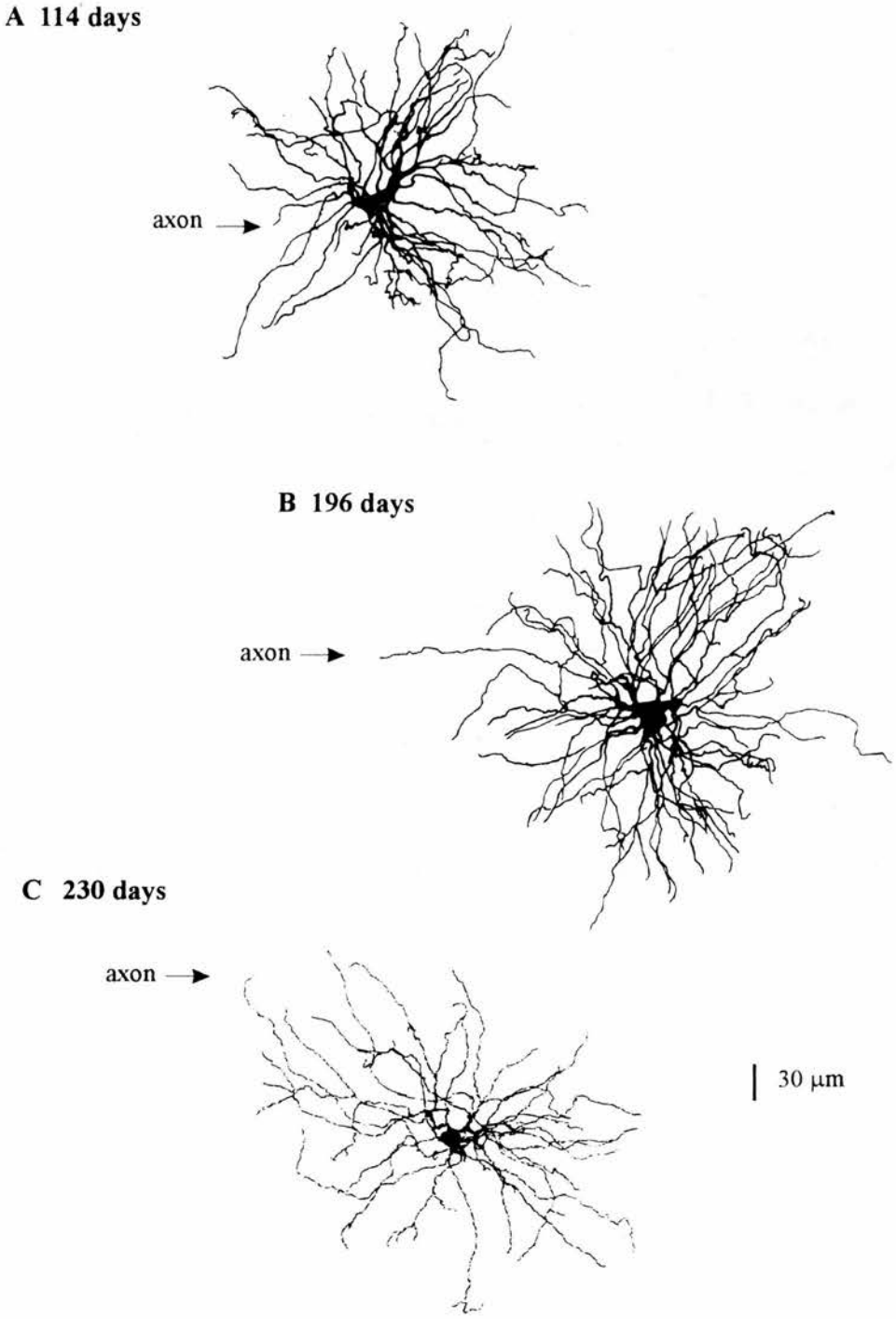


**Fig.45.** A two dimensional representation of the morphology of biocytin labelled dLGN cells in control mice at A, 114 days, B 196 and C, 230 days post-inoculation. The process indicated by the arrow, in this and figs.46 - 48, is thought to be the dLGN cell axon.

**A 85 days**

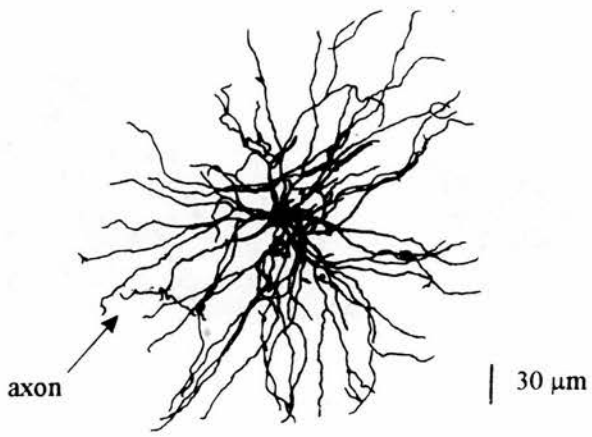


**Fig.46.** A two dimensional representation of the morphology of a biocytin labelled dLGN cell in a scrapie-inoculated mouse at 85 days post-inoculation.

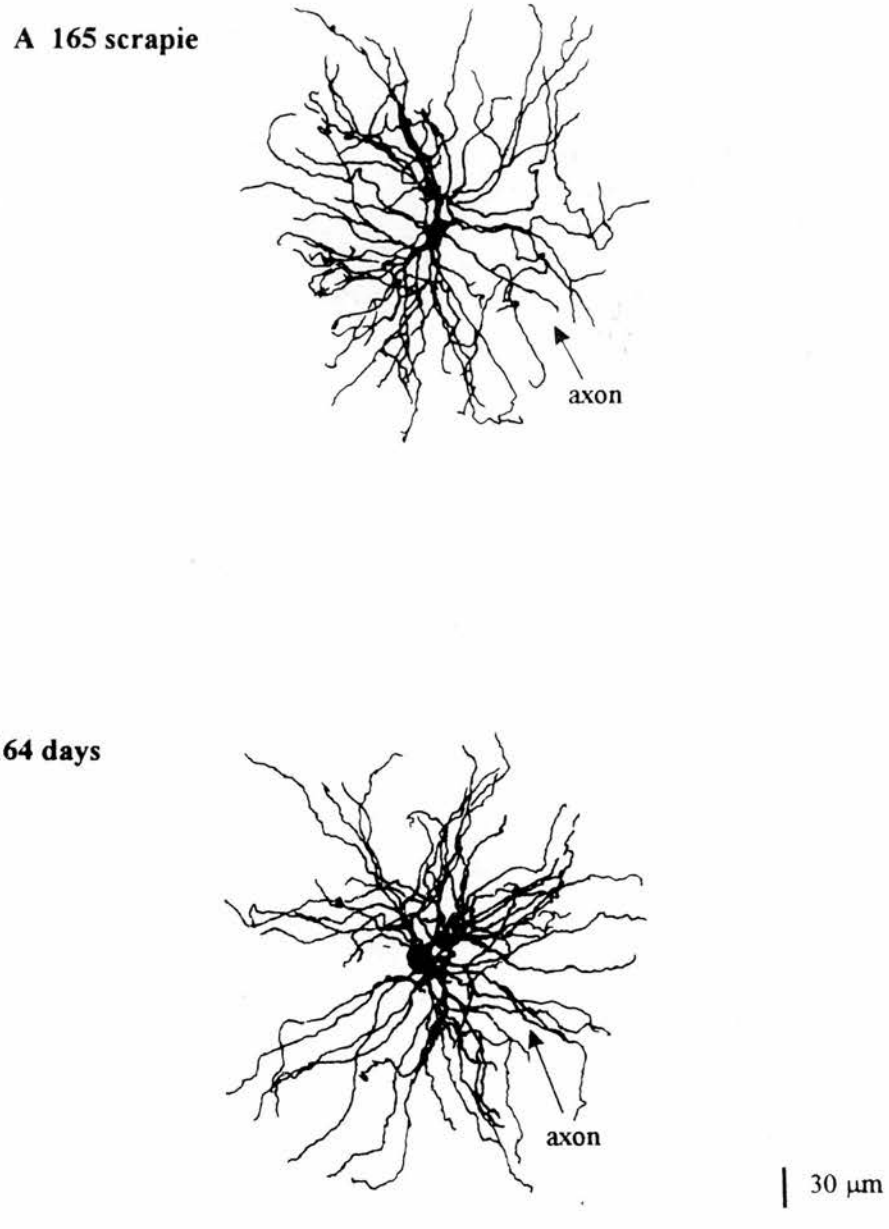


**Fig.47.** A two dimensional representation of the morphology of biocytin labelled dLGN cells in scrapie-inoculated mice at A, 165 and B, 164 days post-inoculation.

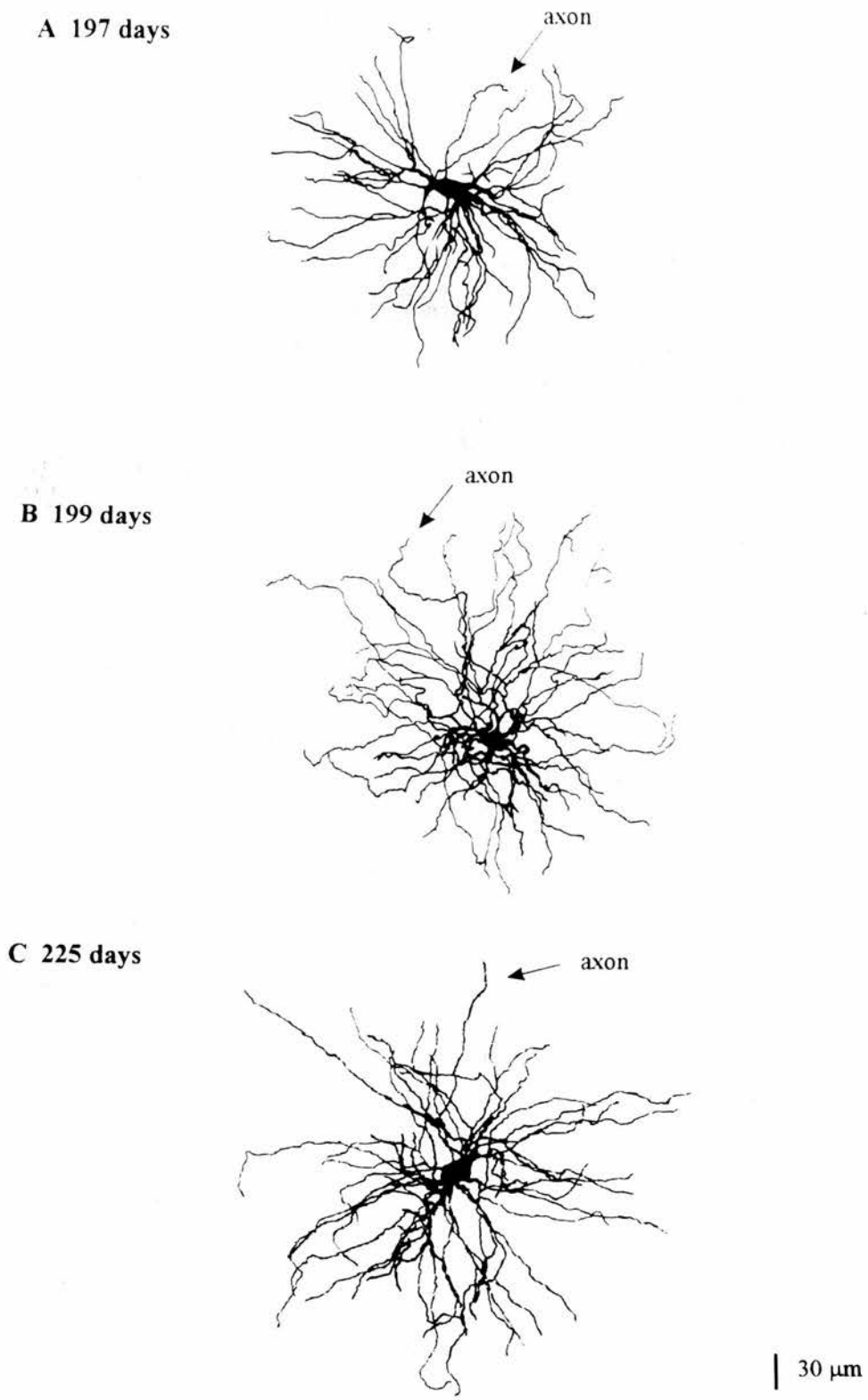


**Fig.48.** A two dimensional representation of the morphology of biocytin labelled dLGN cells in scrapie-inoculated mice at A, 197 B, 199 and C, 225 days post-inoculation.

A

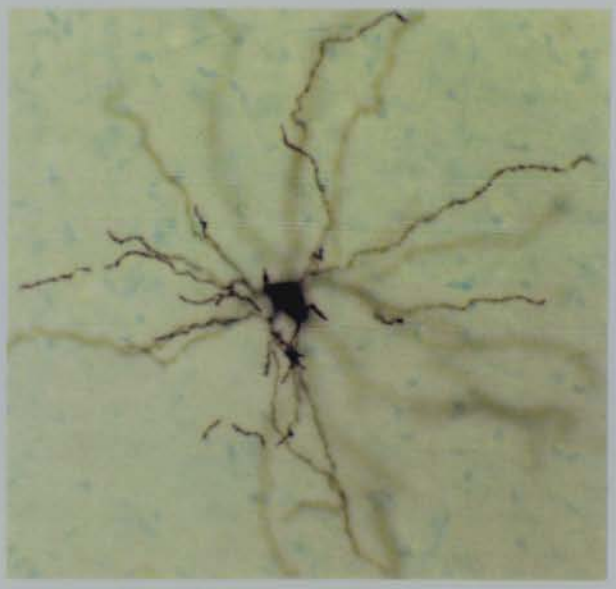

B

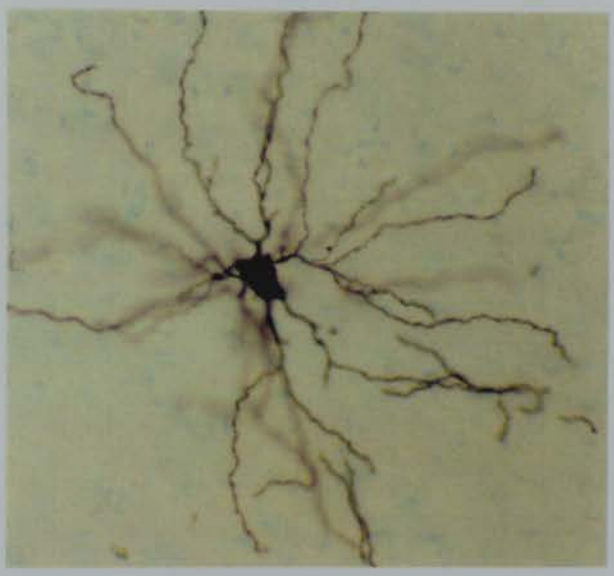

C

**Fig.49.** Photographs illustrating the cell body and dendrites of a biocytin labelled dLGN cell in a control mouse at 194 days post-inoculation. A, B, and C are at different planes of focus in the 70 μm section (x200 magnification).

A

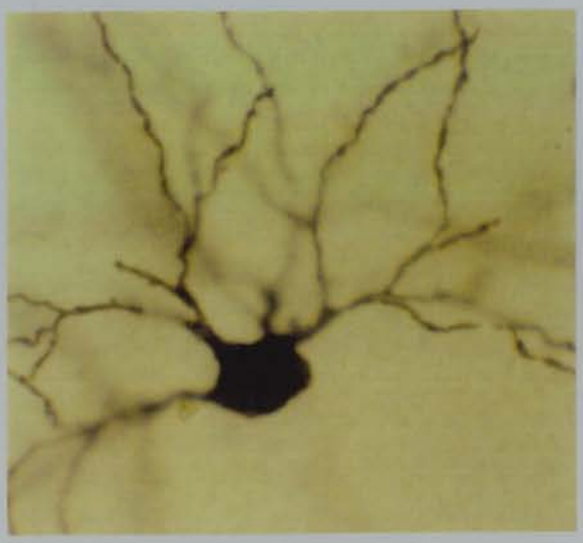

B

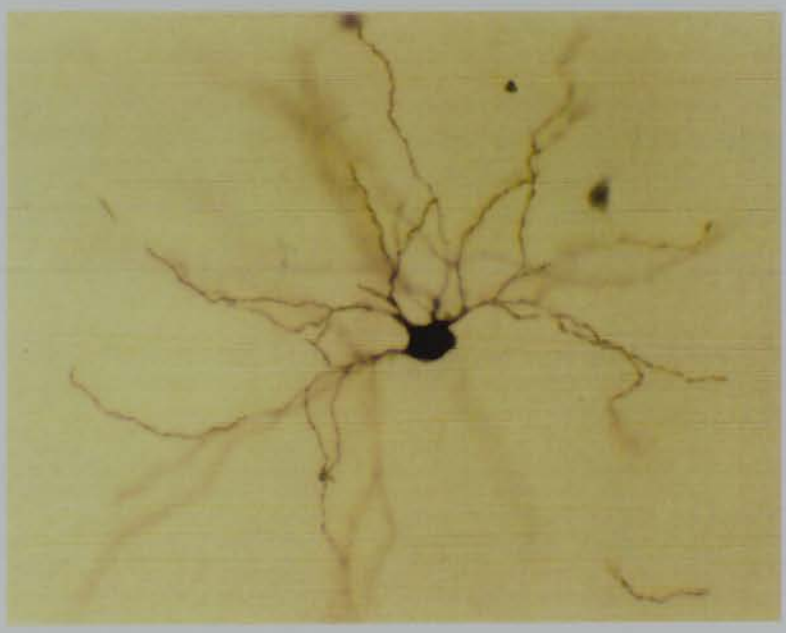

**Fig.50.** Photographs illustrating the cell body and dendrites of a biocytin labelled dLGN cell in a 70 μm section from a scrapie-inoculated mouse at 197 days post-inoculation. A , x600 magnification and B, x200 magnification.

# Chapter 5 - Discussion 1

## The electrophysiological properties of dLGN relay cells in the normal mouse

*5.1.1 Summary of the investigation of dLGN relay cells*

The primary aim of this study was to characterise the electrophysiological properties of murine dLGN relay cells in the normal mouse for comparison with recordings in normal brain inoculated (control) and scrapie-inoculated mice. The intrinsic properties of thalamic relay cells have been extensively investigated in rat and guinea-pig brain slices (see 2.5.1). Jahnsen and Llinas (1984a) first demonstrated that relay cells in the different thalamic nuclei of the guinea-pig, including the dLGN, behave as a homogeneous population. It was established that the properties in the rat are the same as in the guinea-pig (Crunelli et al., 1987a). The electrophysiological properties of murine dLGN relay cells have not been published therefore the aim of the study in normal mice was to establish if murine dLGN relay cells possess similar membrane properties and function as a homogeneous population as reported for the rat and guinea-pig. The basic membrane properties, action potential parameters, and the membrane responses to current injection and optic tract stimulation were monitored in Balb/c mice. This study concluded that the 42 murine dLGN cells sampled appeared to behave as a homogenous population. The basic membrane properties and membrane responses to current injection and optic tract stimulation in murine dLGN relay cells were similar to these properties of dLGN cells in the rat and guinea-pig.

Action potential parameters (spike amplitude; AHP amplitude; rise time; decay time; half width) have not been systematically studied in dLGN relay cells. These parameters were investigated in murine dLGN relay cells from averaged action potential shapes. As previously identified in dLGN cells (Jahnsen and Llinas, 1984b), a biphasic after-hyperpolarisation (AHP) was observed following the repolarisation phase of the spike. In the present study the delayed slow AHP was apamin-sensitive suggesting that it is mediated by the small-conductance calcium-activated potassium current, $I_{AHP}$.

*5.1.2 Membrane properties*

In all 42 cells studied the membrane responses to intracellular current injection were the same as those observed in published studies of thalamic relay cells in the rat and guinea-pig (see 2.5.1). In all murine dLGN cells in this study there was an obvious depolarising sag of the membrane potential in response to the injection of large amplitude hyperpolarising current pulses (fig.10). McCormick and Pape, (1990) demonstrated that this inward

rectification in relay cells is mediated by the mixed cation current, $I_H$. In murine dLGN cells a low threshold spike was evoked at the termination of current pulses that hyperpolarised the cell negative to -60 mV. A similar response has been identified in guinea-pig and rat relay cells which was due to a low threshold calcium spike and was mediated by the calcium current $I_T$; $I_T$ is sensitive to nickel chloride (Crunelli et al. 1989; Hernandez-Cruz and Pape, 1989). In this study the low threshold spike in murine dLGN cells was reduced by nickel chloride showing that it was also mediated by $I_T$. The burst of spikes superimposed on the low threshold calcium spike, and the train of spikes evoked by depolarising pulses were blocked by TTX and were therefore similar to the TTX-sensitive action potentials in guinea-pig and rat dLGN relay cells (Jahnsen and Llinas, 1984b; Crunelli et al., 1987). Jahnsen and Llinas (1984b) demonstrated that when voltage activated sodium currents were blocked, high threshold spikes could be evoked from approximately -20 mV in relay cells, that were reduced in low extracellular calcium. The high threshold voltage-activated calcium current, $I_L$ has been identified in relay cells; this current has a distinct activation range from $I_T$ and is also reduced by nickel chloride (Hernandez-Cruz and Pape, 1989). In the presence of TTX high threshold spikes were evoked from approximately -20 mV in murine dLGN cells. These high threshold spikes were similar in profile and threshold to the spikes observed in the study by Jahnsen and Llinas, (1984b) and were sensitive to nickel chloride. The depolarised threshold of this response and its sensitivity to nickel ions suggests the high threshold spikes were mediated by the high voltage-activated calcium current in relay cells, $I_L$.

When the low threshold spike in murine cells was evoked from membrane potentials in the approximate range of -60 to -70 mV, there was an obvious delay to the onset of the low threshold spike. The transient outward potassium current, $I_A$ is responsible for this delayed phase in thalamic relay cells (Huguenard et al., 1991; Budde et al., 1991) and therefore may have the same role in murine dLGN cells. In response to depolarisation from membrane potentials negative to approximately -60 mV an outward rectification was evident in the cells in this study. A delay between the initiation of the current pulse and the onset of the spike train was observed when depolarising pulses were applied from a membrane potential between approximately -60 and -70 mV. This response in guinea-pig and rat thalamic cells is mediated partially by $I_A$ and also by $I_{AS}$, a potassium current with a similarly fast activation rate to $I_A$ but with slower inactivation kinetics (McCormick, 1991;

Huguenard et al., 1991). Similar currents may therefore be responsible for the delay to action potential generation in murine dLGN cells.

The most prominent difference between intrinsic interneurones and relay cells recorded in current clamp is that interneurones do not display the low calcium threshold potential or the delay to the onset of firing often seen in relay cells with depolarisation from membrane potentials hyperpolarised to -60 mV (see 2.6.4). All 201 murine dLGN cells that satisfied the criteria for inclusion in the study possessed a robust low threshold calcium spike. All impalements of dLGN cells that exhibited weak low threshold spikes did not meet the minimum criteria for this study (see 3.5.6). On this basis it is most probable that cells recorded in the murine dLGN lacking a robust low threshold spike were poor impalements of relay neurones as opposed to interneuronal recordings. In view of the fact that they constitute 25 % of the neuronal population in the dLGN, an obvious question to address is why interneurones were not represented in the population of 201 cells recorded in this study. Interneurones possess smaller cell bodies than relay cells (see 2.2 and Pape et al., 1994) which may result in greater difficulty in obtaining a stable impalement following invasion of the electrode. In a study of rat and cat thalamic relay cells Leresche et al., (1991) recorded from 12 interneurones out of a total population of 289 dLGN cells impaled. This demonstrates the low probability of encountering these cells and the apparent bias of the intracellular technique towards sampling relay cells. This is perhaps reflected by the fact that there are only two published studies focusing purely on the intrinsic properties of dLGN interneurones.

All 42 dLGN cells recorded in the murine dLGN displayed a stable membrane potential without exhibiting spontaneous electrical activity. Relay neurones in the rat and guinea-pig are also electrically silent at rest (see 2.8). The basic membrane properties in the sample of murine dLGN relay cells studied are detailed in Chapter 4 (table 1) of this thesis. The membrane potential and time constant in murine dLGN relay cells (table 1) are similar to published values in relay cells (e.g. Crunelli et al., 1987a; McCormick and Prince, 1987). The mean value for the input resistance is noticeably higher than in the published studies. In the study by Jahnsen and Llinas (1984a) the minimum acceptable resistance was 15 MΩ. This is less than the 30 MΩ set in the present study perhaps explaining the higher mean input resistance in the results presented in this thesis. The lower limit of 30 MΩ was introduced in the present investigation as cells with smaller resistances than this exhibited electrophysiological properties and responses to current injection typical of poor electrode

impalements. The mean action potential threshold has not been reported in studies of relay cells the rat or guinea-pig and therefore cannot be compared.

When the action potential threshold, input resistance and time constant were plotted against resting membrane potential, and the input resistance against time constant, (see fig. 14), there was no indication of distinct focal clusters of data points suggestive of behavioural sub-populations. This demonstrated that the mouse dLGN cells sampled functioned as a homogeneous population. A significant correlation (fig. 14D) was found between the input resistance and time constant in the population of cells studied.

*5.1.3. Action potential properties*

A detailed study of the action potential properties in thalamic relay cells has not been reported. An investigation of the spike amplitude, AHP amplitude, rise time, decay time and half width in murine relay cells was performed for a comparison of these parameters in the inoculated mice in the scrapie study. Two methods were used and compared in this study to collect action potential trains for spike shape averaging. Action potentials were initiated at a rate of 1 - 2 Hz by a constant amplitude depolarisation and then in the same cell single spikes were evoked repetitively by short duration current pulses from a membrane potential 2 mV below threshold. Measurements were subsequently taken from the average spike shape. The parameters of the average action potential shapes recorded by the two methods in 27 murine dLGN cells are detailed in table 2 ( in Chapter 4). The spike amplitude of the evoked spikes was significantly greater than in those initiated by depolarisation to threshold, and the AHP amplitude in the evoked spikes was significantly reduced. A possible explanation for the reduction in AHP amplitude is that the hyperpolarised membrane potential is closer to the equilibrium potential for potassium, which is approximately -110 mV in relay cells (McCormick and Pape, 1990); this may result in a reduction in the outward driving force for potassium during repolarisation and therefore a smaller AHP amplitude.

In voltage clamp experiments in mammalian neurones it has been shown that hyperpolarising pre-pulses prior to membrane depolarisation resulted in the activation of a larger sodium current than depolarising pre-pulses due the de-inactivation of fast sodium channels (Hodgkin and Huxley, 1952; Dodge, 1961). The present study has demonstrated that the TTX-sensitive sodium current ($I_{Na}$) underlies the depolarising phase of action potentials in murine dLGN cells. The increase in spike amplitude observed in the evoked

spikes is probably due a larger sodium influx as an increased number of sodium channels are now available due to the de-activation of sodium channels by the hyperpolarisation. The largest increments when the initiated and evoked spike amplitudes were compared were evident in those cells with the more depolarised action potential thresholds and there was a significant positive correlation between the action potential threshold and the increment in evoked action potential spike amplitude in those cells with thresholds positive to -45 mV (see 4.1.4). In cells with more depolarised thresholds, a larger proportion of the total number of channels will be inactivated; thus the channels de-inactivated by the hyperpolarisation will make a greater contribution to sodium influx during the action potential therefore resulting in a larger spike amplitude. Presumably in cells with thresholds below -46 mV the number of channels de-inactivated by the 2 mV depolarisation is relatively small and the additional sodium influx due their recruitment does not have such a marked effect on the amplitude of the spike.

The scatter of the plots of the relationship between the action potential threshold and the spike and AHP amplitude suggests that in terms of these parameters murine relay cells function as a homogeneous population (see fig.16). The significant negative correlation between the spike amplitude and threshold and AHP amplitude and threshold (see 4.1.4) can be explained in terms of the kinetics of the conventional voltage-gated sodium and potassium currents that shape the action potentials in mammalian neurones. As discussed above, the more depolarised threshold of a cell the greater the proportion of inactivated sodium channels, explaining the smaller amplitudes in these cells. A small spike amplitude will result in a sub-maximal activation of the outward potassium currents repolarising the action potential and hence, in cells with more depolarised thresholds, a smaller AHP amplitude.

*5.1.4 Optic tract-evoked synaptic input*

A quantitative analysis of the "maximum EPSP" ($EPSP_M$) in dLGN cells evoked by optic tract stimulation in normal mice was performed as a control for the measurement of this parameter in the study of normal brain and scrapie-inoculated mice. Cepeda et al. (1992) recorded the $EPSP_M$ in human caudate neurones to assess the efficacy of the input to these cells at different developmental stages. This method of comparing synaptic function over a time period seemed appropriate to studying the strength of the excitatory input to relay cells at different time intervals across the scrapie incubation period. In addition to

evoking an EPSP, optic tract stimulation can indirectly evoke fast and slow IPSP's in relay cells (Crunelli et al., 1988; Crunelli et al., 1987; Hirsch and Bernod, 1990).

At -60 mV the membrane potential was outwith the range of activation of the low threshold spike which could potentially contaminate the data records of the $EPSP_M$. However with membrane hyperpolarisation the $EPSP_M$ evoked a low threshold spike (fig.19). Qualitatively, action potentials evoked by the $EPSP_M$ at depolarised membrane potentials and the low threshold spike and burst of action potentials at hyperpolarised potentials were similar to responses in rat (Crunelli et al., 1987b; Turner et al., 1994) and guinea-pig relay cells (Jahnsen and Llinas, 1984a). In published studies of the optic tract-evoked synaptic input to relay cells, the $EPSP_M$ has not been quantified. Therefore a direct comparison of the peak amplitude, rise time and decay time of this response cannot be made with other species.

The results of this study provide an effective basis for comparison of the electrophysiological properties in normal brain inoculated and scrapie-inoculated mice.

*5.1.5 Apamin-sensitive component of the slow AHP*

In each of the 27 average spike shapes monitored in this study the action potential after-hyperpolarisation was biphasic. The AHP consisted of fast component from the peak of the spike to the point of maximum undershoot that lasted several milliseconds and a slower phase that delayed the return of the membrane to its resting potential by up to 100 ms (fig.17). In the first *in vitro* study of thalamic relay neurones, Jahnsen and Llinas, 1984b) demonstrated that the after-hyperpolarisation of the action potential in these cells was biphasic; both phases of the after-hyperpolarisation were calcium dependent. Voltage clamp experiments in thalamic relay cells have shown that the fast AHP is mediated by the large calcium activated conductance, $I_C$. The conductance underlying the slower calcium-dependent phase of hyperpolarisation has not been identified in relay cells. In the present study a component of the slow AHP was blocked by apamin confirming that it is mediated by the small conductance calcium-activated potassium current, $I_{AHP}$. $I_{AHP}$ mediates a similar hyperpolarisation lasting up to 200 ms in a number of mammalian neurones (e.g. Pennefather et al., 1985; Johnston et al., 1995; Viana et al., 1993; Osmanovic et al., 1990).

In response to depolarisation, a marked increase in the frequency of spike discharge was observed in the presence of apamin (fig.18B *top panel*). There was an apparent broadening of the low threshold spike (fig.18B, arrow 1) and an increase in the number of

spikes superimposed on the low threshold spike (fig.18B, arrow 2). These altered responses to current injection were evident in the absence of a discernible increase in membrane input resistance (fig.18C). This demonstrates that the altered membrane responses were due to a specific effect of apamin and not to a larger depolarisation as a consequence of a non-specific reduction in somatic conductances.

In addition to being apamin-sensitive, Pennefather et al. (1985) demonstrated that the amplitude of $I_{AHP}$ could be partially reduced by muscarinic agonists. The apamin-sensitive $I_{AHP}$ identified in a number of neuronal populations has not been tested for cholinergic sensitivity however Johnston et al., (1994) found that that this potential in MVN neurones was not sensitive to the mixed cholinergic agonist carbachol; this suggests that not all slow calcium-activated conductances mediated by SK channels are sensitive to cholinergic agonists. Another type of slow calcium-activated potassium conductance, that has also been termed $I_{AHP}$, has been identified in hippocampal neurones (Lancaster and Nicoll, 1987); this current is sensitive to muscarinic agonists but it is not sensitive to apamin and therefore is not identical to the $I_{AHP}$ originally identified by Pennefather et al. (1985). McCormick et al. (1992) demonstrated that the slow muscarinic depolarisation in guinea-pig relay cells persisted in the presence of a block of transmembrane calcium currents which led him to suggest that a slow calcium-activated calcium conductance was not present in these cells. However as the evidence presented thus far suggests this result does not negate the possibility that an apamin-sensitive but muscarinic-insensitive $I_{AHP}$ exists in this neuronal population.

Given the original observation of a calcium-dependent slow phase of repolarisation of the action potential in guinea-pig relay cells, it is probable that this finding of $I_{AHP}$ in murine relay cells does not represent a species difference, rather it reflects the fact that the effects of apamin on action potential shapes have not been studied in these species.

# Chapter 5 - Discussion 2

## Summary discussion of the findings in control and scrapie-infected mice

*5.2.1 Impact of the inoculation procedure*

In this study the basic membrane, action potential and synaptic parameters of dLGN cells measured in normal-brain inoculated (control) and normal mice were not significantly different; this demonstrated that the intraocular inoculation procedure performed on the experimental mice did not affect the functional properties of dLGN cells. This established that the inoculation procedure would not mask pathophysiological effects due scrapie-infection. The time intervals studied in this investigation were 60, 88, 112, 140, 168, 198 and 230 days post-inoculation; the mean incubation period in the scrapie inoculated animals in the two series examined were 277 and 274 days post-inoculation.

In this chapter the discussion relates to the results reported in consecutive sections in Chapter four, in which details of the analysis groups (seen in italics in the text below) are also found.

*5.2.2 Comparison of membrane properties*

Relay cells in the dLGN recorded throughout the incubation period in scrapie-infected mice displayed an identical array of voltage-activated currents to those observed in control and normal mice indicating that in the cells sampled, scrapie infection of the dLGN has not compromised the membrane response properties. There were not any *age-related* changes in the resting membrane potential, action potential threshold, membrane time constant and input resistance (basic membrane properties) throughout the period studied. Also there were no differences between the basic membrane properties in the control and scrapie-inoculated groups at each of the incubation intervals studied (*treatment test*). Statistical comparisons of *regrouped* data (60 - 112, 140 - 168 and 198 - 225 days post-inoculation; *see 4.2.4*) and comparisons of *pooled* data (60 - 225 days post-inoculation in control) in both control and scrapie-inoculated mice did not reveal any significant differences with exception of the action potential threshold; when values were *pooled* the firing threshold in scrapie-inoculated mice was significantly negative to that in the control mice. Values for the pooled AHP or spike amplitude in scrapie-infected mice were not significantly different from controls; this would be expected given the significant correlations between firing threshold and both AHP and spike amplitude (see 4.1.4) found in the study of murine relay cells. There is a high degree of overlap in the plots illustrating the relationships between the basic membrane properties in normal, control and scrapie-inoculated mice; this suggests that the cells in mice from each group were sampled from a

single population. The single statistically significant result is an isolated observation therefore a reasonable interpretation of the results is that the basic membrane properties of cells in normal, control and scrapie-inoculated mice constitute a homogeneous population. In the cells sampled the presence of scrapie infection does not appear to have compromised membrane function.

*5.2.3 Comparison of the action potential properties*

The action potential parameters (spike and AHP amplitude; rise and decay time; half width) compared in control and scrapie-inoculated mice at each time interval (*treatment test*) and in the *regrouped* and *pooled data* groups, were not significantly different. A significant difference within the control group (a*ge related test*) was found in the rise time: the rise time at 112 days was significantly different from the values at 60, 140, 168 and 198 days. However the rise times at 60, 140, 168 and 198 days did not differ. This significant difference arose from a global analysis involving comparisons of five action potential variables between two experimental groups and over five incubation period time points. Therefore in context of the multiple comparisons of action potential parameters reported, this single difference must be discounted as not biologically significant. Thus in the control group there appeared to be no evidence of age related changes during the time course of the experiment, similar to the findings in the scrapie-infected group. The scatter of the relationship between threshold, AHP and spike amplitude in cells in normal, scrapie-inoculated and control mice is consistent with the action potentials in each of the experimental groups behaving as a homogenous population.

Essentially, scrapie-infection of the dLGN did not compromise the average action potential shapes quantified in this study.

*5.2.4.Comparison of the maximum EPSP*

The peak amplitude, rise time and decay time of the maximum EPSP ($EPSP_M$) evoked in dLGN relay cells by electrical stimulation of the optic tract fibres in control and scrapie-inoculated mice were quantified. There were not any *age-related* changes in either experimental group of mice; comparison of the mean values at each time interval (*treatment test*) and in the *pooled* and *regrouped* intervals did not reveal any significant differences in the parameters studied. It would therefore appear that throughout the incubation period the efficacy of synaptic transmission between dLGN relay and retinal ganglion cells, in both

scrapie-inoculated and control mice, is essentially similar i.e. the presence of scrapie infectivity does not alter the integrity of the synapse in the population of cells studied.

*5.2.5. Relay cell morphology in control and scrapie-infected mice*

In terms of their morphology, the cells labeled at each incubation period interval (control: 114, 194 and 230 days post-inoculation; scrapie: 85, 164, 165, 197, 199 and 225 days post-inoculation) were subjectively similar to cells found in the Golgi-impregnated murine dLGN (Iwahori and Mazuno, 1984; Rafols and Valverde, 1973). Labeled cells in both groups possessed sites of increased thickening on their dendrites consistent with dendritic enlargements observed at branch points in Golgi-stained neurones. Morphometric analysis of the cells demonstrated that there was a considerable overlap in the cell body length, dendritic process length, extent of dendritic branching and number of primary dendrites in cells from both experimental groups. Candidate axons, identified due to their similarity to axons described in Golgi studies, were labeled but the effects of scrapie-infection on spine integrity could not be assessed due to their inconsistent labeling. Rafols and Valverde, (1973) demonstrated that ultrastructural examination of Golgi-stained murine dLGN relay cells was necessary to study the morphology of dendritic spines in murine dLGN cells.

Cell body sizes and dendritic branching patterns have been studied in the murine dLGN following de-afferentation (Brandes, 1971). In this study a small but significant reduction in the horizontal, but not the vertical diameter of the soma in murine geniculate cells, was reported but the dendritic branch length or branch pattern between normal and de-afferented cells did not differ. Given the small sample of geniculate cells labeled in dLGN in the present study it is therefore not possible to assess if cell body atrophy with a possible link to de-afferentation, has occurred.

The subjective and quantitative analysis of the reconstructed cells (see figs.45 - 48 and table 14) presented in this thesis suggests that, in the population labeled, the morphology of dLGN relay cells is not altered by the scrapie-infection of the dLGN. The cells did not exhibit morphological abnormalities that have been observed in scrapie-infected cortical and hippocampal neurones (see 1.4).

# Chapter 5 - Discussion 3

## Normal relay cell function in the scrapie-infected dLGN

*5.3.1 Review of the scrapie study*

This study characterised the effect of intraocular ME7 scrapie on the functional and morphological properties of murine dLGN relay cells; the basic membrane and action potential properties, the neuronal morphology and the integrity of the synapse between retinal ganglion and dLGN relay cells were investigated. In relating neuronal structure and function to the established pattern of pathological changes and neuronal loss in the scrapie-infected dLGN this study aimed to elucidate the mechanisms of dysfunction preceding cell death.

Despite the expectation of a progressive deterioration in neuronal function during the incubation period, the functional and morphological properties of dLGN cells in mice intraocularly infected with ME7 scrapie were qualitatively and quantitatively identical to the properties of neurones in control and normal mice. These findings are highly surprising when considering that the properties of cells recorded, even at an advanced stage of the disease, were apparently normal at a time when the pathological deposits and neuronal loss associated with this model are well established. These results also contrast with the published findings of a progressive deterioration in the synaptic input and intrinsic properties of hippocampal CA1 and cortical cells (Jefferys et al., 1994; Johnston et al., 1995) and the reports of an altered morphology in hippocampal cells (Johnston et al., 1995; A.R. Johnston, personal communication).

*5.3.2 The presence of scrapie pathology in the dLGN*

The scrapie-inoculated mice utilised in this study exhibited behavioural signs symptomatic of the clinical phase of scrapie infection. The mice designated for calculation of the experimental end-point were culled in accordance with the severity of their clinical symptoms; the mean incubation period was within the expected range for published studies of mice intraocularly infected with ME7 scrapie (240 to 300 days). Although the mice showed the typical clinical signs of succumbing to scrapie infection, in the light of the remarkably normal function of the relay cells in this model it was necessary to demonstrate that the dLGN in the animals investigated was actually targetted with scrapie pathology. In parallel with the electrophysiological investigations, at intervals throughout the incubation period, the onset of histopathological changes in the dLGN (in mice randomly selected from the inoculated groups in the second series of animals) was monitored by staff of the Neuropathogenesis Unit, Edinburgh. Histological and immunolabelling techniques

employed in the study of the dLGN by Jeffrey et al. (1995) were utilised to detect the onset of vacuolar lesions, PrP deposition and altered synaptophysin labeling in the dLGN.

Although the scrapie incubation period of the mice reported in this thesis was approximately 40 days longer than in the published study by Jeffrey et al. (1995), the temporal pattern of pathology in this and the published study was very similar. The onset of vacuolar lesions in scrapie-infected mice was at 168 days post-inoculation, and the severity of vacuolation increased markedly with progression of the incubation period. Disease specific accumulations of PrP were first seen as diffuse deposits at 169 days post-inoculation; at later time intervals areas of diffuse staining were more intense and focal areas of accumulation resembling "plaques" were sparsely evident. Subjectively a slight, but uniform, reduction in synaptophysin labeling, indicative of a loss of synaptic terminal vesicles, was observed at 198 days post-inoculation in the dLGN of scrapie-infected mice. At later intervals there was a more marked reduction in synaptophysin labeling. These findings clearly demonstrate that the dLGN, in which neurones with normal functional properties were recorded, was a definite target of scrapie pathology.

These histopathological observations are clearly similar to the temporal sequence of changes observed in the published study by Jeffrey et al. (1995) in the dLGN of mice intraocularly infected with ME7 scrapie. It can therefore be assumed that a similar temporal sequence of neuronal loss to that reported by Jeffrey et al. (1995), occurred in the dLGN of the mice in the present electrophysiological investigation. The sequential pattern of neuronal loss reported in the published study is illustrated in figure 3.

*5.3.3 Possible limitations resulting in restricted data sampling*

In the view of finding that only neurones with normal intrinsic and functional properties have been sampled in the scrapie-infected dLGN, it is necessary to address the possibility that limitations in the experimental design resulted in the exclusion of functionally compromised neurones from those analysed in this study.

The intracellular recording technique involves puncturing the membrane of the neuronal cell body (diameter approximating between 15 and 35 μm) with an electrode with a tip diameter of approximately one micron. It is reasonable to suggest that a neuronal membrane damaged by scrapie infection may not possess the structural integrity to withstand the physical damage imposed by the electrode; it may not be possible to obtain a

stable recording from such a cell. This could explain the recording of only apparently healthy cells in the dLGN.

Clearly it is possible to envisage a situation in the scrapie-infected slice where the impalement of a cell with a membrane compromised by infectivity (but still able to withstand the physical trauma of impalement) could not be distinguished from the recording of a cell that had been poorly impaled. This situation would amount to the intracellular recording technique being unsuitable for studying the functional integrity of infected neurones.

Whilst advancing intracellular electrodes through the brain slice preparations from normal mice the electrode sometimes impaled a cell which typically possessed low amplitude action potentials, a weak membrane reponse to current injection and a low resistance. Such recordings lacked the robust nature of stable impalements of dLGN relay cells and were designated "poor impalements"; these impalements are attributed to cells that may have been damaged during the slicing procedure, or those in which the electrode has not centrally or cleanly impaled the soma. Poor impalements were seen in similar proportions in the dLGN at different intervals post-inoculation in both control and scrapie-inoculated mice. The criteria for inclusion of cells in this study were identical for the recording of cells obtained in normal, control and scrapie-inoculated mice (see 3.5.6). The accepted values for the action potential and basic membrane parameters were set at the minimum values that allowed the discrimination between neurones that were poorly impaled and those that appeared functionally viable. It is therefore unlikely that these "poor impalements" constitute pathologically compromised cells.

Published intracellular studies of neurones in brain slices from scrapie-infected rodents have successfully impaled neurones with pathologically abnormal membrane and action potential properties (Jefferys et al., 1994; Johnston et al., 1995). This indicates that some neurones infected with scrapie can tolerate electrode impalement. The technique of intracellular recording in brain slices is also used to study neuronal function following acute insult e.g. kainic acid (Ashwood et al., 1986) and 6-hydroxydopamine lesions (Calabresi et al., 1993) and induced anoxia (Cowan and Martin, 1992). Collectively this evidence suggests that the technique of intracellular recording from brain slices is effective in studying the mechanisms of neuronal dysfunction in the diseased and lesioned brain. It is therefore improbable that the findings of normal neuronal function in the scrapie-infected

dLGN reflects a failure to sample, and subsequently analyse, functionally compromised cells.

Arguably the most important finding of this thesis, in terms of the disease process, is that cells with normal intrinsic and synaptic function persist in the dLGN even at an advanced stage of the disease when there has been substantial neuronal loss and very obvious pathological lesions.

*5.3.4 Is there a scrapie-resistant population of cells ?*

Given that the total number of cells from scrapie-inoculated mice included in this study is 81, and therefore few cells were recorded in each infected mouse, it is necessary to consider the possibility that the cells sampled were members of a scrapie-resistant sub-population of dLGN relay neurones. Evidence to support this may come from the morphometric analysis in the dLGN infected with ME7 scrapie (Jeffrey et al., 1995) which found that on average 1000 cells remain at the clinical end point of the disease (see figure 3). The fact that the mice were culled at a defined clinical end-point leaves the possibility that mice in which the disease is left to take its "natural" course may exhibit complete degeneration of the dLGN neuronal population. Analysis of the population of dLGN cells in the normal mice demonstrated that relay cells function as a homogenous population; in terms of their morphology, which has been extensively investigated in Golgi studies (Iwahori and Mazuno, 1984; Rafols and Valverde, 1973), there is no basis for a sub-classification of murine dLGN relay cells. From the results presented in this study it is clear that in terms of electrophysiological properties there is also no evidence for the existence of neuronal sub-populations. Whilst it is still possible that a resistant population of cells exists, in the absence of direct evidence to the contrary I will assume that all cells in the dLGN ultimately die as a result of scrapie infection.

*5.3.5 Transfer of infectivity from retinal ganglion to dLGN relay cells*

The progression of infectivity within the visual pathway, at the rate of slow axonal transport, suggests that neuron to neuron transfer via the synapse is responsible for the transfer of infectivity between the retina, dLGN and visual cortex (Scott et al., 1992). In light of the finding that there is normal synaptic function between retinal ganglion axon terminals and relay cells in the infected dLGN, it is necessary to explore whether all synapses mediate the transfer of infectivity. Retinal ganglion cells comprise small, medium

and large diameter sub-types which may differ in their selective ability to uptake and transmit infectivity. There is a laminar distribution of the inputs from the three classes of retinal ganglion cell to the dLGN (Lund et al., 1976). If a particular class or classes of retinal ganglion cell were involved in the transport of infectivity then one would expect cell death to be initially restricted to a defined region of the dLGN, and advance from that area with progression of the incubation period. The existence of a spatially select neuronal loss could be monitored in a future study by performing neuronal counts in all sectors of the spatially subdivided nucleus. The morphometric study of the dLGN performed by Jeffrey et al. (1995) did not assess if a spatial pattern of neuronal loss was evident in the dLGN. If there is a selective uptake of infectivity by a sub-class of ganglion cells, then during the incubation period the recording of viable cells should occur in a progressively restricted area of the nucleus. In the present study, cells impaled at all stages of the incubation period were randomly located throughout the nucleus; there was no obvious restriction in the location of cells with advancement of the incubation period. Although this may support the uniform uptake of infectivity, this observation must be interpreted with caution due to the limited number of cells recorded in each slice. The subjective reduction in the area the dLGN occupied in brain slices in scrapie-infected mice from 200 days of the approximately 270 day incubation period, suggests that shrinkage of the nucleus had taken place due to neuronal loss; this would obviously result in surviving cells occupying a reduced area, possibly obscuring an observation of cell being recorded in a restricted area of the nucleus. This might also hinder the observation of a spatially select reduction in synaptophysin labeling. However, it is interesting that, when first detected, the reduction in synaptic vesicle labeling is uniform throughout the nucleus; an initial loss of labeling in a distinct region of the nucleus would be expected if a single class of ganglion cells mediated the transfer of infectivity.

On balance of the evidence presented, I will assume that all synapses mediate the transfer of infectivity.

### *5.3.6 The relationship between normal electrophysiological properties, infectivity and neuronal loss: two hypotheses*

Although it is likely that all dLGN cells ultimately die as a result of scrapie infection, the results of this study indicate that the only cells in the infected nucleus that are viable possess normal electrophysiological and optic tract evoked synaptic properties. Two

hypotheses can be put forward in an attempt to explain how scrapie-infection of the dLGN can be reconciled with these findings. The first is that the cells recorded in this study are pre-infected. In view of the dramatic neuronal loss in the dLGN and the fact that cells are not recorded with dysfunctional properties, infection must result in immediate cell death. Secondly, the entire population of dLGN relay cells may be infected from early in the incubation period but their function is not compromised by the presence of infectivity.

The merits of these hypotheses must be gauged in terms of what is known about the profile of neuronal loss in the dLGN. The temporal pattern of the decline in cell numbers in the dLGN both contralateral and ipsilateral to the scrapie-infected and normal brain inoculated eye can be seen in figure 3 (Jeffrey et al., 1995). For each incubation period time interval the mean neuronal number was calculated from dLGN cell counts in five different mice; this study did not discriminate between interneurones and relay cells. It is the nucleus contralateral to the infected eye that has been studied in this electrophysiological investigation. At the first time point of 50 days out of the 240 day incubation period in the published study, the mean neuronal number in the nucleus contralateral to the scrapie-inoculated eye is notably higher than the corresponding values in the nucleus contralateral and ipsilateral to the control, and ipsilateral to the scrapie-inoculated eye; the mean number of cells in the contralateral infected nucleus is approximately 22 000 cells as opposed to between approximately 16 000 and 17 000 in the other groups. As the initial values in all four groups are not significantly different, a more representative value from which to describe the profile of neuronal loss is an average of all the values at this time point; i.e. approximately 18 000 cells. In separate investigation by Heumann et al. (1980) the neuronal number in the dLGN of normal adult mice was found to be around 17 000. This is closer to the average of 18 000 than the value of 22 000 in the contralateral infected dLGN which supports taking the average as a starting value. In the study be Jeffrey et al (1995) a significant neuronal loss between the infected and control groups was not found until 200 days post-inoculation. However it is evident that in both the contralateral and ipsilateral dLGN there may have been a decline in neuronal numbers as early as between 50 to 100 days post-inoculation. Although the mean reduction in neuronal numbers at 150 days was not significant for the group, one mouse at this stage showed a 50 % loss of neurones compared to the surviving numbers in the remaining four mice. This is direct evidence that neuronal loss can occur prior to 150 days post-inoculation. The decline in neuronal numbers appeared initially gradual in both the contralateral and ipsilateral nucleus although for a

similar extent of neuronal loss there was a delay of up to 30 days in the ipsilateral nucleus. Beyond 150 days post-inoculation there was a steeper decline in neuronal numbers bilaterally in the dLGN with approximately 2000 neurons remaining in the ipsilateral and 1000 in the contralateral nucleus by the clinical end point of the disease.

### *5.3.7 Hypothesis one: neurones with normal electrophysiological properties are pre-infected*

Infectivity, as detected by bioassay, is not evident until 77 days post-inoculation in the dLGN. There is evidence from enucleation experiments, that infectivity may access the visual pathways before this (see 1.3.1); bioassay is however the only direct way of assessing the presence of infectivity and therefore 77 days will be considered the first time at which the agent invades the dLGN.

According to the first hypothesis proposed all dLGN cells die as soon as they are with infected with scrapie (see 5.3.6, paragraph one). If we assume that all cells in the retina are simultaneously infected at the time of inoculation and that, as agreed earlier, infection is transferred by axonal transport and across synapses, then widespread cell death should have occurred in the dLGN at approximately 77 days post-inoculation.

There is direct evidence for the onset of neuronal loss between 100 and 150 days post-inoculation, after the time that infectivity is delivered to the dLGN. Scott et al., (1989) demonstrated that infectivity accesses the dLGN over a 30 day period (see 1.3.1). Therefore if infectivity resulted in immediate cell death almost complete cell loss would be expected at approximately 110 days post-inoculation. This cannot be reconciled with the morphometric finding that neurones are lost progressively right up until the terminal stages of the incubation period. The results presented in this thesis demonstrate that neurones can be impaled in the dLGN until late in the incubation period; this argues against the early and relatively synchronous loss of dLGN cells predicted by this hypothesis. The predicted immediate cell loss also cannot account for the observed rise in infectivity titres in the dLGN throughout the incubation period (Scott et al., 1992).

One mechanism that reconciles these observations with the recording throughout the incubation period of surviving pre-infected cells, is if the interneurone population were responsible for the selective uptake and replication of infectivity, subsequently releasing it to target the relay cells. To fulfill this role interneurones would have to uptake and replicate infectivity without succumbing to increasing levels of the agent. Interneurones account for

25 % of neurones and in the dLGN there is ultimately a minimum of 90 % cell death which must therefore eventually include interneurones. Therefore in order for infectivity titres to rise throughout the incubation period another factor would have to be accounted for in this hypothesis that would allow all the interneurones to die last in the dLGN, despite releasing infectivity at high enough levels throughout the incubation period to compromise dLGN cells. In the intraocular ME7 model there is a rise in infectivity titres in the optic nerve in the absence of an obvious retinal ganglion cell loss. Infectivity is detected in this area only after high titres are found in the dLGN, suggesting there is a retrograde transport of detectable levels from the nucleus to ganglion cells following its transfer to and replication at this site (Scott et al., 1992). This evidence does not support the above hypothesis.

The predominant type of synaptic connectivity involving retinal ganglion cells in the dLGN involves a retinal terminal contacting both a relay cell and interneurone. Therefore given the intimacy of this synaptic arrangement it would be necessary to introduce into this hypothesis a second unknown factor that could account for the selective transfer to interneurones and not relay cells of the infectivity in the ganglion cell terminals. The selective loss of photoreceptor cells in the retina with the inoculation of the 79A strain of scrapie supports the possibility that a selective transfer to a neuronal population can occur (Foster et al., 1986) However in this investigation the select loss of photoreceptor cells is associated with particularly high infectivity titres in the retina, some ten fold larger than found with ME7, in which these cells do not appear to degenerate. Scott et al., (1992) suggested that high infectivity titres could therefore be associated with degeneration; this may argue against the capability of interneurones to tolerate extreme levels of infectivity. A study specifically addressing the integrity of interneurones in the dLGN is necessary to test the merits of this hypothesis.

### *5.3.8 Hypothesis two: cells with normal electrophysiological properties are infected without compromised function.*

The second hypothesis proposes that the cells recorded in this study were infected. To date the studies in other scrapie models have reported marked deficits in neuronal function; intracellular investigations of hippocampal cell function in mice infected with ME7 and 263K scrapie, and neocortical cells in 263K scrapie have demonstrated that both the synaptic input and intrinsic properties of cells are compromised by infection (Jefferys et al., 1994; Johnson et al., 1995). The onset of abnormal synaptic properties in cortical and

hippocampal cells was between 30 and 40 days in the approximately 60 day incubation period with 263K scrapie, and at 180 days in the 220 day incubation period with ME7. The onset of spontaneous activity in hippocampal cells in ME7 scrapie was at 180 days; in 263K scrapie 30 % of hippocampal and cortical cells exhibited calcium shoulders to their action potentials during the last few days of the incubation period.

Clearly in the context of these results the findings of normal function in the dLGN are highly unusual; the hypothesis that cells recorded in this study were infected necessitates that all cells in the dLGN tolerate infectivity without exhibiting signs of functional abnormalities. The supposition has been made that all cells in the dLGN (interneurones and relay cells) with equal probability are exposed to infectivity from the retinal ganglion cells; Therefore this hypothesis must account for the accumulation of infectivity in the dLGN throughout the incubation period i.e. agent replication, and also the fact that these cells die as a result of scrapie infection.

Implicit to this hypothesis is the assumption that within each cell infectivity must replicate to a critical level at which it is fatal for that cell. Within a homogeneous population of neurones, such as the murine dLGN cells, one would expect a normal variability in the rate at which individual cells replicate infectivity, a similar variation in both the amount of transferred to each cell and in the rate of transport of infectivity within the retinal ganglion cell axons. These factors in combination would result in a broad normal distribution in the temporal onset of neuronal death in the dLGN following the arrival of infectivity. The cumulative effect of a normal distribution of cell loss would result in a distinctive profile to a plot of the number of days post-inoculation against surviving neuronal number; one would expect there to be an initially slow rate of loss which would accelerate such that the steepest decline in neuronal number would approximate at the time point when half of the neurones had been lost. Towards the latter stage of the disease process one would expect a slowing of the decline in numbers.

The predicted pattern of cell loss according to the hypothesis that neurones are infected and replicate infectivity resulting in a random, and thus normally distributed, cell loss closely mirrors the temporal profile of the decline in neuronal numbers quantified in the study by Jeffrey et al. (1995). Assuming, as discussed above, that the average number of neurones is 18 000 there is initially a slow decline in neuronal numbers between 100 to 150 days of the incubation period, which is after infectivity accesses the dLGN. This decline becomes steeper between 150 and 200 days and appears almost linear by the clinical end-

point of the disease. In the morphometric study there does not appear to be the gradual decline in the rate of neuronal loss towards the clinical stage of the incubation period that would be expected with a temporally normal distribution of cell loss. The final stage at which the neurones were counted was the time at which the mice were culled due to the severity of clinical signs; if however the number of cells was counted in mice at the later time of "natural" death due to scrapie, then perhaps a slowing in the reduction of neuronal numbers similar to the relatively small reduction between 100 and 150 days, might be seen.

If the temporal pattern of cell loss is normal, and the maximum rate of decline in cell numbers (due to the replication of infectivity to a lethal level) is the midpoint between the arrival of infectivity and maximum cell loss, then one would expect the steepest rise in infectivity titres in the initial half of this period; this would correspond to between 77 and around 160 to 170 days post-inoculation in an intraocular model with a 240 day incubation period. In a similar ME7 intraocular model the most rapid increase in infectivity in the dLGN was observed between 77 and 100 to 140 days post-inoculation, with a more gradual rise from approximately 140 days until the end of the incubation period (Scott et al., 1992). Therefore the hypothesis that each neuron replicates the infectious agent to a critical level that triggers cell death, resulting in a temporally normal accumulation of infectivity and distribution of cell loss, to an extent fits with the finding of an increase in titres of infectivity during the incubation period. Infectivity titres in the optic nerve also rise throughout the incubation period (Scott et al., 1992). This introduces the possibility that the rise in titres in the dLGN may be due to a steady influx from the retinal ganglion cells axons, thus weakening the proposal that titre levels in the nucleus are mainly a product of infectivity replication within the dLGN relay cell population. However infectivity in the optic nerve is not detected until approximately 100 days by which time high titres are evident in the dLGN; levels in the optic nerve are restricted to a maximum of 10 % of the titres in the dLGN. Therefore whilst it is possible that throughout the incubation period there is invasion of infectivity to the dLGN this source cannot be solely responsible for the titres in this nucleus. The finding that the relatively high infectivity titres in the retina with 79A scrapie is associated with photoreceptor loss, but levels a magnitude lower with ME7 are not, supports this hypothesis that within each relay cell, replication of infectivity may eventually prove fatal (Foster et al., 1986).

The finding in the present electrophysiological investigation that cells were recorded until a late stage of the incubation period (between 200 and 230 days post-

inoculation), also supports the suggestion that cell death in the scrapie-infected dLGN is temporally asynchronous, and not entirely coincident with the arrival of infectivity at 77 days post-inoculation.

Clearly on balance of the experimental evidence the simplest, and most accountable, hypothesis relating the profile of neuronal loss and the accumulation of infectivity in the dLGN is that relay cells uniformly uptake, and replicate, infectivity to levels fatal for each cell. Therefore in terms of the results of this study, relay cells must house and replicate infectivity without detrimental effects on their basic membrane and action potential properties; in addition the transfer of infectivity from retinal ganglion to dLGN cell via the synapse does not appear to compromise the integrity of synaptic function. The proposed onset of neuronal loss from the time of infection is however highly speculative; whilst there is evidence that neuronal loss is onset before 150 days, a future morphological analysis at more frequent intervals in the incubation period is necessary to assess if the temporal distribution of neuronal loss is actually normal.

*5.3.9 De-afferentation and neuronal morphology*

In the intraocular scrapie model the synapses between retinal ganglion and relay cells are regarded as the site of neuron to neuron transfer of infectivity within the visual pathway (Scott et al.,1992; Scott and Fraser, 1989). Uniform reduction of synaptophysin labeling in axon boutons is observed only after the onset of a significant neuronal loss in the dLGN (Jeffrey et al., 1995) and there is no evidence of retinal ganglion cell degeneration in this model (Foster et al., 1986); the finding in the present study of an apparently normal synaptic input in to relay cells in the infected dLGN further supports the suggestion that cell loss in the dLGN is not a result of degeneration of the ganglion cell terminals mediating infectivity. Following enucleation there is evidence of a reduction in the soma size in murine geniculate cells (Brandes, 1971). This study also reported no differences between the dendritic branch lengths or the branching pattern in normal and de-afferented cells. Therefore, given the small sample of geniculate cells labeled in dLGN, it is not possible to assess if cell body atrophy, with a possible link to de-afferentation, has occurred. The findings of altered synaptic function simultaneous with intrinsic abnormalities in hippocampal cells with ME7 scrapie (Johnston et al., 1995), and prior to changes in hippocampal and cortical cells with 263K scrapie (Jefferys et al., 1994) may indicate that

de-afferentation is a feature in these neuronal populations. However combined synaptophysin labeling and morphometric analysis in these brain areas is necessary to address this possibility.

The finding of dendritic spine loss and vacuolation of the dendrites in all CA1 cells recorded in scrapie-infected mice at the terminal stages of disease (Johnston et al., 1995) contrasts with the morphologically normal cells recorded in the dLGN (figs. 45 - 48). Whilst it is difficult to draw conclusions from the small sample of dLGN cells labeled, this does suggest that, despite the increasing severity of vacuolation observed in the dLGN with progression of the incubation period, not all relay neurones exhibit this pathological lesion. Jeffrey et al. (1995) reported a significant correlation between the increase in vacuolation and the reduction in neuronal numbers in the dLGN with progression of the incubation period; the author postulated that vacuolation may be occurring in cells which were scrapie-resistant or, uninfected. The evidence presented in this discussion suggests that in all probability the entire population of dLGN cells become infected with scrapie and ultimately degenerate as a result of the disease. Not only does there appear to be an absence of a scrapie-resistant population but should the cells reported in this study constitute such a population, in contrast to the suggestion by Jeffrey et al. (1995), they are not vacuolated. Vacuolar lesions have been reported in the axons and dendrites of neuronal populations in Golgi studies of rodent scrapie (Hogan et al., 1987) and the human encephalopathy, Creutzfeld-Jacob Disease (Landis et al., 1981). However the results of the present study suggest this is not a necessary consequence of infectivity in dLGN relay cells. Although the interneurones in the dLGN may constitute a population selectively vulnerable to vacuolation the fact that these neurones also degenerate as a result of infection is difficult to reconcile with the suggestion of resistance to, or the absence of, infectivity.

*5.3.10 Apoptosis:- a possible mechanism of scrapie-associated neuronal loss*

Based on the earlier assumption that the population of cells sampled in this study that did not fulfill the criteria for analysis were poor electrode impalements and not pathologically compromised cells, the degeneration of dLGN relay cells was clearly a rapid process given that obviously deteriorating cells were not recorded in this study. In general, cells are thought to die by two mechanisms, apoptosis and necrosis. A brief overview of the characteristic features of cells undergoing necrosis and apoptosis will be included for the

purposes of this discussion. However, more detailed descriptions can be found in Wyllie and Duvall, (1991); Wyllie et al., (1987); Majno and Jovis., (1995); Ueda and Shah, (1994).

Necrotic death typically affects groups of cells, this process causing mechanical damage to the cell membranes, resulting in the release of cellular debri and the induction of an acute inflammatory reaction. This lysis of the cells results from their loss of capacity for volume homeostasis, with consequent swelling of their mitochondria and the disruption of plasma, organelle and nuclear membranes. Although the initial damage by the external insult is probably by different mechanisms, a failure to regulate the internal calcium concentration, resulting in the activation of phospholipases and proteases which further damage the cells membranes, is thought to be the final common pathway (McConkey et al., 1989).

Apoptosis was first described by Kerr et al. (1972) as a mechanism of regulating cell numbers during development; it is now widely accepted that many cell types retain the ability to undergo apoptotic cell death throughout life. The essential features of apoptosis include a reduction in the cytoplasmic volume, nuclear condensation, recognition and ingestion by phagocytic cells and active protein synthesis (Wyllie, 1987). Apoptosis does not involve cell lysis since membranes remain intact and therefore this process is not accompanied by an acute inflammatory reaction. The reduction in cell volume is due to selective fluid loss that is associated with the compaction of cytoplasmic organelles. This is accompanied by plasma membrane convolution and "blebbing", the latter involving the fusion of distended vesicles of endoplasmic reticulum with the membrane surface. Often the shrinking cell fragments into a number of membrane bound vesicles termed "apoptotic bodies". In addition to aggregation of the chromatin, the activation of a calcium-dependent endonuclease cleaves double strand breaks in the apoptotic cell's DNA causing it to become fragmented (Arends et al., 1990).

Only recently have there been investigations into the molecular mechanisms underlying neuronal loss in the spongiform encephalopathies. Forlioni et al. (1993) investigated the effects of chronic exposure of a synthetic PrP peptide on cultured hippocampal neurones. This peptide corresponded to the region of the PrP gene in the brains of patients with the human encephalopathy Gerstmann-Straussler-Scheinker disease, which is known to be involved in the formation of amyloid protein (aggregated chains of abnormal PrP molecules) *in vivo* (Tagliavini et al., 1991). Fluorescent labeling of DNA demonstrated that in hippocampal cells chronically exposed to the peptide there had been condensation of

the chromatin and electrophoretic analysis demonstrated that there fragmentation of DNA, both features that are typical of an apoptotic mechanism of cell death. In terms of the lifetime of cultured neurones, chronic exposure (days as opposed to hours) was required for apoptosis to occur. The onset of apoptosis was not only asynchronous in different cells, but the extent of neurone loss was dose-dependent with high concentrations of the peptide resulting in a dramatic cells loss. Recently, Fairbairn et al., (1994) identified DNA fragmentation by electrophoresis, consistent with an apoptotic mechanism of cell death in the neurones from the brains of Suffolk sheep with naturally occurring scrapie. This is the first evidence of an apoptotic mechanism of cell death in scrapie.

Clearly the lack of an immune reaction in scrapie, the selective loss of individual cells and the proliferation of microglia, the brain's phagocytic cells, are reminiscent of an apoptotic mechanism of cell loss in this disease. From the discussion of the results presented in this thesis the simplest hypothesis explaining cell loss in the dLGN is that cells uptake and replicate infectivity before a level lethal to the cell is reached. According to this hypothesis loss of individual neurones would be asynchronous and at random locations in the nucleus, features that can be reconciled with an apoptotic mechanism of cell loss.

The fact that dysfunctional cells are not recorded in the nucleus suggests that the actual death of the relay neurones in the dLGN is a rapid process. The clearance of apoptotic cells from tissue is rapid, often within hours of the onset of cell death, and it has been shown that only a small percentage of cells can be observed undergoing cell death by apoptosis even in tissue in which there is massive cell death (Raff et al., 1993). A brief interval between the breakdown of a cell and its ingestion by phagocytes could explain the finding that obviously deteriorating cells were not recorded in the dLGN; rapid clearance of cells, shortly after the onset of apoptosis, would result in a low probability of encountering a dying cell during a brain slice experiment.

The work on hippocampal cultures exposed to the amyloidogenic peptide demonstrated that neurotoxicity was dose-dependent and an asynchronous process (Forlioni et al., 1993). A large amount of evidence suggests that $PrP^{SC}$ is the infectious scrapie agent (see 1.2). Making this assumption it is reasonable to suggest that if $PrP^{SC}$ may be similarly capable of dose-dependent toxicity. This would agree with the hypothesis that the agent replicates to toxic levels in dLGN cells. The accumulation of $PrP^{SC}$ to toxic levels at a different rate in individual dLGN cells would result in asynchronous neuronal loss similar to

that observed in neuronal cultures following exposure to the synthetic, amyloidogenic PrP peptide.

*5.3.11 Summary and conclusions*

This thesis reports the results of an intracellular investigation of the functional properties of dLGN relay neurones following the intraocular inoculation of ME7 scrapie. By this route scrapie infectivity and pathology are targetted to the central visual pathways including the dLGN in the thalamus. The results clearly demonstrate that relay cells with normal membrane, action potential and optic tract evoked synaptic properties are viable in the dLGN even at advanced stages of disease. Neurones with dysfunctional properties are not recorded in the infected nucleus. Perhaps the most plausible explanation for these findings, in view of the replication of infectivity and the neuronal loss profile in the dLGN, is that early in the incubation period relay cells are invaded by and subsequently replicate infectivity until a level fatal to each cell is reached. Were this hypothesis true, in accordance with the findings of this study, adverse effects on the intrinsic properties of relay neurones are not a necessary consequence of the invasion and replication of infectivity in the dLGN. An alternative explanation is that the cells recorded in this study exhibit normal properties because they are pre-infected; it is possible the intrinsic interneurones in the dLGN are responsible for the selective uptake, replication and subsequent release of infectivity to target relay cells.

The transport of infectivity from retinal ganglion to dLGN relay cells does not appear to be associated with compromised function at this synapse. In context of the available literature, the results of this study support the suggestion by Jeffrey et al. (1995) that neuronal loss precedes the loss of synaptic vesicles in this model of scrapie infection and de-afferentation is not primarily involved in neuronal loss. The input from the retinal ganglion cells accounts for approximately 20 % of synapses on relay cells (Guillery, 1971); it is therefore possible there is a post-synaptic deficit in relay cell receptors involved in neurotransmission other than at the ganglion cell synapse, which has gone undetected.

The findings of this study contrast with the abnormal intrinsic and synaptic properties of hippocampal and cortical cells in other rodent scrapie models (Jefferys et al., 1994; Johnston et al., 1995). The viability of the hippocampal and cortical cells when exhibiting signs of dysfunction may support the hypothesis that neurones can house infectivity without immediate cell death. It is possible to speculate that the delayed onset in

the functional changes in these cells is due to the accumulation of infectivity to a level symptomatic for the cells, similar to the hypothesised pattern of replication in dLGN cells. In both the latter published studies not all hippocampal and cortical cells simultaneously show signs of dysfunction which may reflect different rates of accumulation of the infectious agent within individual neurones.

In terms of what is known about scrapie strain targetting, how can the normal function of dLGN relay neurones be reconciled with the findings of altered properties in other neuronal populations ? It is known that scrapie strains can selectively compromise the affinity of receptors and the metabolic enzymes associated with different neurotransmitter systems (see 1.5). The fact that the ME7 strain by the intracerebral route targets scrapie pathology to the hippocampus and by the intraocular route to the dLGN, yet appears to have a different effect on select neuronal populations demonstrates that a single strain can exert quite different effects in different areas of the brain. Given the ability of scrapie strains to selectively target receptors it is therefore possible to speculate that ME7 scrapie in these models may target different receptors on dLGN than on hippocampal cells. The fact that cortical and hippocampal cells exhibit signs of functional abnormalities with scrapie infection and the dLGN relay cells do not, yet the targetting with scrapie pathology is common to all these areas, may suggest that hippocampal and cortical cells constitute more vulnerable populations a with a greater tendency to exhibit pathophysiological signs of infection at the level of the neuronal membrane.

What is significant about the findings in the dLGN is that in experimental scrapie the presence of vacuolation, PrP deposition and neuronal loss are not automatic indicators of a widespread loss of neuronal function. The possibility that de-afferentation occurs in other rodent scrapie models has not been addressed but there is evidence to suggest this phenomenon may occur in other encephalopathies. The study of synaptophysin labeling and synaptic function in the scrapie-infected dLGN indicate that this is not a primary pathological feature in this model. Collectively these findings may indicate that the electrophysiological abnormalities in intrinsic and synaptic function in other models may be secondary consequences of the disease process in those neuronal populations.

In this context the following observation is of interest. In the present investigation field potentials were recorded in the CA1 area of the hippocampus in order to assess the integrity of the brain slice preparation at a stage in the incubation period when the dLGN was electrically quiescent. The hippocampal field potentials at this advanced stage of

disease subjectively appeared similar to those recorded in control mice and not attenuated as found in the published study of intracerebrally ME7-infected mice (Johnston et al., 1995). This finding must be interpreted with caution as the field potentials were not quantified throughout the incubation period in this model. However this introduces the possibility that in the intraocular model the targetting of scrapie infection to the central "clinical target areas" results in the death of the animal without affecting hippocampal function. If this is the case this finding would suggest that whilst monitoring the effects of different scrapie strains on different neuron populations may inform on the specific effects in those cells, such studies may not be characterising the key functional deficits underlying the onset of clinical symptoms and eventual death of the host.

Relay cells in dLGN intraocularly infected with ME7 scrapie do not exhibit the pathophysiological abnormalities evident in hippocampal and cortical cells, nevertheless the dLGN is clearly subject to neuronal loss and pathological changes. These observations permit the speculation that this is a less complex model for investigating the mechanisms of agent replication and cell death in scrapie.

# Appendix

## Recipes from *The Glasgow Cookbook* (1962 edition)

## SHEEP'S HEAD BROTH

**Ingredients:**

Sheep's Head (split).
4 quarts Water.
4 oz. Barley.
2 oz. dried Peas (soaked overnight).
2 small Carrots.
6 oz. Turnip.
1 Onion.
2 Leeks.
Salt and Pepper.
4 oz. Cabbage.
Parsley.

**Method:**

1. **Remove brains from head and soak in cold water.**
2. **Wash the head with warm water and soak overnight in cold water.**
3. **Put in pan, cover with cold water and bring to boiling point.**
4. **Wash and clean the head thoroughly.**
5. **Put on again in 4 quarts water with scalded barley and soaked peas. Bring slowly to boiling point and cook 1½ hours.**
6. **Add diced vegetables and seasoning and simmer 2 hours.**
7. **Chop the cabbage and add along with the chopped brains ½ hour before serving.**
8. **Add 1–2 tablespoonfuls chopped parsley.**

*Note:* Traditionally a singed head was used.

## HAGGIS

**Ingredients:**

1 Sheep's Bag and Pluck.
¼ lb. Suet.
4 medium-sized Onions (blanched).
½ lb. pinhead Oatmeal.
2–4 level tablespoonfuls Salt.
1 level teaspoonful black Pepper.
1 level teaspoonful powdered Herbs.

**Method:**

1. **Wash the bag in cold water, scrape and clean it well. Leave overnight in cold water.**
2. **Wash the pluck and put it in a pan of boiling water and boil for 2 hours, with the windpipe hanging out; have a small basin under the windpipe to catch any drips.**
3. **Place the cooked pluck in a basin, cover with liquor in which boiled and leave overnight.**
4. **Next day, cut off the windpipe, grate the liver, chop the heart, lights, suet and onions.**
5. **Add the oatmeal which should first be toasted, but not coloured, salt, pepper, herbs and 1 pint of liquid in which the pluck was boiled.**
6. **Mix well, fill the bag rather more than half full of the mixture, then sew it up and prick it.**
7. **Place in boiling water, simmer for 3 hours, pricking occasionally to keep from bursting.**
8. **If liked, the bag may be cut into several pieces to make smaller haggis; cook 1½–2 hours.**

**Alternative Method of Preparing and Using the Stomach Bag:**

1. **Get the stomach bag cleaned by the butcher.**
2. **Wash it thoroughly and put it on in cold water, bring to boiling point; this will cause the bag to contract.**
3. **Take it out of the pan immediately, wash and scrape it well and lay in salted water till required.**
4. **Take the stomach bag, keep the fat or smooth side inside and fill it, but not quite full; sew up the opening.**
5. **Put into boiling water and simmer for 3 hours.**

## References

AIRAKSINEN, M. S. & PANULA, P. (1988). The histaminergic system in the guinea-pig central nervous system. Journal of Comparative Neurology 273, 163-186.

ALPER, T. , CRAMP, W. A., HAIG, D. A. & CLARKE, M. C. (1967). Does agent of scrapie replicate without a nucleic acid. Science 214, 764-766.

ARENDS, M. J., MORRIS, R. G. & WYLLIE, A. H. (1990). Apoptosis: the role of endonucleases. American Journal of Pathology 136, 593-608.

ASHWOOD, J. Y., LANCASTER, B. & WHEAL, H. V. (1986). Intracellular electrophysiology of CA1 hippocampal pyramidal neurones in slices of kainic acid lesioned hippocampus of the rat. Experimental Brain Research 62 (1), 189-198.

AVANZINI, G. , DE CURTIS, M. , PANZICA, F. & SPREAFICO, R. (1989). Intrinsic properties of nucleus reticularis thalami neurones of the rat studied *in vitro*. Journal of Physiology 416, 111-112.

BAL, T. , VON KROSIGK, M. & MCCORMICK, D. A. (1995). Role of the ferret perigeniculate nucleus in the generation of synchronized oscillations *in vitro*. Journal of Physiology 483 (3), 665-685.

BASLER, K. , OESCH, B. , SCOTT, M. , WESTAWAY, D. , WALCHLI, M. , GROTH, D. F., MCKINLEY, M. P., PRUSINER. S, & WEISSMAN, C. (1986). Scrapie and cellular PrP isoforms are encoded by the same chromosomal gene. Cell 46, 417-428.

BASSANT, M. H., CATHALA, F. , COURT, L. , GOURMELON, P. & HAUW, J. J. (1984). Experimental scrapie in rats: first electrophysiological observations. Brain Research 308, 182-185.

BASSANT, M. H., COURT, L. & CATHALA, F. (1987). Impairment of the cortical and thalamic electrical activity in scrapie-infected rats. Electroencephalography and clinical Neurophysiology 66, 307-316.

BELLINGER-KAWAHARA, C. , DIENER, T. O., MCKINLEY, M. P., GROTH, G. F., SMITH, D. R. & PRUSINER, S. B. (1987). Purified scrapie prions resist inactivation by procedures that hydrolyse, modify or shear nucleic acids. Virology 160, 271-274.

BENDHEIM, P. E., BROWN, H. R., RUDELLI, R. D., SCALA, L. J., GOLLER, N. L., WEN, G. Y., KASCSAK, R. J., CASHMAN, N. R. & BOLTON, D. C. (1992). Nearly ubiquitous tissue distribution of the scrapie agent precursor protein. Neurology 42, 149-156.

BENSON, D. L., ISACKSON, P. J., GALL, C. M. & JONES, E. G. (1992). Contrasting patterns in the localisation of glutamic acid decarboxylase and $Ca^{2+}$ calmodulin protein kinase gene expression in the rat central nervous system. Neuroscience 46, 825-849.

BIGNAMI, A. & PARRY, H. B. (1972). Electron microscopic studies of the brain of sheep with natural scrapie. I The fine structure of neuronal vacuolation. Brain 95, 319-326.

BLATZ, L. A. & MAGLEBY, K. L. (1986). Single apamin-blocked Ca-activated K channels of small conductance in cultured rat skeletal muscle. Nature 323, 718-720.

BORSCHELT, D. R., SCOTT, M. , TARABOULOS, A. , STAHL, N. & PRUSINER, S. B. (1990). Scrapie and cellular prion protein differ in their kinetics of synthesis and topology in cultured cells. Journal of Cellular Biology 110, 743-752.

BOUTHENET, M. L., RUAT, M. , SALES, N. , GARBARG, M. & SCHWARTZ, J. C. (1988). A detailed mapping of histamine H1-receptors in guinea-pig central nervous system identified by autoradiography with [$^{125}$I] iodobolpyramine. Neuroscience 26, 553-600.

BRANDES, J. S. (1971). Dendritic branching patterns in lateral geniculate nucleus following deafferentation. Experimental Neurology 31, 444-450.

BRUCE, M. E., MCBRIDE, P. A. & FARQUAR, C. F. (1989). Precise targeting of the pathology of the sialoglycoprotein, PrP, and vacuolar degeneration in mouse scrapie. Neuroscience Letters 102, 1-6.

BRUCE, M. E., MCCONNELL, I. , FRASER, H. & DICKINSON, A. G. (1991). The disease characteristics of different strains of scrapie in *Sinc* congenic mouse lines: implications for the nature of the agent and host control of pathogenesis. Journal of General Virology 72, 595-603.

BRUCE, M. E., MCBRIDE, P. A., JEFFREY, M. & SCOTT, J. R. (1994). PrP pathology and pathogenesis in scrapie-infected mice. Molecular neurobiology 8, 105-112.

BUDDE, T. , MAGER, R. & PAPE, H. (1992). Different types of potassium outward current in relay neurons acutely isolated from the rat lateral geniculate nucleus. European Journal of Neuroscience 4, 708-722.

BUELER, H. , FISCHER, M. , LANG, Y. , BLUETHMANN, H. , LIPP, H. , DEARMOND, S. , PRUSINER, S. B., AGUET, M. & WEISSMAN, C. (1992). Normal development and behaviour of mice lacking the neuronal cell-surface PrP protein. Nature 356, 577582

CALABRESI, C. , MERCURI, N. B., SANCESARIO, G. & BERNARDI, G. (1993). Electrophysiology of dopamine-denervated striatal neurons: Implications for Parkinson's Disease. Brain 116 (2), 433-452.

CAUGHEY, B. , NEARY, K. , BULLER, R. , ERNST, D. , PERRY, L. L., CHESBRO, B. & RACE, B. (1990). Normal and scrapie-associated forms of the prion protein differ in their sensitivities to phospholipase and proteases in intact neuroblastoma cells. Journal of Virology 64, 1093-1101.

CAUGHEY, B. , RACE, R. & CHESEBRO, B. (1992). Effects of scrapie infection on cellular PrP metabolism. In Prion diseases of humans and animals, eds. PRUSINER, S. B., COLLINGE, J. , POWELL, J. & ANDERTON, B. , pp. 445-456. Chichester: Ellis Horwood Limited.

CEPEDA, C. , WALSH, J. P., PEACOCK, W. , BUCHWALD, N. A. & LEVINE, M. S. (1994). Neurophysiological, pharmacological and morphological properties of human caudate neurones recorded *in vitro*. Neuroscience 59 (1), 89-103.

CHANDLER, R. L. (1961). Encephalopathy in mice produced by inoculation with scrapie brain material. Lancet i, 107-108.

CHOU, S. M., PAYNE, W. M., GIBBS, C. J. & GAJDUSEK, D. C. (1980). Transmission and scanning electron microscopy of spongiform change in Creutzfeld-Jacob disease. Brain 103, 885-904.

CLARKE, M. C. & MILLSON, G. C. (1976). Infection of a cell line of mouse L fibroblasts with scrapie agent. Nature 261, 144-145.

CLARKE, P. B. S., SCHWARTZ, R. D., PAUL, S. M., PERT, S. B. & PERT, A. (1985). Nicotine binding in rat brain: Autoradiographic comparison of [3H]acetylcholine, [3H]nicotine, and [125i]alpha-bungarotoxin. Journal of Neuroscience 5, 1307-1315.

CLINTON, J. , FORSYTH, C. , ROYSTON, M. C. & ROBERTS, G. W. (1993). Synaptic degeneration is the primary neuropathological feature in prion disease: a preliminary study. NeuroReport 4, 65-68.

COLLING, S. B., KING, T. M., COLLINGE, J. & JEFFERYS, J. G. R. (1995). Prion protein null mice: abnormal intrinsic properties of hippocampal CA1 pyramidal cells. Brain Research Association Abstracts 12 (10.7), 49(Abstract)

COLLINGE, J. , WHITTINGTON, M. A., SIDLE, K. C. L., SMITH, C. J., PALMER, M. S., CLARKE, A. R. & JEFFERYS, J. G. R. (1994). Prion protein is necessary for normal synaptic function. Nature 370, 295-297.

COWAN, A. I. & MARTIN, R. L. (1992). Ionic basis of membrane-potential changes induced by anoxia in rat vagal motoneurones. Journal of Physiology 455, 89-109.

CROPPER, E. C., EISENMAN, J. S. & AZMITIA, A. C. (1984). An immunocytochemical study of the serotoninergic innervation of the thalamus of the rat. Journal of Comparative Neurology 224, 238-250.

CRUNELLI, V. , KELLY, J. S., LERESCHE, N. & PIRICHIO, M. (1987a). The ventral and dorsal lateral geniculate nucleus of the rat: intracellular recordings *in vitro*. Journal of Physiology 384, 587-601.

CRUNELLI, V. , KELLY, J. S., LERESCHE, N. & PIRICHIO, M. (1987b). On the excitatory post-synaptic potential evoked by stimulation of the optic-tract in the rat lateral geniculate nucleus. Journal of Physiology 384, 603-618.

CRUNELLI, V. , HABY, M. , JASSIK-GERSCHENFELD, D. & PIRICHIO, M. (1988). $Cl^-$ and $K^+$-dependent inhibitory postsynaptic potentials evoked by interneurones of the rat lateral geniculate nucleus. Journal of Physiology 399, 153-176.

CRUNELLI, V., LIGHTOWLER, S. & POLLARD, C. E. (1989). A T-type calcium current underlies low-threshold calcium potentials in cells of the cat and rat lateral geniculate nucleus. Journal of Physiology 413, 543-561.

CUILLE, J. & CHELLE, P. L. (1936). La maladie dite tremblente du mouton est-elle inoculable ?. Comptes Rendus des Seances de l'Academie des Sciences 203, 1552-1554.

DE CURTIS, A. D., CONTI, F., VAN EYCK, S. L. & MANZONI, T. (1989). Excitatory amino acids mediate responses elicited *in vitro* by stimulation of cortical afferents to reticularis thalamic neurons of the cat. Neuroscience 33, 275-283.

DEARMOND, S. J., MOBLEY, W. C., DEMOTT, D. L., BARRY, R. A., BECKSTEAD, J. H. & PRUSINER, S. B. (1987). Changes in the localization of brain prion proteins during scrapie infection. Neurology 37, 1271-1280.

DESCHENES, M., PARADIS, M., ROY, J. P. & STERIADE, M. (1984). Electrophysiology of neurons of lateral thalamic nuclei in cat: Resting properties and burst discharges. Journal of Neurophysiology 51 (6), 1196-1219.

DESCHENES, M. & HU, B. (1990). Electrophysiology and pharmacology of the corticothalamic input to lateral thalamic nuclei: an intracellular study in the cat. European Journal of Neuroscience 2, 140-152.

DICKINSON, A. G., MEIKLE, V. M. H. & FRASER, H. (1968). Identification of a gene which controls the incubation period of some strains of scrapie in mice. Journal of Comparative Pathology 78, 293-299.

DODGE, F. A. (1961). Ionic permeability changes underlying nerve excitation. In Biophysics of physiological and pharmacological action, eds. Anonymous, pp. 119-143.

DRAGER, U. C. (1974). Autoradiography of tritiated proline and fucose transported transneuronally from the eye to the visual cortex in pigmented and albino mice. Brain Research 82, 284-292.

DREHER, B., SEFTON, A. J., NI, S. Y. K. & NISBETT, G. (1985). The morphology, number and distribution of class I cells in the retina of albino and hooded rats. Brain Behaviour and Evolution 26 (1), 10-48.

ENDO, T., GROTH, D., PRUSINER, S. B. & KOBATA, A. (1989). Diversity of oligosaccharide structures linked to asparaganines of the scrapie-prion protein. Biochemistry 28, 8380-8388.

FAIRBAIRN, D. W., CARNAHAN, K. G., THWAITS, R. N., GRIGSBY, R. V., HOLYOAK, G. R. & O'NEILL, K. L. (1994). Detection of apoptosis induced DNA cleavage in scrapie-infected sheep brain. FEMS Microbiology Letters 115, 341-346.

FAMIGLIETTI, E. V. & PETERS, A. (1972). The synaptic glomerulus and the intrinsic interneurone in the dorsal lateral geniculate nucleus of the cat. Journal of Comparative Neurology 144, 285-344.

FERSTER, D. & LINDSTROM, S. (1983). An intracellular analysis of geniculo-cortical connectivity in area 17 of the cat. Journal of Neuroscience 342, 181-215.

FORLIONI, G. , ANGERETTI, N. , CHIESA, R. , MONZANI, E. , SALMONA, M. , ORSO, B. & TAGLIAVANI, F. (1993). Neurotoxicity of a prion protein fragment. Nature 362 (8), 543-546.

FOSSE, V. M., KOLSTAD, J. & FONNUM, F. (1986). A bioluminescence method for the measurement of L-glutamate: Applications the study of changes in the release of L-glutamate from lateral geniculate nucleus and superior colliculus after visual cortical ablation in rats. Journal of Neurochemistry 47, 340-349.

FOSTER, J. D., FRASER, H. & BRUCE, M. E. (1986). Retinopathy in mice with experimental scrapie. Neuroscience Letters 72, 111-114.

FRASER, H. (1982). Neuronal spread of scrapie agent and targeting of lesions within the retino-tectal pathway. Nature 295, 149-150.

FRASER, H. & DICKINSON, A. G. (1968). The sequential development of brain lesions of scrapie in three strains of mice. Journal of Comparative Pathology 78, 301-311.

FUKUDA, Y. (1977). A three group classification of rat retinal ganglion cells: Histological and physiological studies. Brain Research 119, 327-344.

FUKUDA, Y. , SUGIMOTO, T. & SHIROKAWA, T. (1982). Strain differences in the quantitative analysis of the rat optic nerve. Experimental Neurology 75, 525-532.

GABBOTT, P. L. A., SOMOGYI, M. G., STEWART, M. G. & HAMORI, J. (1986). A quantitative investigation of the neuronal composition of the rat DLG nucleus using GABA-immunocytochemistry. Neuroscience 19, 101-111.

GAJDUSEK, D. C., GIBBS, C. J. & ALPERS, M. (1966). Experimental transmission of a Kuru-like syndrome to chimpanzees. Nature 209, 794-796.

GAJDUSEK, D. C. & ZIGAS, V. (1957). Degenerative disease of the central nervous system in New Guinea: The endemic occurrence of "Kuru" in the native population. New England Journal of Medicine 257, 974-978.

GIUFFREDA, R. & RUSTIONI, A. (1988). Glutamate and aspartate immunoreactivity in corticothalamic neurons of rats. In Cellular Thalamic Mechanisms, eds. BENTIVOGLIO, M. & SPREAFICO, R. , pp. 311-320. Amsterdam: Elsevier.

GRAFSTEIN, B. & FORMAN, D. S. (1980). Intracellular transport in neurones. Physiological Reviews 60, 1167-1283.

GRAY, E. G. (1963). Electron microscopy of presynaptic organelles in the spinal cord. Journal of Anatomy 97, 101-106.

GRIFFITH, J. S. (1967). Self-replication and scrapie. Nature 215 (105), 1043-1044.

GROSSMAN, A. , LIEBERMAN, A. R. & WEBSTER, K. E. (1973). A Golgi study of the rat lateral geniculate nucleus. Journal of Comparative Neurology 150, 441-466.

GUILLERY, R. W. (1971). Patterns of synaptic interconnections in the dorsal lateral geniculate nucleus of the cat and monkey: a brief review. Vision Research Supplement 3, 211-227.

GUTNICK, M. J., LOBEL-YAAKOV, R. & RIMON, G. (1985). Incidence of neuronal dye-coupling in neocortical slices depends on the plane of section. Neuroscience 15, 659-666.

HADLOW, W. J. (1959). Scrapie and Kuru. Lancet ii, 289-290.

HERNANDEZ-CRUZ, A. & PAPE, H. (1989). Identification of two calcium currents in acutely dissociated neurons from the rat lateral geniculate nucleus. Journal of Neurophysiology 61, 1271-1273.

HEUMANN, D. & RABINOWICZ, T. (1980). Postnatal development of the dorsal lateral geniculate nucleus in the normal and enucleated albino mouse. Experimental Brain Research 38, 75-85.

HIRSCH, J. C., FOUREMENT, A. & MARC, M. E. (1983). Sleep-related variations of membrane potential in the lateral geniculate body relay neurons of the cat. Brain Research 259, 308-312.

HIRSCH, J. C. & BURNOD, Y. (1987). A synaptically evoked late hyperpolarisation in the rat dorsolateral geniculate neurons *in vitro*. Neuroscience 23 (2), 457-468.

HODGKIN, A. L. & HUXLEY, A. F. (1952). A quantitative description of membrane current and its application to conduction and excitation in nerve. Journal of Physiology 117, 500-544.

HOGAN, N. R., BARINGER, J. R. & PRUSINER, S. B. (1987). Scrapie infection diminishes spines and increases varicosities of dendrites in hamsters: a quantitative Golgi analysis. Journal of Neuropathology and Experimental Neurology 46 (4), 461-473.

HORIKAWA, K. & ARMSTRONG, W. E. (1988). A versatile means of intracellular labelling: injection of biocytin and its detection with avidin conjugates. Journal of Neuroscience Methods 25, 1-11.

HOUSER, C. R., VAUGHN, J. E., BARBER, R. P. & ROBERTS, E. (1980). GABA neurons are the major cell type of the nucleus reticularis thalami. Brain Research 200, 341-354.

HUGUENARD, J. R., COULTER, D. A. & PRINCE, D. A. (1991). A fast transient potassium current in thalamic relay neurons: kinetics of activation and inactivation. Journal of Neurophysiology 66 (4), 1304-1315.

HUNTER, N. , DANN, J. C., BENNETT, A. D., SOMERVILLE, R. A., MCCONNELL, I. & HOPE, J. (1992). Are *Sinc* and the PrP gene congruent? Evidence from PrP gene analysis in *Sinc* congenic mice. Journal of General Virology 73, 2751-2755.

IQBAL, K. , SOMERVILLE, R. A., THOMPSON, C. H. & WISNIEWSKI, H. M. (1985). Brain glutamate decarboxylase and cholinergic enzyme activities in scrapie. Journal of the Neurological Sciences 67, 345-350.

IWAHORI, I. & MIZUNO, N. (1984). The dorsal lateral geniculate nucleus in the mouse: a Golgi study. Neuroscience Research 1, 443-455.

JAHNSEN, H. & LLINAS, R. (1984a). Electrophysiological properties of the guinea-pig thalamic neurones: an *in vitro* study. Journal of Physiology 349, 205-226.

JAHNSEN, H. & LLINAS, R. (1984b). Ionic basis for the electroresponsiveness and oscillatory properties of guinea-pig thalamic neurones *in vitro*. Journal of Physiology 349, 227-247.

JEFFREY, M. , SCOTT, J. R. & FRASER, H. (1991). Scrapie inoculation of mice: light and electron microscopy of the superior colliculi. Acta Neuropathologica 81, 562-571.

JEFFREY, M. , GOODSIR, C. M., BRUCE, M. E., MCBRIDE, P. A., SCOTT, J. R. & HALLIDAY, W. G. (1992). Infection specific prion protein (PrP) accumulates on plasmalemma in scrapie infected mice.. Neuroscience Letters 147, 106-109.

JEFFREY, M. , GOODSIR, C. M., BRUCE, M. , MCBRIDE, P. A., SCOTT, J. R. & HALLIDAY, W. G. (1994). Correlative light and electron microscopy studies of PrP localisation in 87V scrapie. Brain Research 656, 329-343.

JEFFREY, M. , FRASER, J. R., HALLIDAY, W. G., FOWLER, N. , GOODSIR, C. M. & BROWN, D. A. (1995). Early unsuspected neuron and axon terminal loss in scrapie-infected mice revealed by morphometry and immunocytochemistry. Neuropathology and Applied Neurobiology 21, 41-49.

JEFFERYS, J. G. R., EMPSON, R. M., WHITTINGTON, M. A. & PRUSINER, S. B. (1994). Scrapie infection of transgenic mice leads to network and intrinsic dysfunction of cortical and hippocampal neurones. Neurobiology of Disease 1, 3-15.

JOHNSTON, A. R., MACLOUD, N. K. & DUTIA, M. D. (1994). Ionic conductances contributing to spike repolarisation and after-potentials in rat medial vestibular nucleus neurones. Journal of Physiology 481 (1), 61-77.

JOHNSTON, A. R., BLACK, C. J., FRASER, J. R. & MACLOUD, N. K. (1995). Physiological and morphological properties of scrapie-infected CA1 hippocampal pyramidal cells. Brain Research Association Abstracts 12 (10.6), 49(Abstract)

JONES, E. G. (1985). The thalamus. New York: Plenum press.

KANEKO, T. & MIZUNO, N. (1988). Immunohistochemical study of glutaminase-containing neurons in the cerebral cortex of the rat. Journal of Comparative Neurology 267, 590-602.

KAYAMA, Y. (1985). Ascending, descending and local control of neuronal activity in the rat lateral geniculate nucleus. Vision Research 25, 339-347.

KAYAMA, Y. (1989). Effects of stimulating the dorsal raphe nucleus of the rat on neuronal activity in the dorsal lateral geniculate nucleus. Brain Research 489, 1-11.

KERR, J. F. R., WYLLIE, A. H. & CURRIE, A. R. (1972). Apoptosis: a basic biological phenomenon with wide-ranging implications in tissue kinetics . British Journal of Cancer 26, 239-257.

KIM, J. H. & MANUELIDIS, E. E. (1987). Neuronal alterations in experimental Creutzfeld-Jakob disease: a Golgi study. Journal of the Neurological Sciences 89, 93-101.

KIMBERLIN, R. (1982). Reflections on the nature of the scrapie agent. Trends in the Biochemical Sciences 7, 392-394.

KOCISKO, D. A. , COME, J. H . , PRIOLA, S. A. , CHESEBRO, B. , RAYMOND, G. J. , LANSBURY, P. T. , CAUGHEY, B. (1994). Nature 370, 471 - 474.

KRETZCHMAR, H. A., PRUSINER, S. B., STOWRING, L. E. & DEARMOND, S. J. (1986). Scrapie prions are synthesised in neurones. American Journal of Pathology 122, 1-5.

KRISTENSSON, G. B. , & WISNIEWSKI, H. M. (1974). Study on the propagation of herpes simplex virus (type 2) into the brain after intraocular injection. Brain Research 69, 189-201.

KRISTENSSON, K. , FEUERSTEIN, B. , TARABOULOS, A. , HYUN, W. C., PRUSINER, S. B. & DEARMOND, S. J. (1993). Scrapie prions alter receptor-mediated calcium responses in cultured cells. Neurology 43, 2335-2341.

KROMER, L. F. & MOORE, R. Y. (1980). A study of the organisation of the locus coeruleus projections to the lateral geniculate nuclei in the albino rat. Neuroscience 5, 255-271.

LAMPERT, P. , HOOKS, J. , GIBBS, C. J. & GAJDUSEK, D. C. (1971). Altered plasma membranes in experimental scrapie. Acta Neuropathologica 19, 81-93.

LANCASTER, B. & ADAMS, P. R. (1986). Calcium-dependent current generating the after-hyperpolarisation of hippocampal neurons. Journal of Neurophysiology 55, 1268-1282.

LANCASTER, B. & NICOLL, R. A. (1987). Properties of two calcium-activated hyperpolarisations in rat hippocampal neurones. Journal of Physiology 389, 187-203.

LANDIS, D. M. D., WILLIAMS, R. S. & MASTERS, C. L. (1981). Golgi and electronmicroscopic studies of spongiform encephalopathy. Neurology 31, 538-549.

LASHLEY, K. S. (1934). The mechanism of vision. IV. The projection of the retina on the primary optic areas in the rat. Journal of Comparative Neurology 59, 341-373.

LERESCHE, N. , LIGHTOWLER, S. , SOLTESZ, I. , JASSIK-GERSCHENFLED, D. & CRUNELLI, V. (1991). Low-frequency oscillatory activities intrinsic to rat and cat thalamocortical cells. Journal of Physiology 441, 155-174.

LIEBERMAN, A. R. & WEBSTER, K. E. (1972). Presynaptic dendrites and a distinctive class of synaptic vesicle in the rat dorsal lateral geniculate nucleus. Brain Research 42, 196-200.

LIEBERMAN, A. R. & WEBSTER, K. E. (1974). Aspects of the synaptic organisation of intrinsic neurones in the dorsal lateral geniculate nucleus. An ultrastructural study. Journal of Neurocytology 3, 677-710.

LINDEN, R. & PERRY, V. H. (1983). Massive retinotectal projection in rats. Brain Research 272, 145-149.

LIVINGSTONE, M. S. & HUBEL, D. H. (1981). Effects of sleep and arousal on the processing of visual information in the cat. Nature 291, 554-561.

LLINAS, R. & SUGIMORI, M. (1980). Electrophysiological properties of *in vitro* purkinje cell dendrites in mammalian cerebellar slices. Journal of Physiology 305, 197-213.

LLINAS, R. & YAROM, Y. (1981). Properties and distribution of ionic conductances generating electroresponsiveness of mammalian inferior olivary neurones *in vitro*. Journal of Physiology 315, 549-567.

LUND, J. S., REMINGTON, F. L. & LUND, R. D. (1976). Differential central distribution of optic nerve components in the rat. Brain Research 116, 83-100.

LUND, R. D. (1965). Uncrossed visual pathways in albino and hooded rats. Science 149, 1506-1507.

LUND, R. D. & CUNNINGHAM, T. J. (1972). Aspects of synaptic and laminar organisation of the mammalian lateral geniculate body. Investigative Ophthalmology 11, 291-302.

M'GOWAN, J. P. (1914). Investigations of the disease of sheep called "scrapie". Edinburgh: Blackwood.

MAJNO, G. & JOVIS, I. (1995). Apoptosis, oncosis and necrosis: an overview of cell death. American Journal of Pathology 146 (1), 3-15.

MARTIN, K. A. C. (1988). The lateral geniculate nucleus strikes back. Trends in Neurosciences 11 (5), 192-194.

MARTY, A. (1981). Calcium-dependent channels with large unitary conductance in chromaffin cell membranes. Nature 291, 497-500.

MASLIAH, E. & TERRY, R. D. (1993). The role of synaptic proteins in the pathogenesis of disorders of the central nervous system. Brain Pathology 3, 77-85.

MATTHEWS, M. A. (1973). Death of the central neuron: An electron microscopic study of thalamic retrograde degeneration following cortical ablation in the rat. Journal of Neurocytology 2, 265-288.

MCCONKEY, D. J., HARTZELL, P. , NICOTERA, P. & ORRENIUS, S. (1989). Calcium-activated DNA fragmentation kills immature thymocytes. FASEB Journal 3, 1843-1848.

MCCORMICK, D. A. (1991). Functional properties of a slowly inactivating potassium current in guinea-pig dorsal lateral geniculate relay neurons. Journal of Neurophysiology 4, 1176-1189.

MCCORMICK, D. A. (1992). Cellular mechanisms underlying cholinergic and noradrenergic modulation of neuronal firing mode in the cat and guinea-pig dorsal lateral geniculate nucleus. Journal of Neuroscience 12 (1), 278-289.

MCCORMICK, D. A. & PAPE, H. (1988). Acetylcholine inhibits identified interneurones in the cat lateral geniculate nucleus. Nature 334, 246-248.

MCCORMICK, D. A. & PAPE, H. (1990a). Noradrenergic and serotoninergic modulation of a hyperpolarisation-activated cation current in thalamic relay neurones. Journal of Physiology 431, 319-342.

MCCORMICK, D. A. & PAPE, H. (1990b). Properties of a hyperpolarisation-activated cation current and its role in rhythmic oscillation in thalamic relay neurones. Journal of Physiology 431, 291-318.

MCCORMICK, D. A. & PRINCE, D. A. (1986). Mechanisms of ascending control of thalamic neuronal activities: acetylcholine and norepinephrine. Society of Neuroscience Abstracts 12, 903(Abstract)

MCCORMICK, D. A. & PRINCE, D. A. (1987). Actions of acetylcholine in the guinea-pig and cat medial and lateral geniculate nuclei, *in vitro*. Journal of Physiology 392, 147-165.

MCCORMICK, D. A. & PRINCE, D. A. (1988). Noradrenergic modulation of firing patterns in guinea pig and cat thalamic neurones, *in vitro*. Journal of Neurophysiology 59, 978-996.

MCCORMICK, D. A. & WANG, Z. (1991). Serotonin and noradrenaline excite GABAergic neurones of the Guinea-pig and Cat thalamic reticular nucleus. Journal of Physiology 442, 235-255.

MCCORMICK, D. A. & WILLIAMSON, A. (1991). Modulation of neuronal firing mode in cat and guinea pig dLGN by histamine: Possible cellular mechanisms of histaminergic control of arousal. Journal of Neuroscience 11, 3188-3199.

MCKINLEY, M. P., BOLTON, D. C. & PRUSINER, S. B. (1983). A protease-resistant protein is a structural component of the scrapie prion. Cell 35, 57-62.

MERZ, P. A., SOMERVILLE, R. A., WISNIEWSKI, H. M. & IQBAL, K. (1981). Abnormal fibrils from scrapie-infected brain. Acta Neuropathologica 54, 63-74.

METIN, C. , GOUDEMENT, P. & SAILLOUR, P. I.,M (1983). Physiological and anatomical study of retinogeniculate projections in the mouse. Comptes Rendus des Seances de l'Academie des Sciences Series III 296, 157-162.

MEYER, N. , ROSENBAUM, V. , SCHMIDT, B. , GILLES, K. , MIRENDA, C. & GROTH, D. (1991). Search for a putative scrapie genome in purified prion fractions reveals a paucity of nucleic acids. Journal of General Virology 72, 37-49.

MEYER, R. K., MCKINLEY, M. P. & BOWMAN, K. A. (1986). Separation and properties of cellular and scrapie prion proteins. Proceedings of the National Academy of Sciences 83, 2310-2314.

MONAGHEN, D. T., YAO, D. T., OLVERMAN, H. W. & COTMAN, C. W. (1984). Autradiography of D-2-[3H]amino-5-phosphopentanoate bindings sites in rat brain. Neuroscience Letters 52, 253-258.

MONAGHEN, D. T. & COTMAN, C. W. (1982). The distribution of [3H]kainic acid binding sites in rat CNS as determined by autoradiography. Brain Research 252, 91-100.

MONAGHEN, D. T. & COTMAN, C. W. (1985). The distribution of N-Methyl-D-Aspartate-sensitive L-[3H] glutamate-binding sites in rat brain. Journal of Neuroscience 5, 2909-2919.

MONTERO, V. M. & GUILLERY, R. W. (1968). Degeneration in the dorsal lateral geniculate nucleus of the rat following interruption of retinal or cortical connections. Journal of Comparative Neurology 143, 211-242.

MONTERO, V. M. & SCOTT, G. L. (1981). Synaptic terminals in the dorsal lateral geniculate nucleus from neurons of the thalamic reticular nucleus. Neuroscience 6, 2561-2577.

MONTERO, V. M. & WENTHOLD, R. J. (1989). Quantitative immunogold analysis reveals high glutamate levels in retinal and cortical synaptic terminals in the lateral geniculate nucleus of the Macaque. Neuroscience 31, 639-647.

MONTERO, V. M., BRUGGE, J. F. & BIETEL, R. E. (1968). Relation of the visual field to the lateral geniculate body of the albino rat. Journal of Neurophysiology 31, 221-236.

MUKHAMETOV, L. M. & RIZZOLATTI, G. (1970). The responses of lateral geniculate neurons to flashes of light during the sleep-waking cycle. Archives of Italian Biology 108, 348-368.

NI, S. Y. K. & DREHER, B. (1981). Morphology of rat retinal ganglion cells projecting to the thalamus and midbrain. Proceedings of the Australian Physiological and Pharmacological Society 12, 97P(Abstract)

OESCH, B. , WESTAWAY, D. , WALCHI, M. , MCKINLEY, M. P., KENT, S. B. H., AEBERSOLD, R. , BARRY, R. A., PRUSINER, S. B. & WEISSMAN, C. (1985). A cellular gene encodes scrapie PrP 27-30 protein. Cell 40, 735-746.

OHARA, P. T., LIEBERMAN, A. R., HUNT, S. P. & WU, J. P. (1983). Neural elements containing glutamic acid decarboxylase (GAD) in the dorsal lateral geniculate nucleus of the rat: immunohistochemical studies by light and electron microscopy. Neuroscience 8 (2), 189-211.

OHARA, P. T. & LIEBERMAN, A. R. (1985). The thalamic reticular nucleus of the adult rat: experimental anatomical studies. Journal of Neurocytology 14, 364-411.

OSMANOVIC, S. S., SHEFNER, S. A. & BRODIE, M. A. (1990). Functional significance of the apamin-sensitive conductance in rat locus coerulus neurons. Brain Research 530, 283-289.

OTTERSON, O. P. & STORM-MATHISEN, J. (1984a). GABA-containing neurons in the thalamus and pretectum of the rodent: An immunocytochemical study. Anatomy, Histology and Embryology 170, 197-207.

OTTERSON, O. P. & STORM-MATHISEN, J. (1984b). Glutamate- and GABA-containing neurones in the mouse and rat brain, as demonstrated with a new immunocytochemical technique. Journal of Comparative Neurology 229, 374-392.

PAN, K. , BALDWIN, M. , NGUYEN, J. , GASSET, M. , SERBAN, A. , GROTH, D. , MEHLHORN, I. , HUANG, Z. , FLETTERICK, R. J., COHEN, F. E. & PRUSINER, S. B. (1993). Conversion of alpha helices to beta sheets features in the formation of the scrapie prion proteins. Proceedings of the National Academy of Sciences 90, 109622-10966.

PAPE, H. , BUDDE, T. , MAGER, R. & KISVARDAY, Z. F. (1994). Prevention of $Ca^{2+}$-mediated action potentials in GABAergic local circuit neurones of rat thalamus by a transient $K^+$ current. Journal of Physiology 478 (3), 403-422.

PARNAVELAS, J. G., MOUNTY, E. J., BRADFORD, R. & LIEBERMAN, A. R. (1977). The postnatal development of neurons in the dorsal lateral geniculate nucleus of the rat: a golgi study. Journal of Comparative Neurology 171, 481-500.

PENNEFATHER, P. , LANCASTER, B. , ADAMS, P. R. & NICOLL, R. A. (1985). Two distinct Ca-dependent K currents in bullfrog sympathetic ganglion cells. Proceedings of the National Academy of Sciences 82, 3040-3044.

PERRY, V. H. (1979). The ganglion cell layer of the retina of the rat. Proceedings of the Royal Society of London 204, 363-375.

POCCHIARI, M. , MUNSON, P. J., COSTA, T. , GAJDUSEK, D. C. & GIBBS, C. J. (1985a). Serotoninergic system in scrapie-infected hamsters. Journal of Neurochemistry 44, 862-868.

POCCHIARI, M. , MASULLO, C. , LUST, W. D., GIBBS, C. J. & GAJDUSEK, D. C. (1985b). Isonicotinic hydrazide causes seizures in scrapie-infected hamsters with shorter latency than in control animals: a possible GAGAergic defect. Brain Research 326, 117-123.

POCCHIARI, M. , SCHMITTINGER, S. & MASULLO, C. (1987). Amphoteracin B delays the incubation period of scrapie in intracerebrally inoculated hamsters. Journal of General Virology 1987, 68-219.

PRUSINER, S. ,B. (1982). Novel proteinaceous infectious particles cause scrapie. Science 216, 136-144.

PRUSINER, S. B., GROTH, D. F., COCHRAN, S. P. & MASIARZ, F. R. (1980). Molecular properties, partial purification, and assay by incubation period measurements of the hamster scrapie agent. Biochemistry 19, 4883-4891.

PRUSINER, S. B., SCOTT, M. , FOSTER, D. , PAN, K. , GROTH, D. , MIRENDA, C. , TORCHIA, M. , YANG, S. , SERBAN, D. , CARLSON, G. A., HOPPE, P. C., WESTAWAY, D. & DEARMOND, S. J. (1990). Transgenetic studies implicate interactions between homologous PrP isoforms in scrapie prion replication. Cell 63, 673-686.

PRUSINER, S. B., GROTH, D. , SERBAN, A. , KOEHLER, R. , FOSTER, D. , TORCHIA, M. , BURTON, D. , YANG, S. & DEARMOND, S. (1993). Ablation of the prion protein (PrP) gene in mice prevents scrapie and facilitates production of anti-PrP antibodies. Proceedings of the National Academy of Sciences 90, 10608-10612.

QUINN, M. R., KIM, Y. S., LOSSINSKY, A. S. & CARP, R. I. (1988). Influence of stereotaxically injected scrapie on neurotransmitter systems of mouse cerebellum. Brain Research 445, 297-302.

RAFF, M. C., BARRES, B. A., BURNE, J. F., COLES, H. S., ISHIZAKI, Y. & JACOBSON, M. D. (1993). Programmed cell death and the control of cell survival: lessons from the nervous system. Science 262, 695-700.

RAFOLS, J. A. & VALVERDE, F. (1973). The structure of the dorsal lateral geniculate nucleus in the mouse. A Golgi and electron microscopic study. Journal of Comparative Neurology 150, 303-332.

ROCHE-LUBIN, (1848). Records in Medical and Veterinary Services 3 (5), 698

ROGOWSKI, M. & AGHANHANIAN, G. H. (1982). Activation of lateral geniculate neurones by locus coerulus or dorsal noradrenergic bundle stimulation: Selective blockade by the Alpha1-adrenocepor antagonist prazosin. Brain Research 50, 31-39.

ROTTER, R. , BIRDSALL, N. J. M., BURGEN, A. S. V., FIELD, P. M., HULME, E. C. & AISMAN, G. (1979). Muscarinic receptors in the central nervous system of the rat.. Brain Research Reviews 1, 141-165.

SATO, Y. , OHTA, M. & TATEISHI, J. (1980). Experimental transmission of human subacute spongiform encephalopathy to small rodents. II Ultrastructural study of spongy state in the grey and white matter. Acta Neuropathologica 51, 135-140.

SCHEIBEL, M. E. & SCHEIBEL, A. B. (1966). The organisation of the nucleus reticularis thalami: A Golgi study. Brain Research 1, 43-62.

SCOTT, J. R., REEKIE, L. J. D. & HOPE, J. (1991). Evidence for the intrinsic control of scrapie pathogenesis in the murine visual system. Neuroscience Letters 133, 141-144.

SCOTT, J. R., DAVIES, D. & FRASER, H. (1992). Scrapie in the central nervous system: neuroanatomical spread of infection and *Sinc* control of pathogenesis. Journal of General Virology 73, 1637-1644.

SCOTT, J. R. & FRASER, H. (1984). Degenerative hippocampal pathology in mice infected with scrapie. Acta Neuropathologica 65, 62-68.

SCOTT, J. R. & FRASER, H. (1989). Enucleation after intraocular scrapie injection delays the spread of infection. Brain Research 504, 301-305.

SCOTT, M. , FOSTER, D. , MIRENDA, C. , SERBAN, D. , COUFAL, F. , WALCHLI, M. , TORCHIA, M. , GROTH, D. , CARLSON, G. , DEARMOND, S. J. & PRUSINER, S. B. (1989). Transgenic mice expressing hamster prion protein produce species-specific scrapie infectivity and amyloid plaques. Cell 59, 847-857.

SEFTON, A. J. & DREHER, B. (1985). Visual system. In Forebrain and midbrain, ed. PAXINOS, G. , pp. 169-221. Australia: Academic Press.

SEFTON, A. J. & SWINDBURN, M. (1981). Cortical projections to visual centres in the rat: An HRP study. Brain Research 215, 1-13.

SHERMAN, S. M. & KOCH, C. (1986). The control of retinogeniculate transmission in the mammalian geniculate nucleus. Experimental Brain Research 63, 1-20.

SHERMAN, S. M. & KOCH, C. (1990). Thalamus. In The synaptic organisation of the brain, ed. SHEPHERD, G. M., pp. 246-278. Oxford: Oxford University Press.

SIGURDSSON, D. (1954). Rida, a chronic encephalitis of sheep. With general remarks on infection which develops slowly and some of their special characteristics. British Veterinary Journal 110, 341-354.

SILINSKY, E. M. (1992). Intracellular recording methods for neurons. In Monitoring neuronal activity, a practical approach., ed. STAMFORD, J. A., pp. 29-57. Oxford: IRL Press.

SNIDER, W. D. (1988). Nerve growth factor enhances dendritic arborisation of sympathetic ganglion cells in developing mammals. Journal of Neuroscience 8 (7), 2628-2634.

SOFRONIEW, M. V., PRIESTLEY, J. V., CONSOLAZIONE, A. , ECKENSTEIN, F. & CUELLO, A. C. (1985). Cholinergic projections from the midbrain and pons to the thalamus in the rat, identified by combined retrograde tracing and choline acetyltransferase immunohistochemistry. Brain Research 329, 213-223.

SOLSTESZ, I. , LIGHTOWLER, S. , LERESCHE, N. , JASSIK-GERSCHENFELD, D. , POLLARD, C. E. & CRUNELLI, V. (1991). Two inward currents and the transformation of low-frequency oscillations of rat and cat thalamocortical cells. Journal of Physiology 441, 175-197.

SPIELMAYER, , SEE COLLINGE, J. & PRUSINER, S. B. (1992). Terminology of Prion Diseases. In Prion Diseases of Humans and Animals, eds. PRUSINER, S. , COLLINGE, J. , POWELL, J. & ANDERTON, B. , pp. 5-29. London: Ellis Horwood.

STERIADE, M. , DOMICH, L. & OAKSON, G. (1986). Reticular thalami neurons revisited: Activity changes during shifts in states of vigilance. Journal of Neuroscience 6, 68-81.

STERIADE, M. , DOMICH, L. & OAKSON, G. (1987). The deafferented reticular thalamic nucleus generates spindle rhythmicity. Journal of Neurophysiology 57, 260-273.

STERIADE, M. , PARE, D. , HU, B. & DESCHENES, M. (1990a). The visual thalamocortical system and its modulation by the brain stem core. Progress in Sensory Biology 10,

STERIADE, M. , JONES, E. G. & LLINAS, R. (1990b). The thalamus as a neuronal oscillator. New York: Wiley.

STERIADE, M. , PARE, D. , OAKSON, G. & CURRO DOSSI, R. (1990c). Neuronal activities in brainstem cholinergic nuclei related to tonic activation processes in thalamocortical systems. Journal of Neuroscience 10, 2541-2559.

STERIADE, M. , MCCORMICK, D. A. & SEJNOWSKI, T. J. (1993). Thalamocortical oscillations in the sleeping and aroused brain. Science 262, 679-685.

STERIADE, M. & LLINAS, R. R. (1988). The functional states of the thalamus and the associated neuronal interplay. Physiological Reviews 68, 649-742.

STERIADE, M. & MCCARLEY, R. W. (1990). Brainstem control of wakefulness and sleep. New York: Plenum ress.

STORM, J. F. (1987). Action potential repolarisation and a fast after-hyperpolarisation in rat hippocampal pyramidal neurones. Journal of Physiology 365, 733-759.

SUDHOF, T. C. & JAHN, R. (1991). Proteins of synaptic vesicles involved in exocytosis and membrane recycling. Neuron 6, 665-677.

SWANSON, L. W., SIMMONS, D. M., WHITING, P. J. & LINDSTROM, J. (1987). Immunohistochemical localisation of neuronal nicotinic receptors in the rodent central nervous system. Journal of Neuroscience 7 (10), 3334-3342.

TAGLIAVINI, F. (1991). Amyloid protein of Gerstmann-Straussler-Scheinker disease (Indiana kindred) is an 11 Kd fragment of a protein with a N-terminal glycine at codon 58. The EMBO Journal 10, 513-519.

THE GLASGOW COOKBOOK BOOK, (1962). Glasgow: John Smith and Son.

THOMSON, A. (1988). Inhibitory postsynaptic potentials evoked in thalamic neurons by stimulation of the reticularis nucleus evoke slow spikes in isolated rat brain slices. Neuroscience 25 (2), 491-502.

TSUMOTO, T. , CREUTZFELDT, O. D. & LEGENDY, C. R. (1978). Excitatory amino acid transmitters in neuronal circuits of the cat visual cortex. Experimental Brain Research 32, 345-354.

TURNER, J. ., LERESCHE, N. , GUYON, A. , SOLTESZ, I. & CRUNELLI, V. (1994). Sensory input and burst firing output of rat and cat thalamocortical cells: the role of NMDA and non-NMDA receptors. Journal of Physiology 480 (2), 281-295.

UEDA, N. & SHAH, S. V. (1994). Apoptosis. Journal of Laboratory and Clinical Research 124 (2), 169-177.

VALVERDE, F. (1968). Structural changes in the area striata of the mouse after enucleation. Experimental Brain Research 5, 274-292.

VIANA, F. , BAYLISS, D. . & BERGER, A. J. (1993). Multiple potassium conductances and their role in action potential repolarisation and repetitive firing behaviour of neonatal rat hypoglossal motoneurons. Journal of Neurophysiology 69 (6), 2150-2163.

VON KROSIGK, M. , BAL, T. & MCCORMICK, D. A. (1993). Cellular mechanisms of synchronized oscillation in the thalamus. Science 261, 361-364.

WARREN, R. , AGMON, A. & JONES, E. G. (1994). Oscillatory synaptic interactions between ventroposterior and reticular neurones in mouse thalamus *in vitro*. Journal of Neurophysiology 72 (4), 1993-2003.

WEGIEL, J. & WISNIEWSKI, H. M. (1990). The complex of microglial cells and amyloid star in three-dimensional reconstruction. Acta Neuropathologica 81, 116-124.

WILESMITH, J. W., RYAN, J. B. M. & ATKINSON, M. J. (1991). Bovine spongifrom encephalopathy: epidemiological studies on origin. Veterinary Record 128, 199-203.

WILLIAMS, A. E., LAWSON, L. J., PERRY, V. H. & FRASER, H. (1994). Characterization of the microglial response in murine scrapie. Neuropathology and Applied Neurobiology 20, 47-55.

WYLLIE, A. H. (1987). Apoptosis: cell death in tissue regulation. Journal of Pathology 153, 313-316.

WYLLIE, A. H. & DUVALL, E. (1994). Cell death. In Oxford Textbook of Pathology, pp. 141-156.